



**University of
Zurich^{UZH}**

Ammonoid size variation during the Smithian- Spathian climatic upheavals

ESS 511 Master's Thesis

Author

Lara Locatelli
10-947-794

Supervised by

Prof. Dr. Hugo Bucher (hugo.fr.bucher@pim.uzh.ch)

Faculty representative

Prof. Dr. Hugo Bucher

29.01.2019

Department of Geography, University of Zurich



Table of Contents

ABSTRACT	1
1. INTRODUCTION	2
2. SETTINGS	5
2.1 STRATIGRAPHY	5
2.2 PALAEOGEOGRAPHY	5
2.3 AMMONOID RECOVERY	7
2.4 SMITHIAN-SPATHIAN PALAEOCLIMATE AND THE END SMITHIAN EXTINCTION — A BRIEF OVERVIEW.....	8
2.5 PALAEOECOLOGY OF THE SMITHIAN-SPATHIAN TIME; AN AMMONOIDS' PERSPECTIVE	9
3. MATERIAL AND METHODS	12
3.1 DATASET.....	12
3.2 SPATIAL SUBDIVISIONS	15
3.3 ANALYSIS OF MAXIMAL SIZE THROUGH TIME	16
3.3.1 <i>Mann-Whitney-U test</i>	16
3.3.2 <i>Kolmogorov-Smirnov test</i>	16
3.4 <i>Size patterns across space</i>	17
4. RESULTS	18
4.1 <i>SIZE TRENDS ACROSS TIME</i>	18
4.2 <i>SIZE PATTERNS ACROSS SPACE</i>	45
5. DISCUSSION	53
5.1 INTERACTIONS BETWEEN ENVIRONMENTAL AND ECOLOGICAL PARAMETERS AND BODY SIZE.....	53
5.1.1 <i>Temperature</i>	53
5.1.2 <i>Nutrients</i>	53
5.1.3 <i>Oxygen availability</i>	54
5.1.4 <i>Calcium carbonate saturation level</i>	54
5.1.5 <i>Body size and trophic relations</i>	55
5.2 <i>SIZE CHANGES THROUGHOUT SMITHIAN AND SPATHIAN — AN OVERVIEW ON CLIMATE UPHEAVALS</i>	56
5.3 <i>SIZE REDUCTION FROM SMITHIAN TO SPATHIAN</i>	57
5.4 <i>THE SOUTH CHINA BLOCK AND THE PALAEO-TETHYS</i>	58
5.5 <i>THE NEOTETHYS</i>	60
5.6 <i>THE BOREAL DOMAIN</i>	61
5.7 <i>THE PULL-APART BASINAL AREA OF THE WESTERN U.S.</i>	62
5.8 <i>SIZE RANGE AND DIVERSITY GRADIENTS</i>	63
6. CONCLUSION	65
7. OUTLOOK	67



ACKNOWLEDGMENTS	68
BIBLIOGRAPHY	69
APPENDIX – PART 1.....	I
APPENDIX – PART 2.....	VI
MAIN OUTPUT COMPONENTS OF MULTIPLE LINEAR REGRESSION	VII
MAIN OUTPUT COMPONENTS OF SIMPLE LINEAR REGRESSION	XV
PERSONAL DECLARATION	A

Abstract

The Smithian-Spathian time interval was a time of major climatic upheavals which resulted in a massive extinction event at the end of the Smithian stage (about 2.5 Myr after the end-Permian extinction) and profoundly impacted ammonoid and conodont faunas. A large positive amplitude carbon excursion globally characterises the shift from a middle Smithian hot and humid climate to late Smithian-early Spathian cooler and more arid environmental conditions. Biotic crisis associated with strong climatic changes are usually accompanied by significant changes in size, as a result of the associated biotic and abiotic stressors. Body size is in fact affected by different factors and it is in turn related to many faunal ecological features that can impact trophic relationships, the main link between the organisms of an ecosystem. Here, for the first time, the response of ammonoids in terms of body size evolution is analysed on a global scale throughout Smithian and Spathian, based on both published and unpublished material that is grounded into a solid stratigraphy. When taking into account different palaeoregions, contrasting results emerge, of which the most striking is the complete absence of size change throughout the considered time period in South China and in the Palaeotethys domain. Putative explanations that take into account the palaeoposition and the palaeoecology of the two areas are advanced, mainly focused on the warmer temperatures proper of equatorial locations (which might imply a smaller environmental impact during the warmest middle Smithian times), and on the associated smaller amount of oxygen that can be dissolved in warmer seawater. The latter might have kept Smithian ammonoids at a smaller size compared to other palaeolatitudes. Most of the other analysed regions show an expected significant size reduction between Smithian and Spathian as well as between late Smithian and early Spathian, in connection to the extinction event. Size reduction was also observed in most cases associated with the shift from cooler to warmer conditions between early to middle Smithian and early to middle Spathian, in agreement with Atkinson's (1994) "temperature-size rule". No latitudinal or longitudinal trend is observed, a fact which is ascribed either to the global nature of the climatic upheavals, or to the paucity of sampled palaeolocations.

1. Introduction

The Early Triassic (252.2-247.2 Ma; Cohen et al. 2013) is a time of faunal recovery following the Permian-Triassic boundary mass extinction (PTBME) that took place ~ 252 Ma ago (Burgess et al. 2014). The PTBME was the most devastating extinction, reshaping marine communities more than any event since the Cambrian (Erwin 1994). It led to the loss of more than 90% of marine species (Raup 1979), and thus allowed the diversification of new marine ecosystems which still prevail in the modern oceans (Erwin 1994). A common view asserts that the biotic recovery following the extinction was slowed down until the beginning of the Middle Triassic, 5 Myr after the extinction (e.g. Hallam 1991; Retallack et al. 2011). Unfavourable climatic/oceanic conditions persisting until the Early-Middle Triassic boundary (Brayard et al. 2006, Retallack et al. 2011) have long been considered as the main putative causes of such delay.

However, recent studies focusing on benthic fauna from the Griesbachian of South China have challenged this paradigm by asserting a correlation between the benthos low diversification rates and post-extinction low levels of competition. According to these late findings, interspecific competition is a likely primary driver of diversification during the early stages of communities restoration, as it leads to niche differentiation. When interspecific competition is too weak, as it is expected in the aftermath of an extinction with such high magnitude as the PTBME, speciation is prevented and recovery is thus delayed (Hautman et al. 2015). As opposed to sessile primary consumers, competition among nektonic predators is considered to be more intense, and this could be one of the reasons behind the observed first diversification pulses that occurred less than 1.5 Myr after the extinction. These pulses concerned in fact mainly ammonoids (Brayard et al. 2006, Brayard et al. 2009c, Brühwiler et al. 2010a; see section 2.3) and conodonts (Orchard 2007), although they seem to have been observed also for trace fossils assemblages (ichnofauna) from Canada (Beatty et al. 2008), Eastern Greenland (Hautmann et al. 2011), the Alps (Hofmann et al. 2011) and for some benthic faunas such as foraminifera and calcareous algae (Song et al. 2011b)

While higher interspecific competition might be a valid explanation for the faster recovery of nektonic organisms, it might however be only one of the possible reasons. With regard to ammonoids, Brayard et al. (2009c) suggest, for example, a connection between their high taxonomical and morphological diversity and the possible exploitation of a wider range of trophic resources and niches colonization. This would agree with the recently advanced hypothesis (Scheyer et al. 2014; Brayard et al. 2017) of Early Triassic trophic webs that were not as annihilated as it would be expected, rather based on a substantial variety of primary producers (despite still being less complex than those of the Permian and of the Middle-Late Triassic; Brayard et al. 2009c).

The biotic recovery phases that took place throughout the Early Triassic were interrupted in the late Smithian, (ca. 2.5 Myr after the PTBME; Ovtcharova et al. 2006) by a major setback, when the end Smithian extinction generated severe perturbations in the carbon cycle and caused, among other faunal repercussions, the biggest recorded ammonoid turnover of the Early Triassic (Brayard and Bucher 2015). The extinction had a magnitude

comparable to that of the PTBME (Brayard and Bucher 2015) and it is associated with drastic climatic changes, that saw a shift from a middle Smithian hot, humid climate to late Smithian- early Spathian cooler and more arid environmental conditions (Brayard et al. 2006; Romano et al. 2013; Goudemand et al. 2019).

A common repercussion of mass extinctions is the smaller size of surviving species, often interpreted as a consequence of the selectivity acting against larger (and/or more specialized) species (see review of McKinney, 1997) or, more generally, as a consequence of the environmental biotic and abiotic disturbances associated to climatic changes, such as temperatures maxima, salinity fluctuations, oxygen depletion, acidification, or primary productivity disturbances (Twitchett 2007, Harries and Knorr 2009, He et al. 2010, Schaal et al. 2016). This has been already documented in various evolutionary lineages, mostly for the PTBME (e.g. Twitchett 2007, He et al. 2010, Metcalfe et al. 2011, Payne et al. 2011, Song et al. 2011a), although latest research has brought evidence of contrasting responses within marine lineages (e.g. Brayard et al. 2010, 2015, Schaal et al. 2016). Most studies have analysed size change from Permian throughout Middle Triassic times within larger time intervals (e.g. Schaal et al. 2016; Romano et al. 2016).

This study investigates the response of ammonoids to climatic disturbances at the finer time resolution of Smithian and Spathian stages, following recent studies that focused on the reaction of conodonts within the same time frame (Chen et al. 2013, Leu et al. 2018). While the latter have observed a significant size decrease of this nektonic clade at the SSB (but see Leu et al. 2018), other works have found evidence that would speak against a Lilliput effect extending up to Smithian-Spathian times in the aftermath of the PTBME (Brayard et al. 2010, 2015, Schaal et al. 2016). Expanding our knowledge on how biota responded to climatic upheavals in times of environmental crisis can help to better understand not only the dynamics of the climatic changes that occurred at the time, but also how the ecosystem reacts in times of environmental stress, which, in light of the current global warming, seems to be a most topical question. Latest research has shown, for example, that some extant marine ectothermal organisms already exhibit smaller sizes as a consequence of the current global warming (e.g. Daufresne et al. 2009)

Size plays a crucial role in the survival of species and, as such, it is of fundamental importance in order to unravel the ecological, biological but also environmental change that prevailed during the time of extinction (Twitchett, 2006). Body size is in fact controlled by many environmental parameters, such as temperature (which, in case of extant cephalopods, seems to be the main factor influencing body size; Rosa et al. 2012), oxygen availability (whose solubility in water is inversely proportional to the water temperature; Atkinson and Sibly, 1997), food availability (although this does not seem to be the decisive size limiting factor in case of extant cephalopods; Wood and O'Dor 2000, Rosa et al. 2012) or calcium carbonate saturation level (Gazeau et al. 2007, Fabry et al. 2008). The close relation between environmental parameters and body size explains why the examination of body size evolution can aid the understanding of the dominating palaeoenvironmental conditions. In addition, body size is a crucial morphological parameter that plays a key role in the evolutionary history, the ecology and the physiology of organisms (Schmidt-Nielsen 1984). One of the most important aspects is the influence of size over trophic relations of organisms. Body size is in fact related to many ecological aspects which, in turn, impact

the structure of food webs (Woodward et al. 2005, Warren 2005, Arim et al. 2010). To cite a few, it is related to a species productivity, its energetic demands, life history traits, longevity, spatial use of resources, biomass abundance or interactions with the other components of the food web, i.e. prey and predators (Woodward et al. 2005; see also Locatelli-Academic Internship Report 2017). With regard to ammonoids, body size has also been interpreted as an important determinant of swimming speed (Jakobs and Chamberlain, 1996), and thus affects (for ammonoids but also for most other marine species) predatory strategies as well as their escape abilities and vulnerability with respect to predators (Greene, 1986). As such, body size influences the position that species occupy in the trophic pyramid (Elton 1927, Sholto-Douglas et al. 1991, France et al. 1998, Warren 2005, Trebilco et al. 2013), and it is a more reliable parameter than species identity to identify and predict the trophic position of an organism within the marine realm (Jennings 2005). Most aquatic species are in fact usually characterised by ontogenetic changes in diets, due to ontogenetic morphological development, which induces them to rise up the trophic chain (Jennings 2005). As a consequence, as stated by Jennings (2002, p. 88): *“comparison among species are most usefully made at an identifiable and comparable stage in life history (e.g. size at maturity) or, if detailed life history data are lacking, at a fixed proportion of maximum body size”*. Maximal size measurements can thus be used as a proxy to infer changes of trophic level of a clade through time and, more generally, to evaluate the impact of unstable environments on the clade. This, in turn, allows a better understanding of the related palaeoenvironmental and climatic drivers.

Through the aid of published and unpublished material, based on the most recent zonation's available, and taking recent or new taxonomic synonymisations into account (in order to reduce taxonomic oversplitting to a minimum), this work aims at exploring the evolution of ammonoid body size throughout Smithian and Spathian times on a global scale. Statistically significant changes in body size will be discussed in the context of the climatic upheavals of the late Early Triassic, and an attempt to interpret the results in the light of the latest findings will be made.

2. Settings

2.1 Stratigraphy

Stage subdivisions of the Early Triassic are still controversial. Commonly two (Induan and Olenekian; Kiparisova and Popov 1956), three (Griesbachian, Nammalian, Spathian; Guex 1978) or four stages (Griesbachian, Dienerian, Smithian, Spathian; Tozer 1967, 1974, Brayard et al. 2006) are recognized. The Subcommittee on Triassic Stratigraphy officially decided on the original two-fold partitioning (Cohen et al. 2013); however, the debate on the definition of the Induan-Olenekian boundary is still ongoing. In fact, while the Induan stratotype is located in the Tethyan domain of Salt Range (Pakistan) and the Indian Himalayas, the Olenekian type locality is located in the Olenek Basin, in northern Siberia, i.e. in the Boreal realm (Kiparisova and Popov 1956; see also Brühwiler et al. 2010c). Because the magnitude of the ammonoid turnover at this boundary has been minor compared to that of other intra-Triassic events, a definite stratigraphic correlation between the two geographic domains is yet to be achieved (Brayard et al. 2006, Ovtcharova et al. 2006, Brosse et al. 2013; see Krystyn et al. 2007a,b and Brühwiler et al. 2010c for recent Induan-Olenekian GSSP – Global Stratotype Section and Point –

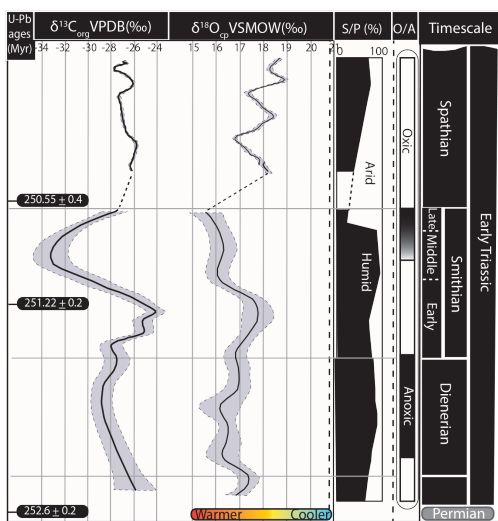


Figure 1: Simplified Early Triassic chronostratigraphy, with indications of the palaeoclimatic and palaeoenvironmental conditions and associated (organic) carbon and oxygen isotopes curves. Radiometric ages from Mundil et al. (2004); Ovtcharova et al. (2006) and Galfetti et al. (2007b). Modified after Romano et al. 2013.

candidate at Mud, Northern India). On the other hand, the boundaries of the fourfold subdivision established by Tozer (1967) are better defined both in terms of ammonoid and conodont events, which is why such subdivisions are more frequently used in most of the Lower Triassic research and hereafter (Ovtcharova et al. 2006, Brayard et al. 2006, Brosse et al. 2013; see fig. 1).

In terms of time span, calibration between zircon U-Pb radiometric ages and ammonoid zones has proven the four stages to be characterised by a very uneven duration: a maximal duration of 1.4 ± 0.4 Myr has been estimated for the Griesbachian-Dienerian stages, while the duration of the Smithian is estimated to 0.7 ± 0.6 Myr (Galfetti et al. 2007b). The Spathian stage amounts to at least half of the duration of the entire Early Triassic i.e. ca. 2.5 to 3 Myr (Ovtcharova et al. 2006).

2.2 Palaeogeography

The Early Triassic is characterised by the relatively simple and stable Pangean palaeogeography (Brayard et al. 2009b; fig. 2) whose main lines were already in place in the earliest Permian times, when Gondwana had completed its amalgamation with Laurentia, Siberia and Kazakhstan (Metcalf 1999).

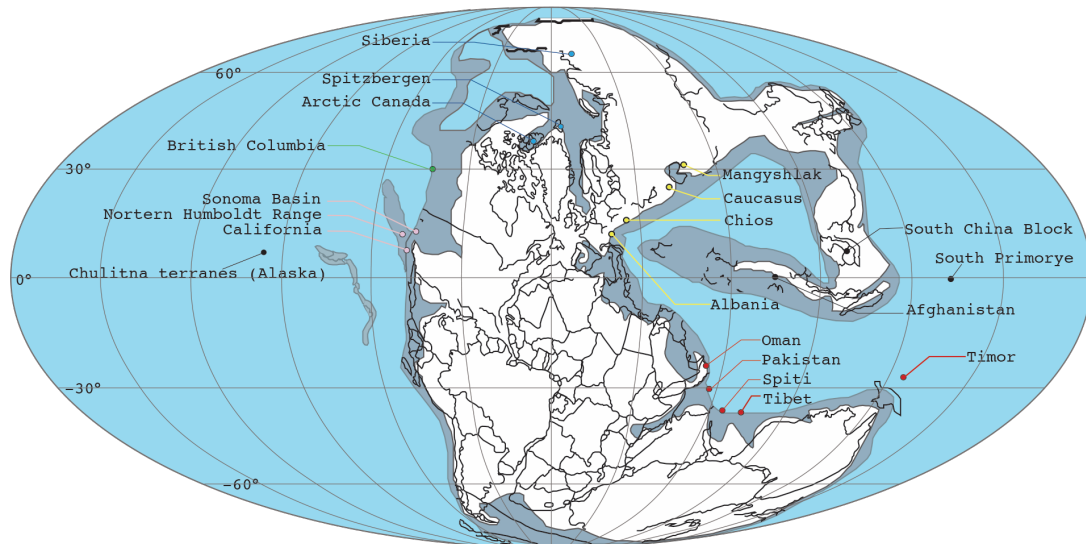


Figure 2: Simplified representation of the Early Triassic Pangea. Different coloured dots and lines refer to the different recognized palaeoregions: light blue = boreal domain; green = British Columbia; pink = Western U.S. Sonoma Basin; yellow = Palaeotethys; red = Neotethys; black = terranes. Modified after Scotese and Schettino 2017, Leu et al. 2018, Brosse et al. 2013.

In the Early Palaeozoic (Late Ordovician-Silurian) rifting of the northern Gondwana margin led to the opening of what was later defined as the PalaeoTethys ocean (Stampfli et al. 1991; Stampfli and Borel 2002). The Early Triassic was thus characterised by the large oceanic domain of Panthalassa (i.e. the Palaeopacific), which constituted roughly 90% of the end-Permian ocean, while the remaining 10% was occupied by the Tethyan ocean domain, centred on the Equator, encroached in the crescent shaped Pangea and connected to the East with Panthalassa (Scotese and Schettino 2017). Despite the simple Pangean palaeogeography, the Early Triassic was also characterised by several microcontinents and terranes drifting across the Tethys (Sengör 1984) and the Panthalassa, moving towards convergence zones (e.g. see Nichols and Silberling 1979, Tozer 1982, Kojima 1989, Natal'in 1993, Parfenov et al. 1993, Belasky et al. 2002, Yancey et al. 2005, Scotese and Schettino 2017).

During the Late Carboniferous - Early Permian and throughout the Triassic, after Pangea had been formed, the northern Gondwana margin was affected by several rifting phases (Stampfli et al. 1991), which led to the progressive opening of the Neotethys. This rifting event was associated with the formation of the Cimmerian microcontinents, an almost continuous belt of continental blocks which separated from the northern Gondwana margin and encompassed today's Iran, parts of Afghanistan and Tibet and western Indochina. Such blocks started drifting northward within the Tethys, due to the subduction of the Palaeotethys below the Eurasian margin (Sengör 1979, 1984, Stampfli et al. 1991, Metcalfe 1996, Besse et al. 1998, Stampfli and Borel 2002). The northward subduction caused the formation of various back-arc basins (Stampfli and Borel 2002) and their drifting led to the complete closure of the Palaeotethys ocean in Middle Triassic times and to their final accretion to the Siberia/Kazakhstan Asian area (Laurasia) by the end of the Triassic (Metcalfe 1999, Stampfli and Borel 2002, Xu et al. 2015).

Drifting on the eastern edge of the Tethyan domain was the Cathaysian microcontinent (Metcalfe 1996, 1999), encompassing the South China block, most of Indochina and East Malaya. Both lands had started their separation from the Gondwana margin during the Late Devonian and by the Early Carboniferous times they had completely

separated from Gondwana and had amalgamated, losing all floral and faunal affinities with Gondwana (Metcalf 1999). During the Early Triassic this microcontinent was located at an approximately equatorial position (Metcalf 1996, Sengör 1979, 1984, Xu et al. 2015).

Lastly, recent work of Brayard et al. (2009b) has revised the Smithian-Spathian palaeogeographic position of some drifting terranes, such as the Chulitna terranes (Alaska) and South Prymorie (Russia).

Based on the analysis of ammonoids assemblages, they confirmed Nichols and Silberling's (1979) sub-equatorial position of the Chulitna terranes, on the western side of the Pangea, and identified an equatorial position for South Prymorie at the Tethys/Panthalassa interface. Both terranes were probably in a position relatively close to the South China block (Brayard et al. 2009b).

2.3 Ammonoid recovery

Ammonoids were among the organisms most affected by the end-Permian extinction. Yet research has shown that ammonoid recovery was much faster than that of many other benthic groups, despite repeated harsh environmental and climatic conditions (Brayard et al. 2006; Brayard et al. 2009c; Brühwiler et al. 2010a). Only 3 ceratitid lineages survived the extinction (Brayard et al. 2007b): the genus *Otoceras* is considered the last descendant of the Permian Araxoceratidae family, whose life span expanded through the Griesbachian stage only (Brayard et al. 2007b); the genus *Proharpoceras* has been confirmed to be derived from the Late Permian Anderssonoceratidae (Brayard et al. 2007a); finally, the Xenodiscidae are widely accepted as ancestor of most ammonoids of the Triassic order Ceratitida (Tozer 1981; see also Brayard et al. 2006 and 2007b). Recent works would suggest that ammonoids were the first marine invertebrates to fully recover by the middle Spathian (Brayard et al. 2006) and within 2 Myr after the PTB, ammonoid diversity had already reached diversity levels comparable (if not higher) to those of the Permian (Brayard et al. 2009c). More than 200 genera were generated in less than 5 Myr (Brayard et al. 2009c), characterised by new distributions and diversity patterns (Brayard et al. 2006). A clear latitudinal diversity gradient, contrasting a previous cosmopolitan pattern, starts emerging during Smithian times, characterized by an unimodal shape that shows an increase of diversity from high to low latitudes. This pattern was interpreted as a consequence of a steepening of the Sea Surface Temperature (SST) gradient. The gradient steepens during the Spathian stage, when it develops an asymmetric bimodal character in proximity of the equator and a relative higher boreal generic richness (Brayard et al. 2006). A longitudinal gradient, likely associated to a weak ocean circulation, is also observed between the Tethyan and the Panthalassa realms during the Smithian (with diversity decreasing westward, through the Tethys). This disappears during Spathian times, when ocean circulation intensifies, thus indicating a progressive homogenisation of the primary controlling factors of spatial distribution within the two realms (Brayard et al. 2006).

Generally speaking, five main stages are usually recognized during the ammonoid biotic recovery: I) A low-diversity, cosmopolitan phase during the Griesbachian. II) A global increase in taxonomical diversity from Dienerian throughout Smithian times. Boreal ammonoids, compared to Tethyan specimens, seem however to have reached the highest diversification level during the Spathian and were in general characterized by a lower

diversification degree (Brayard et al. 2006). Such increase was characterized by an increasing latitudinal gradient of both generic richness and endemism. It would seem that high turnover rates, i.e. intense restructuring of communities rather than accumulation of new taxa with high origination rates have characterized the recovery during Smithian times (Brühwiler et al. 2010a). III) A massive extinction at the end of the Smithian (see next section 2.4), which caused the largest ammonoid turnover of the Early Triassic at the Smithian-Spathian boundary. IV) A recovery of endemism and diversity during the Spathian. V) Another significant, though less devastating, global decrease of generic diversity at the Spathian-Anisian boundary (Brayard et al. 2006, 2007b, 2009b,c; Brosse et al. 2013). This gradual recovery is also characterised by the evolution of the ammonoid morphological disparity, which shifts from three extreme morphospaces observed during the Griesbachian stage, to a prevalence of involute ammonoids during Dienerian times, a very broad morphological landscape during early-middle Smithian times, and a loss of disparity in the late Smithian which is eventually replaced by a morphospace comparable to that of early-middle Smithian in the Spathian (Brosse et al. 2013). Attempts have been made to assign different morphotypes to different trophic habits (e.g. see Westermann 1996). As such, morphotypes disparity could be an indication of a change in predatory strategies and feeding habits. However, such interpretations linking shell shape to feeding habits remain highly speculative.

More than one explanation could be advanced in order to explain the quicker (compared to other biota) recovery of ammonoids; Brayard et al. (2009c) suggested that the high taxonomical and morphological diversity characteristic of ammonoids might have favoured the exploitation of a wider range of trophic resources as well as the colonization of various niches. Schaal et al. (2016) proposed that the nektonic mode of life of ammonoids might have aided them to escape local unfavourable environmental conditions. Recently, Hautman et al. (2015) suggested that the higher interspecific competition that characterizes nektonic organisms might be the primary driver for their faster recovery (see section 1), a model which is consistent with the two main nektonic clades, i.e. ammonoids and conodonts.

[2.4 Smithian-Spathian palaeoclimate and the end Smithian extinction – a brief overview](#)

The Early Triassic biotic recovery was interrupted by a severe extinction at the end of the Smithian, followed by a massive radiation in the early Spathian (Galfetti et al. 2007c, Brayard and Bucher, 2015). The extinction had a magnitude comparable to that of the PTB extinction, and severely decimated nekto-pelagic organisms such as conodonts (Orchard, 2007) and ammonoids (Brayard et al. 2006, 2009c). However, benthic communities do not seem to have been impacted as much (Song et al. 2011b; Hofmann et al. 2014). Only four ammonoid lineages, encompassing a limited number of species, survived: xenoceltitids (which are considered the potential ancestor of most of the Spathian taxa; Galfetti et al. 2007a), sagerceratids, palaeophyllitids and proptychitids (Brayard and Bucher, 2015).

Smithian and Spathian times were characterized by pronounced carbon and oxygen isotopic excursions (see fig. 1), as well as by alterations of the net water balance between evaporation and precipitation, all of which is suggestive of massive climate changes (Payne et al. 2004; Galfetti et al. 2007a,c; Romano et al. 2013,2016; see

section 5.2 for details). Research has shown the Smithian-Spathian boundary (SSB) is distinguished by a global positive C-isotopic excursion associated with a cooling event (Romano et al. 2013) that started during the early late Smithian (Goudemand et al. 2019) and peaked at the SSB (Galfetti et al. 2007c), accompanied by a matching positive oxygen isotope peak measured in biogenic phosphate (Romano et al. 2013, fig. 1). While the middle Smithian was a time characterized by a temperature maximum (Goudemand et al. 2019) and humid conditions, the late Smithian-early Spathian (i.e. the SSB) saw a shift to dryer and cooler conditions associated to a more homogeneous Spathian climate (Hochuli et al. 2016, Hermann et al. 2011, Hochuli and Vigran 2010, Romano et al. 2013, Goudemand et al. 2019). The most prominent characteristic of the SSB is (as previously mentioned) the drastic turnover in ammonoid and conodont faunas, which both saw a collapse in diversity and a resurgence of cosmopolitanism, both of which have been interpreted to reflect a flat SST gradient (Galfetti et al. 2007c; but see section 5.8). At the onset of Spathian times ammonoid diversity started rising again (Brayard et al. 2006) while different latitudinal climatic conditions developed, more oxic conditions prevailed (compared to previous suboxic ones) and clastic sediment input diminishes (Galfetti et al. 2007a).

The most common view is that temperature change during late Smithian, in combination with ocean acidification and increased levels of pCO₂ in the atmosphere (which led to reduced pH and thus to reduced carbonate ion concentration and calcium carbonate oversaturation in sea water; Galfetti et al. 2007a) might have been the causes of ammonoid extinction (Galfetti et al. 2007c); however, the interactions of climate change with the other environmental factors are still under debate (H. Bucher ongoing work; see section 5.2).

2.5 Palaeoecology of the Smithian-Spathian time; an ammonoids' perspective

Very little is known of ammonoid feeding habits. The buccal mass of ammonoids consists of a jaw (to cut food) and a radula (to transport food to the stomach), and it is therefore comparable with that of modern Cephalopoda such as *Nautilus*, *Octopoda* and *Decapoda* (Lehman and Weitschat 1973; Kennedy and Cobban 1976, Kruta et al. 2011).

Knowledge on stomach and crop contents is limited to a very few specimens, mostly from Middle and Late Triassic (e.g. Lehman and Weitschat 1973; Lehman 1975). It indicates that ammonoids were nektonic carnivores (see also reviews of Lukeneder 2015 and Westermann 1996) and also suggests feeding habits similar to Octopoda. However, as opposed to them, the absence of a sharp cutting edge on the jaw of ammonoids would speak against strong biting abilities of larger and more active prey, and their more limited mobility would deny a pursuit capability of very agile preys (Lehman and Weitschat 1973). Recent work (Kruta et al. 2011) has brought to light new excellently preserved specimens of the Late Cretaceous heteromorph genus *Baculites*, from South Dakota, whose radulae contain remnants of planktic preys (isopods and a benthic gastropod larva), thus giving a clear indication of feeding strategies directed more towards planktic, rather than benthic organisms during Jurassic-Cretaceous times. From the Early Triassic, gastric content from only one specimen of the Spathian *Svalbardiceras* was recovered, containing remnants of ostracods and foraminifera and thus confirming the pelagic nektonic carnivore nature of Early Triassic plan spiral ammonoids (Westermann 1996). Generally speaking, ammonoids are commonly considered to occupy a mid-order omnivore trophic level with feeding

strategies ranging from planktotrophic to microphagous (Lukeneder 2015). Their main prey seems to have been mainly zooplankton, which included, aside from smaller ammonoids, planktic crustaceans and pseudoplanktic ostracods and microgastropods (Westerman 1996). Ammonoids belonged to the pelagic food chain, and occupied various trophic levels; in fact, while smaller taxa as well as neanic and juvenile stages of larger taxa probably fed on mikroplankton, they were also cannibalised by the mid-sized ammonoids, which, in turn, were preyed upon by the largest of their kind and vertebrates (Westermann 1996). Ammonoids' main predators may have comprised larger oxyconic ammonoid species, but also fish, reptiles and teuthoids (see e.g. Frenzen 1936, Kauffman and Kesling 1960, Martill 1990, Ward and Hollingworth 1990, Kauffman 1990, 2004, Tsujita and Westermann 2001, Gale et al. 2017).

A recent study by Scheyer et al. (2014) investigates the global spatial and size distribution of the most common marine predators (fishes, amphibians and reptiles) of the Early Triassic (and Anisian) in order to understand the height of trophic pyramids following the end-Permian mass extinction.

They summarized evidence for the presence, on a global scale, of a wide range of predators diffused throughout the entire Early Triassic. For Smithian and Spathian times, they gathered data on Trematosauroida (temnospondyl amphibians, top piscivorous predators preying preferentially nearshore marine habitats fauna; Hammer 1987) in the Early Smithian Ceratite Marls of Salt Range (Pakistan), in the middle-late Smithian Fish Niveau of Spitzbergen, in the Spathian stage of the Moenkopi Formation of Arizona and in the Smithian and Spathian of Western Australia. Also they brought evidence of Spathian Sauropterygia from Germany, China and North America (large top carnivores and piscivorous ambush predators; Storrs 1991). Their review also includes documentation of the piscivorous Thalattosauria reported by Bardet (1995) in the Spathian sections of British Columbia, and of many Ichthyopterygia from the Spathian of Svalbard, Japan, North America and China.

Ichthyopterygia seem to have achieved during Spathian times a high diversification level as well as a global distribution. Within the clade, some species show the crushing dentition typical of durophagous organisms; for example, dental analysis seems to suggest that hard shelled organisms such as ammonoids and bivalves might have been a main component of Omphalosauria's diet, a taxon found both in the low latitudes of Nevada and in the higher ones of Spitzbergen (Sander and Faber, 2003). The dentition of the Ichthyopterygia *Grippia longirostris* also seems to indicate an affinity of this late Spathian species with the crunching guild (Motani 1997), which Massare (1987) identifies as a guild whose feeding habits possibly encompassed thin shelled ammonoid predators. Furthermore, many similarities have been found between this boreal species (recovered in Spitzbergen), and the lower latitudes' Ichthyopterygia *Utatsusaurus hataii*, from Japan; the latter, as in case of Omphalosauria (Buffrenil et al. 1987), also show the specialization needed for manoeuvrable swimming and cruising in a pelagic marine environment (Nakajima et al. 2014), a characteristic which, together with the observed dentition, could make of *U. hataii* a probable ammonoid predator. Nakajima and Izumi (2014) recently found various coprolites in the Spathian of the Osawa Formation (Japan). They suggest that the size variation observed in these coprolites is an indication of the presence of a hierarchy of marine carnivores and the larger ones were probably excreted by large fishes or marine reptiles akin to the basal Ichthyosaur *U. hataii*. While such faecal remains do not allow the distinction of specific ammonoid predators, they are a clear evidence of the existence of a more complex trophic structure than what can be derived from the regional fossil records

(Nakajima and Izumi 2014). Scheyer et al. (2014) also report the presence of Chondrichthyes species either with tearing teeth or with durophagous habits and of marine bony fishes (Osteichthyes) species with either fast-swimming large predator characteristics or small to large ambush predator features; both lineages may thus potentially have included ammonoids in their diet (see table 1 p. 14 of Scheyer et al. 2014).

Further marine fish and reptile assemblages from the Chaohu locality (South China) dating back specifically to Smithian-Spathian times are also reported by Benton et al. (2013), while, more recently, Brayard et al. (2017) brought to light a complex, phylogenetically diverse marine ecosystem from the early Spathian of Idaho (North America), incorporating a trophically complete ecosystem, from lower level primary producers to top predators (such as Ichthyosauria or Chondrichthyans). It is an ecosystem composed both of long ranging Palaeozoic taxa and younger taxa originated in a closer pre-Spathian time; it also includes taxa previously unknown from this time interval or taxa presenting anatomic characteristics that had been assumed to have only developed later (such as crinoids, whose advanced morphological characters give proof of an intense diversification that started during or even before the early Spathian).

This fossil record thus proves that in the aftermath of the Permian-Triassic extinction and throughout the Early Triassic the global marine ecosystem did not consist of primary producers only, rather included enough trophic levels that could allow the proliferation of large aquatic predators placed high up in the trophic pyramid that needed enough abundance of lower-levels preys for their survival (Scheyer et al. 2014).

3. Material and Methods

3.1 Dataset

The database includes both published and, in smaller amount, unpublished material (the latter stored in the Paleontological Institute and Museum of Zurich). Taken into account were mostly relatively recently published monographs, journals and research papers grounded in a detailed stratigraphy. Older monographs whose taxonomy has been partly synonymised in the more recent works were also considered. For the latter, in case of a lack of synonymisation, illustrated specimens that featured a good preservation were revised specifically for the purpose of this research by courtesy of H. Bucher and T. Brühwiler (of the University of Zurich, personal communication) at the species level or at the genus level with a species assignment kept in open nomenclature. The locations from which measurements were collected and the relative references used are given in table 1. From each considered location, the biggest specimen for each occurring species was recorded.

The database features 1211 observations, of which 783 belong to the Smithian and 428 to the Spathian stage. As much information as possible was included in the dataset, such as the location and the respective palaeoposition, the zone, the formation's name and the palaeoenvironmental characteristics in which the specimens were found. The reference from which each measured specimen was obtained, the page of its taxonomical description as well as the plate featuring the illustration, the original taxonomical identification (in case of a synonymised specimen) and the reference of the work responsible for the synonymisation are also given.

The analyses were performed at the species level; in the cases where a taxonomical identification was only possible at the genus or at the family level, the species resp. the genus was left in open nomenclature. Families identifications have been given, where possible, for each specimen, according to the latest revisions of the taxonomical framework at the family level. Families' assignments derived from older works, for which no new published synonymisation was available, were kept, despite being outdated.

Palaeopositions were either taken from the published literature or, when not available, inferred from the newest Early Triassic map found, provided by Scotese and Schettino (2017). Because the measurements extrapolated from the map could only be approximated and measurements taken from the literature, based mostly on the palaeomap of Brayard et al. (2009b), did not match with absolute accuracy the newest map (on which the Pangea seems slightly more clockwise rotated), the two maps were compared and an uncertainty of $\pm 5^\circ$ can be asserted for the recorded palaeolatitudes and palaeolongitudes.

Despite the zone in which the specimens were found is given for each sample, a global correlation at the zone level for both Smithian and Spathian has not yet been properly developed (Brayard et al. 2006, H. Bucher, personal communication). Hence, the size analyses were implemented at the stage level (Smithian and Spathian) and at the level of the "substages" recognised by the most recent literature (e.g. Brühwiler et al. 2012b,c, Jattiot et al. 2017) i.e. early, middle, late. In the dataset, additional subdivisions were introduced (early/middle, middle/late, early-to-late) whenever the lack of a detailed biostratigraphy made it impossible to assign longer

ranging ammonoids species to any of the smaller time subdivisions.

As previously mentioned, the data recorded in the dataset consist of the maximal diameter of the largest specimen found for each species in each land. As an additional information, where the last septum was visible, measurements of the phragmocone diameter were also given. Furthermore, distinctions were made between specimens that could be undisputedly recognised as phragmocones, as adult forms, or juveniles. (*Note*: to distinguish adult forms, main features such as the preservation of the aperture, the approximation of septa towards the end of the phragmocone, a change in ornamentation and/or in geometry of the adult body chamber, and a clearly egressive umbilicus were considered). In specific cases, an estimation of the maximal size that the species could have reached was either given by the author or could be estimated from the illustrations in the plates or from the available material. In such occasions, the measurable diameter was averaged with the estimated reachable size, and the mean value was used to perform the analyses.

Table 1: Localities and relative references from which dataset specimens were measured. References marked with a star indicate manuscripts that are not referenced in the dataset, which were however checked for synonyms and/or for the presence of bigger specimens.

Data Location	References
Afghanistan	Collignon 1973; Kummel 1968a; Kummel and Erben 1968
Albania	Arthaber, 1911
Canada BC Arctic Canada	Tozer 1961, 1962, 1963*, 1965, 1967, 1984*, 1994
Chulitna Terranes (Alaska)	Nichols and Silberling 1979
Chios Island (Greece)	Renz and Renz 1948
Mangyshlak	Shevyrev 1968;
N.W. Caucasus	Shevyrev 1995;
Oman	Brühwiler et al. 2012a
Siberia	Dagys and Ermakova 1988, 1990
Timor	Jattiot 2017 (PhD dissertation), Jattiot et al. 2015, Kummel 1968b, Nakazawa and Bando 1968, Wanner 1911, Welter 1922
Salt Range (Pakistan)	Brühwiler et al. 2011, 2012 c, De Koninck 1863a*,b*, Mojsisovics 1895, Noetling 1905, Guex 1978, Kummel 1966, Pakistani-Japanese Research Group 1985*, Spath 1934, Waagen 1895
South China Block	Brayard and Bucher 2008, Chao 1950*, 1959; Ji et al. 2015, Monnet et al. 2013, Shigeta et al. 2014, Tong and Zakharov 2004, Tong et al. 2004
South Primorye	Shigeta and Kumagae 2016, Shigeta et al. 2009
Spiti	Brühwiler et al. 2010c, 2012b, Diener 1897, Krafft and Diener 1909, Krystyn et al. 2007a,b
Spitzbergen	Frebold 1930, Kummel 1961*, Mørk et al. 1999, Weitschat 2008, Weitschat and Lehmann 1978, Spath 1934, Piazza 2015, Piazza et al. 2017
Tulong (Tibet)	Brühwiler et al. 2010b
Western U.S. Basin (Sonoma Basin ¹ ; Star Peak Group ² ; California)	Brayard et al. 2009a, Brayard et al. 2013, Guex et al. 2010, Jattiot et al. 2017, Jenks 2007, Jenks et al. 2010, Jenks et al. 2013, Jenks and Brayard 2018, Kummel and Steele 1962, Monnet et al. 2013, Silberling and Wallace 1969, Smith 1932, Stephen et al. 2010

3.2 Spatial subdivisions

Each region was treated separately for the detection of a size trend through time (see figure 2).

First, the whole of the Pangea was considered, to get an idea of the size spread at a global level in each considered time bin, and to examine the contingency of a size trend through time at a global level. Then, boreal palaeolatitudes were separated from lower latitudes in order to detect the main differences between the two latitudinal belts; the low latitudinal belt ranges from 35°S to 35°N. A common choice to define the *low palaeolatitudinal* zone usually corresponds to 30°S-30°N (see e.g. Romano et al. 2016). However, because of the acknowledged uncertainty of $\pm 5^\circ$ previously mentioned (section 3.1), 35° seemed like a more reasonable choice. The Boreal palaeoregion includes occurrences from Arctic Canada, Siberia and Spitzbergen, whereas the low palaeolatitudes comprise all the other locations (see table 1), including, among the rest, the British Columbia, the Afghanistan block and the terranes of south-central Alaska (Chulitna terranes) and South Primorye. According to their palaeogeographic position these locations should actually be considered each on its own. However, not enough specimens from these sites could be measured to allow their statistical analyses at the fine timescale of early, middle, late Smithian and Spathian, hence their inclusion in such an extensive region as the low palaeolatitudes.

Additional smaller palaeoregions were recognized within the lower latitudes. The Tethys area was first subdivided into Palaeotethys (including Albania, Chios, Mangyshlak and Caucasus) and Neotethys (comprising Oman, Pakistan, Spiti, Timor, South Tibet and Afghanistan).

During the Early Triassic the South China block (which includes also today's North-Eastern Vietnam), was a continental block fluctuating between Palaeo- and Neotethys (see section 2.2) and, as such, it was considered on its own. A similar palaeogeographic position was true for Afghanistan, which was part of the Cimmerian blocks that started to separate from Gondwana land in the Permian throughout the Triassic time (Sengör 1987, Scotese and McKerrow 1990). To obviate the aforementioned insufficiency of measured samples, Afghanistan, was also included as part of the Neotethys palaeoregion. However, for the sake of precision, and to make sure that no contingent change that might have happened to the Afghanistan fauna during the drifting of the block would affect the analysis on the whole of the Neotethyan locations, statistical analyses on the Neotethys palaeoregion were also performed after removal of the Afghanistan block from the area. Statistical tests could also be implemented on the Afghanistan block alone but only at the stage level (i.e. at Smithian and Spathian level). Each stage included in fact the sufficient amount of specimens to allow the identification of size changes between the two (results may however be biased by the poor amount of measurements available and care must therefore be taken when interpreting them).

Two additional subdivisions were further recognized within the Neotethys: the Northern Indian Margin (Spiti, Pakistan - Salt Range - and South Tibet), and the offshore seamount occurrences of Oman and Timor. Lastly, the palaeoregion of the Western America Basin was considered, composed of the localities of the Western America Sonoma Basin (including North-East Nevada, South East Idaho and Utah), California and the Star Peak Group (North-West Nevada, Silberling and Wallace 1969, Silberling and Nichols 1982).

As previously mentioned, to build the dataset, all species that have been recorded within each considered location have been taken into account. Therefore, when grouping such locations into the above mentioned palaeoregions and implementing the analyses at the palaeoregions scale, the same species is likely to be present more than once within the region. It would however be ill-advised, to simply pick the biggest size over the all the smaller ones, as it might be the case that a locality is characterised by smaller ammonoid sizes compared to another locality of the same palaeoregion, and it would be mostly incorrect to dismiss such information. The best possible way to solve this issue was through the aid of a sorting function compiled in R: after distinguishing the different time subsets of early, middle and late Smithian and Spathian within a certain palaeoregion, for each subset the distributions of the different localities included have been compared with one another, with the aid of the Kolmogorov-Smirnov test (see later for the detailed description of the test). If, according to the test, the ammonoids from each locality are proven to be taken from populations with equal distributions, then the biggest specimen for each of the species in question was chosen. If, however, the test recognized the two compared distributions as unequal, or in case too few specimens were available in one of the distributions for the test to be implemented, then both measurements were kept. This thus ensures consistency throughout the analyses and limits to a minimum the multiple occurrences of the same species within each palaeoregion.

3.3 Analysis of maximal size through time

3.3.1 Mann-Whitney-U test

In order to uncover a possible trend in size change throughout the analysed time span, this first statistical test aims to compare the medians of each pair of time-wise sequential subgroups.

It is a non-parametric statistical test, which thus, by definition, does not assume any specific distribution in the sample population (Hammer and Harper 2006). The choice of the implementation of a non-parametric test, as opposed to a more robust parametric one, is driven by the proven absence of normality in most part of the distributions of the analysed subgroups (see section 4.1).

The test compares two independent samples based on the null hypothesis that *“the data are drawn from populations with the same median values”* (Hammer and Harper 2006, p. 27). A p-value smaller than 0.05 gives evidence of a statistically significant difference between the medians.

3.3.2 Kolmogorov-Smirnov test

This is again a non-parametric test, which does not make any assumptions concerning the distribution of the data. *“It compares the complete shapes and positions of two distributions”* that contain a minimum of 8 data points and it is based on the null hypothesis that *“the two samples are taken from populations with equal distributions”*. (Hammer and Harper 2006, p. 30). In this case as well, a p-value smaller than 0.05 indicates a significant difference in distributions.

3.4 Size patterns across space

In order to investigate the possible presence of a latitudinal/longitudinal size trend the median size of the samples measured at a specific palaeolatitude or palaeolongitude or at both coordinates at the same time is calculated, both separately for Smithian and Spathian and for the two stages taken together. A multiple linear regression is performed when the median size is investigated as a function of both palaeolatitude and palaeolongitude, while simple linear regressions are implemented for the size regarded as a function of either one of the palaeocoordinates. For the detailed description of the output elements (and the relative interpretation) of the regressions, the reader is referred to the Appendix-Part 2.

4. Results

4.1 Size trends across time

The size of the maximal diameter shows some statistically significant fluctuations within the considered time span.

For an overview of the number of samples available for the analyses in each considered palaeogeographic area and time stage, and of their relative size range and medians, the reader is referred to table 2.

For a better visual grasp, only data subsets including at least 10 specimens were represented as histograms (so that all histograms could be based on the same binwidth), while only those composed of at least 8 specimens have been depicted in boxplots (according to the minimum number required for necessary statistic tests).

Further tables reporting the detailed outcomes (p-values) of the Mann-Whitney-U and the Kolmogorov-Smirnov tests can be found in the Appendix (Part 1, pages I-IV).

In a few specific cases, which will be described in detail in this paragraph and/or in the *Discussion* chapter (5), the absence of a significant difference in median or in distribution of the statistical populations of two considered time stages, is likely to be due to an insufficient amount of data. Hence, the statistical results obtained from such small samples, will not be considered of primary importance for the shaping of the overall size trend observable during Smithian and Spathian.

As previously mentioned (see section 3.1), the subdivisions of early/middle, middle/late and early-to-late Smithian and Spathian have been included in the dataset for the sake of precision, in case of a lack of a high resolution assignment to any of the subdivisions presented by recent works (early, middle, late). Therefore, such samples were only taken into account when considering the Smithian and Spathian substages as a whole, but were not regarded as distinctive statistical populations that could yield reasonable results.

With this in mind, the maximal ammonoid size within each palaeogeographic region can now be analysed.

Table 2: Number of specimens (identified by “# ”), size range, interquartile range (IQR) and median size for each palaeoregion in each time bin. Dashes indicate absence of data. The first line represents all specimens that were measured in each palaeoregion for both Smithian and Spathian. The number of specimens given for the different time bins represents only the specimens that were used for the analysis, once species originally present multiple times (according to the different localities included in a palaeoregion) were removed. See section 3.2 for detailed explanations.

	Global	Low Paleolat.	Boreal Paleolat.	Neotethys	Neotethys seamounts	NIM	Palaeo-tethys	South China	Western USA
Total # of specimens available	# 1211	# 1089	# 122	# 444	# 157	# 250	# 121	# 224	# 225
SMITHIAN	# 578	# 536	# 52	# 315	# 126	# 203	# 11	# 130	# 98
Size range (mm):	11.6-400	11.6-361.5	18.5-400	12.5-350	12.5-275	12.5-350	21-122	12-200	11.6-361.5
IQR (mm):	42-98	41.4-95	42.7-177.50	43.7-95	42.1-86.9	45.0-98.0	28.0-54.9	29.7-87.7	44.1-105.2
Median (mm):	63.5	62.9	65.5	63.7	60.4	66	34.3	58.5	65.92
SPATHIAN	# 412	# 354	# 60	# 31	# 11	# 13	# 107	# 94	# 113
Size range (mm):	13-300	13-270	15-300	20-178	24-58	20-178	15.3-178	18.5-270	13-160
IQR (mm):	32.0-66.8	31.6-67.5	36.9-69.1	31.5-47.9	36.0-44.9	31.0-57.5	31.6-60.5	34-81.5	31.0-65.0
Median (mm):	46	45	49.5	38.5	39	37	46	50	43
EARLY SMITHIAN	# 225	# 224	# 1	# 138	# 35	# 105	-	# 56	# 9
Size range (mm):	12.3-350	12.3-350	-	23.3-350	25-275	23.3-350	-	12.5-180	32.5-142.5
IQR (mm):	45.0-100.0	44.7-99.2	-	56.7-104.7	55.5-95.7	58-124.3	-	29.5-82.0	52.0-106.0
Median (mm):	67	67	-	78.7	73	80.8	-	56.5	70
MIDDLE SMITHIAN	# 264	# 233	# 32	# 137	# 81	# 72	# 11	# 58	# 56
Size range (mm):	11.6-400	11.6-361.5	18.5-400	12.5-265	12.5-229	12.5-265	21-122	18-200	11.6-361.5
IQR (mm):	34.9-99	34.7-96	42.5-183.1	32-86.6	34.5-86.6	31.7-76.4	28.0-54.9	38.9-97.5	34.5-97.2
Median (mm):	57.5	55.8	78.25	53.1	52.7	50.2	34.3	59.7	60.65
LATE SMITHIAN	# 91	# 74	# 23	# 42	# 15	# 24	-	# 14	# 16
Size range (mm):	19.4-263.5	19.4-165	26-263.5	22-90	23.1-90.0	32-85	-	20-108.15	19.4-165
IQR (mm):	42.7-75.0	48.5-77.1	37.7-64.5	42.3-66.7	51.7-68.5	40-66.2	-	47.0-87.0	60.6-115
Median (mm):	60	61	50	53.5	61.9	51.9	-	83	80.65
EARLY SPATHIAN	# 117	# 109	# 8	# 7	# 1	# 5	# 20	# 36	# 44
Size range (mm):	13-130.7	13-130.7	34-100	-	-	-	23.7-130.7	22-115	13-107
IQR (mm):	33.3-72.2	33.2-72.0	41.7-86.9	-	-	-	33.1-64.2	35-71.2	33.7-72.6
Median (mm):	50	49	59.7	-	-	-	42.05	55.5	50.5
MIDDLE SPATHIAN	# 176	# 155	# 21	# 19	# 7	# 7	# 55	# 40	# 44
Size range (mm):	14-270	14-270	26-135	20-132.6	-	-	15.3-165	18.5-270	14-160
IQR (mm):	29.5-56.2	29.0-54.5	41-59	33-46	-	-	29.7-55.5	31.1-68.4	24-52.2
Median (mm):	40.5	38.5	52	38	-	-	40	44	33.5
LATE SPATHIAN	# 90	# 63	# 28	# 4	# 2	# 1	# 8	# 14	# 25
Size range (mm):	14 - 300	14-213	15-300	-	-	-	24-88	22-136	14-110
IQR (mm):	33-79	33.5-82.0	32.7-61.0	-	-	-	36.5-77.5	47.1-118.7	33.0-64.0
Median (mm):	47.8	50	46	-	-	-	47.5	83.5	45

Table 3: Time intervals which were found to be statistically significantly different according to the Mann-Whitney-U and the Kolmogorov-Smirnov tests. Ticks represent significant difference (below the trend of the median in that time range is given), crosses indicate the absence of a significant change. Dashes point to a lack of data that did not allow the comparison of the time intervals. Question marks indicate that the two tests gave opposite results or ambivalent ones (p -value ≈ 0.05)

Statistical Significance	Global	Low Palaeolatitudes	Boreal Palaeolatitudes	Neotethys	Neotethys seamounts	NIM	Palaeotethys	South China	Western USA
Smithian - Spathian	✓ median-decrease	✓ median-decrease	✓ median-decrease	✓ median-decrease	✓ median-decrease	✓ median-decrease	✗	✗	✓ median-decrease
Early - Middle Smithian	✓ median-decrease	✓ median-decrease	-	✓ median-decrease	✓ median-decrease	✓ median-decrease	-	✗	✗
Middle - Late Smithian	✗	?	✗	?/✗	✗	✗	-	✗/✗	✗
Late Smithian - Early Spathian	✓ median-decrease	✓ median-decrease	✗	-	-	-	-	✗	✓ median-decrease
Early - Middle Spathian	✓ median-decrease	✓ median-decrease	✗	-	-	-	✗	✗	✓ median-decrease
Middle - Late Spathian	✓ median-increase	✓ median-increase	✗	-	-	-	✗	?	?

On a global scale (figs.3-5), histograms (fig. 3) and boxplots (fig. 4) help to give a general and clear view of the spread of size ranges. The Smithian-Spathian boxplot (fig. 4B) reveals that the Smithian stage is characterised by a bigger spread than the Spathian. Subdividing the two stages in smaller time bins, it can be noticed that the widest spread is to be found in the early and middle Smithian as well as in the late Spathian. The middle Spathian, on the other hand, shows the smallest spread (see table 2 for the precise size measurements included within the lower and upper quartile - interquartile range, IQR- of the boxes). Down to the smallest time partitioning, all the obtained histograms (fig. 3) show positively skewed distributions (mean larger than the median), which indicates a prevalence of samples smaller than the median within the considered population. Late Smithian and early Spathian appear to have the closest to symmetrical distribution, with very close mean and median values and with the least number of samples recognized as outliers within boxplots. However, a Shapiro-Wilk's test reveals that none of the considered statistical population is characterised by a normal distribution. This is not all too surprising considering that the test is most sensitive to outliers (Leu et al. 2018), and both the skewness of the histograms and boxplots themselves indicate that, in all cases, samples categorised as outliers are quite numerous.

The Mann-Whitney-U and the Kolmogorov-Smirnov tests reveal a significant difference between the distributions and the medians of Smithian and Spathian populations, indicated by the very small p values of both (Mann-Whitney-U: $7.462e-13$; Kolmogorov-Smirnov: $2.101e-12$; see table 3 and table 1A in the Appendix – Part 1). This thus points to a statistically significant size reduction from the Smithian to the Spathian (medians: rel. 63.5 and 46 mm, table 2; (see fig. 4B). On smaller timescales, a statistically significant size reduction (see table 3) occurred between the early and middle Smithian, the late Smithian and the early Spathian, the early and middle Spathian (fig. 5). Statistically significant size increase occurred between the middle and late Spathian (fig. 5) (see figs. 4 and 5 for a clear view over the medians size change and table 1A in the Appendix-part 1 for the

precise p-values).

With a first subdivision into two palaeolatitudinal belts, high (i.e. boreal, figs. 6-8)) palaeolatitudes (in our case, above 35° N up to 90° N) can subsequently be compared to lower ones (included between 35° S and 35° N, figs. 9-11). For specifications on the choice of palaeolatitudinal zones and palaeogeographic regions see section 3.2). 89.9% of the available measured specimens belong to the low palaeolatitudinal range. This induces some obvious biases within the comparison, but it is still worth analysing ammonoids that come from undisputedly much higher palaeogeographic domains separately from those that were part of palaeo- tropical/subtropical areas, in order to assess any potential strong differences between the two subsets.

Only 122 specimens could be measured within the Boreal realm (see table 2), and while such a number turns out to be quite scanty when it comes to the finer time subdivisions (early, middle and late), it is still sufficient for statistics performed at the stage level. In terms of smallest time bins, the early Smithian included only a single measured specimen, and it could therefore not be taken into account in the analysis.

A first look on the Smithian-Spathian histograms and boxplots (figs. 6 and 7) reveals that, once again, the broadest size range is to be found in Smithian times, while in the Spathian size diversity is characterised by a smaller spread. In particular, it is the middle Smithian which shows the relative largest size spread, while size in the middle Spathian has the smallest span (fig. 7A, and see table 2 for detailed interquartile ranges).

The histograms (figs. 6) all present a very strong positive skewness, thus reflecting a preponderance of smaller sizes. Furthermore, as expected by the shape of their distribution as well as by the amount of outliers in the boxplots, the Shapiro-Wilk's test confirms once again that none of the identified subsamples fulfils normality assumptions, except for the early Spathian, which is the only subsample for which no outliers are to be recognized in the boxplots. (*Note:* as previously notified, no histogram has been depicted of the latter subgroup since it contains less than 10 specimens).

Figure 7 and 8 illustrate the evolution of the median size throughout the Smithian and Spathian substages in the boreal palaeolatitudes. At the level of the Smithian and Spathian stages, a statistically significant reduction of median size could be detected between the Smithian (median: 65.5 mm) and the Spathian (median: 49.5 mm) times (p-value: 0.009583), alongside with a similar statistically significant difference of size distribution (p-value: 0.02272).

On the other hand, in terms of the smaller time bins identified, no statistically significant differences could be found (see table 3 and Appendix-Part 1, table 2A).

The low palaeolatitude belt (figs. 9-11), on the other hand, yields convergent results with those obtained at the global scale analysis (see table 3A, Appendix – Part 1). This was expected, since, as previously mentioned, almost 90% of the studied samples come from the low palaeolatitudes. Thus, once again, statistically significant differences in medians and distributions could be recognized not only between Smithian and Spathian stages (*significant* size reduction; medians resp. 62.9 and 45 mm, see table 2 and 3), but also between the early and middle Smithian, the late Smithian and early Spathian (size reduction in both cases), the early and middle Spathian (size reduction) and the middle and late Spathian (size increase) (see table 2). Figure 11 illustrates the

evolution of the median size throughout the considered time bins.

Histograms (fig. 9) and boxplots (fig. 10) show that the removal of boreal specimens did not affect the results both in terms of statistical significance, but also with regard to the distribution of the subsamples.

All histograms are still positively skewed and all deviate from normality (according to the Saphiro-Wilk's test).

The size span included within the interquartile range of Smithian - Spathian boxplot is almost identical to that at global level and here as well, early and middle Smithian as well as late Spathian retain the widest IQR spread, while middle Spathian still maintains the smallest (see table 2 for details).

However, the complete size ranges of both Smithian and Spathian display a somewhat smaller size span than the size ranges observed at a global scale (table 2), which indicates that some of the biggest measured samples have been recovered in the boreal latitudes.

Further considering smaller palaeoregions of the Pangea, the two main provinces of the Tethys domain, the Palaeotethys (figs. 12-14) and the Neotethys (figs. 15-17) were then analysed.

In the Palaeotethys area (figs. 12-14) almost all available data are concentrated in the Spathian (i.e. 107 analysed ammonoids), while the remaining 11 specimens all belong to the middle Smithian time. For this reason, it is not possible to draw any solid conclusion based on the comparison of Smithian and Spathian each taken as a whole, as it was done for the other palaeoregions. Indeed, neither the Mann-Whitney-U test, nor the Kolmogorov-Smirnov test reveal statistically significant differences between the (middle) Smithian and the rest of the Spathian ammonoids, but this can hardly question the statistical difference that the other analysed regions have shown.

As seen from the histograms and the boxplots (figs. 12-13), both size ranges and distribution spreads of the considered time bins are comparable to each other (see also table 2), and none of the subgroups fulfils normality, with the exception of the late Spathian (once again another subgroup whose boxplot does not show any outliers).

In contrast to what has been observed in the other regions up to this point, no statistically significant difference is recognized between any of the considered subgroups (middle Smithian to early Spathian, early to middle Spathian or middle to late Spathian, see table 3 and Appendix-Part 1, table 4A). Note that the number of specimens included is not much lower than in other cases in which a *significant* change has indeed been found.

Things appear different when moving into the Neotethys area. This includes 444 specimens and, contrary to the Palaeotethys, most of them are of Smithian age (315 analysed) and only very few of Spathian age (31 analysed; see table 2). Therefore, while early, middle and late Smithian subsets could be recognized, the Spathian stage was handled in a twofold manner. First only samples from the middle Spathian were considered and juxtaposed to the late Smithian group, to observe whether the size diversity in the middle of the younger stage is comparable to that at the end of the previous older stage. Then all Spathian ammonoids were considered as a whole (i.e. including the few samples from the early and late subdivisions) and were analysed not only in comparison to the whole Smithian, as was done for all other palaeoregions, but also to the late Smithian subset only, to see if any significant change could be observed already between the fauna right at the Smithian-Spathian

boundary and the one of the younger Spathian stage.

As it can be seen from the boxplots (fig. 16), both middle Spathian and the entire Spathian distributions show the smallest spread, while early and middle Smithian present once again the widest size spread. Just as for the above analysed palaeoregions, in the Neotethys as well, the Spathian shows a much smaller IQR spread and size range compared to the entire Smithian stage (fig. 15A-B and FIG. 16C). The latter, on the other hand, still maintains many samples categorised as outliers, as illustrated by fig. 16C. Once more, all histograms (fig. 15) are characterised by a positive skewness and all deviate from a normal distribution, with the exception of late Smithian. This subgroup is recognized by the Saphiro-Wilk's test as fulfilling normality expectations and because no outliers are recognized in this time stage, this outcome is not surprising.

In terms of *significant* size changes (see table 3), a statistically significant reduction in size and difference in distributions can be observed once again from Smithian to Spathian times (medians being respectively 63.7 and 38.5, see table 2) and also from early to middle Smithian and from late Smithian to middle Spathian. Also statistically significant is the size reduction and size distribution between late Smithian and the whole Spathian (see table 3 and Appendix-Part 1 table 5A for the detailed p-values). The tests give opposite results as far as middle to late Smithian substages are concerned: while the Kolmogorov-Smirnov test recognises a difference in the two distribution, the Mann-Whitney-U test does not recognise any significant change in medians, which in fact, are almost identical. Such disagreement ultimately prevents any confident statement as to whether a trend towards a size change might be present; however, the indistinguishable medians of the two subgroups (53.1 in the middle and 53.5 in the late Smithian) would speak against it.

The two tests were performed also after removing Afghanistan from the Neotethys area, which corresponds to 29 specimens measured from the Smithian (mostly middle) and 8 from the Spathian stage, very poorly distributed in the smaller time substages. The same results were obtained in terms of *significance* (see table 5A, Appendix – Part 1). This indicates that the Afghanistan fauna does not have a big impact on the trend and it might be considered an evidence that no crucial difference might be present between the two faunas.

It is however worth mentioning that when considering Smithian and Spathian time intervals for Afghanistan alone (median sizes resp. 48 mm and 39 mm), no significant size change can be detected between the two stages. Moreover, when both tests were performed in order to compare the Afghanistan fauna of each time stage with the fauna of the other palaeoregions (see Appendix – Part 1, table 10A), a significant difference of distributions and median sizes could be observed in the Smithian (but not in the Spathian), with a smaller maximal median size observed in the Afghanistan record. The insufficient number of specimens measured from Afghanistan makes it however impossible to analyse the considered time intervals at a finer resolution.

To analyse things in as much detail as possible, two further subdivisions were applied to the Neotethys area. The palaeoenvironment from which ammonoids from Oman and Timor have been collected has been identified in both cases as isolated oceanic seamounts (Brühwiler et al. 2012a; Jattiot et al. 2015), in contrast to the terrigenous siliciclastic-carbonate deposits that characterise the Northern Indian Margin (NIM) localities (Brühwiler et al. 2012b). Hence the offshore seamounts of Oman and Timor were analysed separately from the NIM localities of Spiti, Pakistan and South Tibet. In both cases, similar results to those of the whole Neotethys

have been obtained.

Just like for the Neotethys region, for both the seamounts (figs. 18-20) and the NIM (figs. 21-23) most of the measured specimens are of Smithian age (203 analysed ammonoids in the NIM and 126 in the seamounts), while only very few of Spathian age were measured (13 in the NIM and 11 in the seamounts). Therefore, while the Smithian could be subdivided in the smaller time bins corresponding to early, middle and late, the Spathian stage could only be considered as a whole for the analyses.

Once again, when looking at the histograms and the boxplots (figs. 18-19, 21-22), it is evident that the Smithian is characterised by the largest size spread. The Spathian size range appears the smallest in the seamount occurrences as opposed to the NIM but also to any other analysed region (see table 2); however, given the restricted amount of specimens available, a reasonable comparison can only be made with the Northern Indian Margin region. In addition, the late Smithian presents in both cases a much smaller size range and IQR compared to early and middle Smithian, and, according to the Shapiro-Wilk's test, this and the whole Spathian stage of the seamounts are the only normally distributed subgroups (although the latter might be due to a lack of a large enough samples measured and an overall limited amount of available specimens).

Once again, the histograms are (both for the seamounts and for the NIM; figs. 18, 21) all positively skewed, with the exception of the late Smithian seamounts fauna, for which a median larger than the mean indicates a prevalence of sizes bigger than the median.

As far as *significant* changes are concerned (see table 3 and tables 6A and 7A in the Appendix – Part 1), the Mann-Whitney-U test and the Kolmogorov Smirnov test show a significant change in size and distribution between the whole Smithian and Spathian stages of both regions (thus characterized by a size reduction), as well as between early and middle Smithian of both regions and between late Smithian and whole Spathian of the seamounts (in both cases a reduction in median size could be detected. See figs. 20, 23 for details of the evolution of median size in the two considered palaeoregions). In the Northern Indian Margin, while a significant difference between the late Smithian and the Spathian distributions is detected by the Kolmogorov-Smirnov test, no significant change in size could be detected by the Mann-Whitney-U test.

The South China block (figs. 24-26) seems to show more similarities with the Palaeotethys rather than with any of the other considered palaeolocations. It includes 224 specimens, quite evenly distributed within the Smithian and the Spathian (see table 2).

None of the histograms (fig. 24) seems to show an obvious normal distribution, but the Shapiro-Wilk's test reveals normality for late Smithian and late Spathian subdivisions. Just like for the Neotethys seamounts, the late Smithian histogram is in addition the only one to display a negative skewness.

The boxplot (fig. 25A) indicates that the late Spathian presents the widest IQR spread, while the other subgroup distributions have a roughly comparable and smaller spread. When comparing Smithian to Spathian stages, though (fig. 25B), they seem to have an almost identical distribution, which is confirmed by both Mann-Whitney-U and the Kolmogorov-Smirnov test. In fact, none of the tests can detect any change from Smithian to Spathian times nor between the smaller subdivisions of the stages (see table 2 and Appendix-Part 1 table 6A). The only exception can be found between middle and late Spathian, for which the Mann-Whitney-U test does detect a

statistically significant increase of the median size (resp. 44 to 83.5 mm, see Appendix-Part 1, table 8A for p-values), but no *significant* change in the distribution of the two populations can be detected by the Kolmogorov-Smirnov test. This divergence ultimately precludes any further and more precise comparison between the two time intervals.

Finally, the last palaeogeographic entity to be analysed is the Western U.S. Sonoma basin (figs. 27-29). It includes a total of 225 specimens, of which 98 analysed for Smithian age, and 113 of Spathian age. The specimens are suitably distributed among the smaller time subdivisions of both stages, so that all of them could be statistically analysed.

Once again, all histograms (fig. 27) present a positive skewness. The Saphiro-Wilk's test reveals that early and late Smithian, as well as late Spathian, are characterised by normal distributions, while in case of the early Spathian subgroup a p-value of 0.05157 makes it impossible to reject or confirm normality (see table 9A, Appendix-Part 1).

Fig. 28B shows that the size range (both the whole and the interquartile size range) in the Smithian once again reaches higher values than in the Spathian, and fig. 28A indicates that throughout the Smithian, the size distribution of the smaller time subgroups remains close to identical (see IQR of early, middle and late Smithian in table 2). This observation is corroborated by both the Mann-Whitney-U test and the Kolmogorov-Smirnov test, none of which can find any statistical difference among the Smithian subdivisions (see table 2 and table 9A, Appendix-part 1). A first statistically significant change is found between the late Smithian and the early Spathian, both in median values (with a decrease from 80.65 to 50.5 mm, see also fig. 29 for a clear view of the evolution of median sizes) and in distribution. The transition from early to middle Spathian is also characterized by such a statistically significant change, i.e. by a *significant* reduction of median size (50.5 to 33.5 mm, see fig. 29 and table 2) and a *significant* change in distributions.

When comparing Smithian and Spathian, a *significant* reduction of medians and change in distribution can be detected (Mann-Whitney-U p-value: 6.361e-07 and Kolmogorov-Smirnov p-value 4.01e-05, see table 9A, Appendix-Part 1) just as was the case for most of the analysed palaeoregions.

The most important results can thus be summarized as follows:

- A statistically significant median size reduction, accompanied by a statistically significant change in shape and relative *position* (see Hammer and Harper 2006, p. 30) of the respective distribution is detected between **Smithian and Spathian** at a global scale and for all considered palaeoregions, with the exception of Palaeotethys and the South China block.
- From the subdivision of both Smithian and Spathian into early, middle and late time bins, no consistent pattern can be observed among the different palaeoregions (see table 3). On the whole it can only be stated that:
 - Statistically different distributions characterised by a reduction in median size can be observed between **late Smithian and early Spathian** only at a global level, in the low palaeolatitudes and, in specific, of the single palaeoregions included in the latter, only within the western USA.

No data from Early Spathian are available from the Neotethys; however, when comparing the **late Smithian** with **middle Spathian** and the **whole Spathian**, in both cases the reduction in median and the difference in distributions are found to be significant.

- The only clear and constant pattern observed is the lack of a *significant* difference between the **middle** and the **late Smithian**.
- All histograms (except for two, see above concerning the South China block and the Neotethys seamounts) display a positive skewness, which indicates a prevalence of specimens smaller than the median value.
- When comparable (which is not the case for Palaeotethys area), the maximal size range reaches a broader spectrum in the Smithian, rather than in the Spathian, with the exception of South China, in which the distributions are comparable to each other and some bigger sizes are to be found in the middle Spathian, rather than in the Smithian.
- In the majority of cases, the largest IQR values are to be found either in the **early** (fig. 22A), and/or in the **middle Smithian** (figs. 4A, 7A, 10A, 16A, 19A, 28A) and/or in the **late Spathian** (figs. 13A, 25A; see also table 2).
- Very few of the identified statistical populations are normally distributed, most likely due to the sensitivity of the Shapiro Wilk's test to outliers; in fact, only those whose boxplot display no outliers fulfil normality.

For the sake of consistency, it is worth mentioning that British Columbia does not include enough specimens for a statistical analysis at the substages (early, middle, late) level, as previously mentioned. There would however be just the right amount of specimens to compare body size at the stage level (with 27 specimens for Smithian and 11 for Spathian time), just as it has been done in case of Afghanistan. However, as asserted for the latter, such a limited amount of specimens could lead to biased outcomes, and while the results obtained through the statistical analysis of Afghanistan could be considered and critically examined in the light of the surrounding Tethyan domain, British Columbia represents a quite isolated position. Therefore, the location was not considered for a separate statistical analysis, rather it was only included within the low palaeolatitudes and the global statistical analysis (as previously mentioned, see section 3.2).

Global

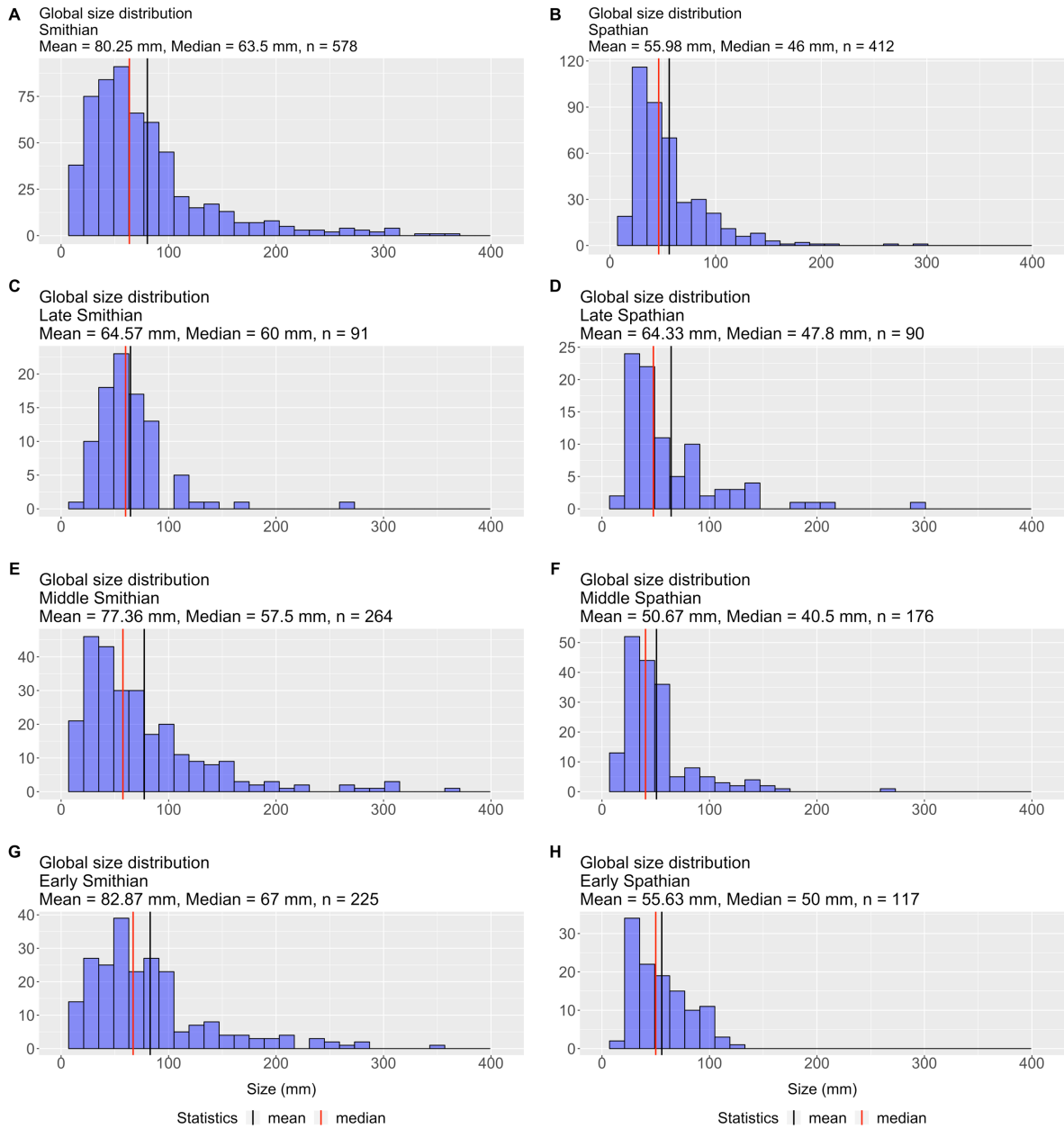


Figure 3: Size distribution of ammonoid species through time on a global scale. All histograms positively skewed and none normally distributed.

Global

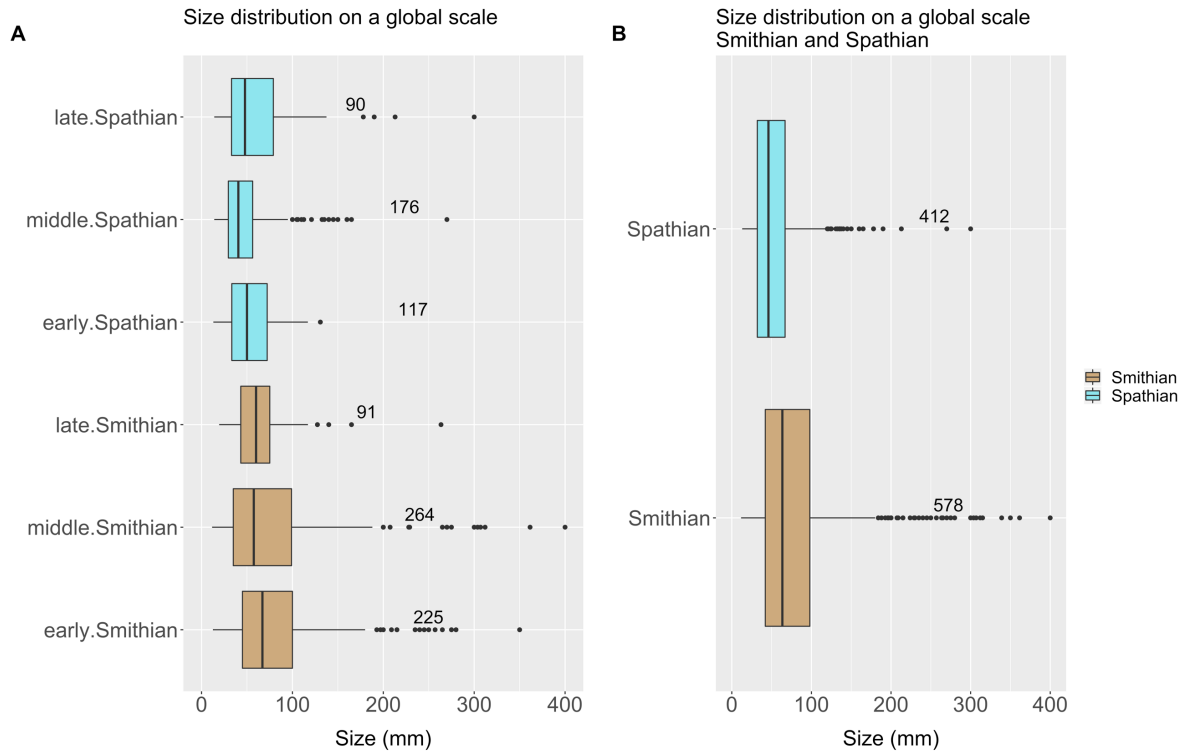


Figure 4: Boxplots based on all data gathered from the whole Pangea. Statistical tests reveal a significant size reduction between Smithian and Spathian, as well as between Early and Middle Smithian, Late Smithian and Early Spathian, Early and Middle Spathian. A significant size increase is detected between Middle and Late Spathian.

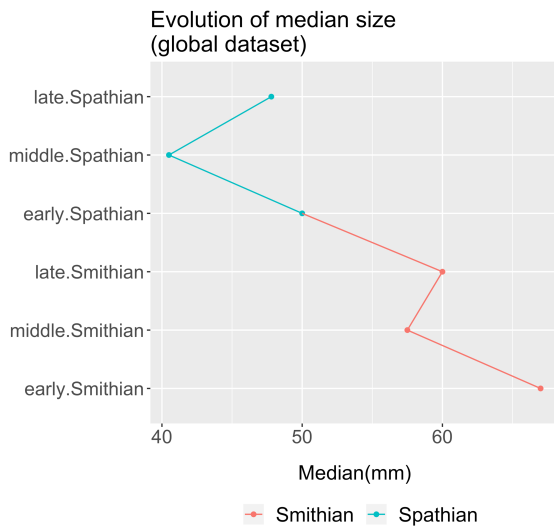


Figure 5: Evolution of the median size through time. Palaeogeographic region considered: Pangea as a whole.

Boreal Palaeolatitudes

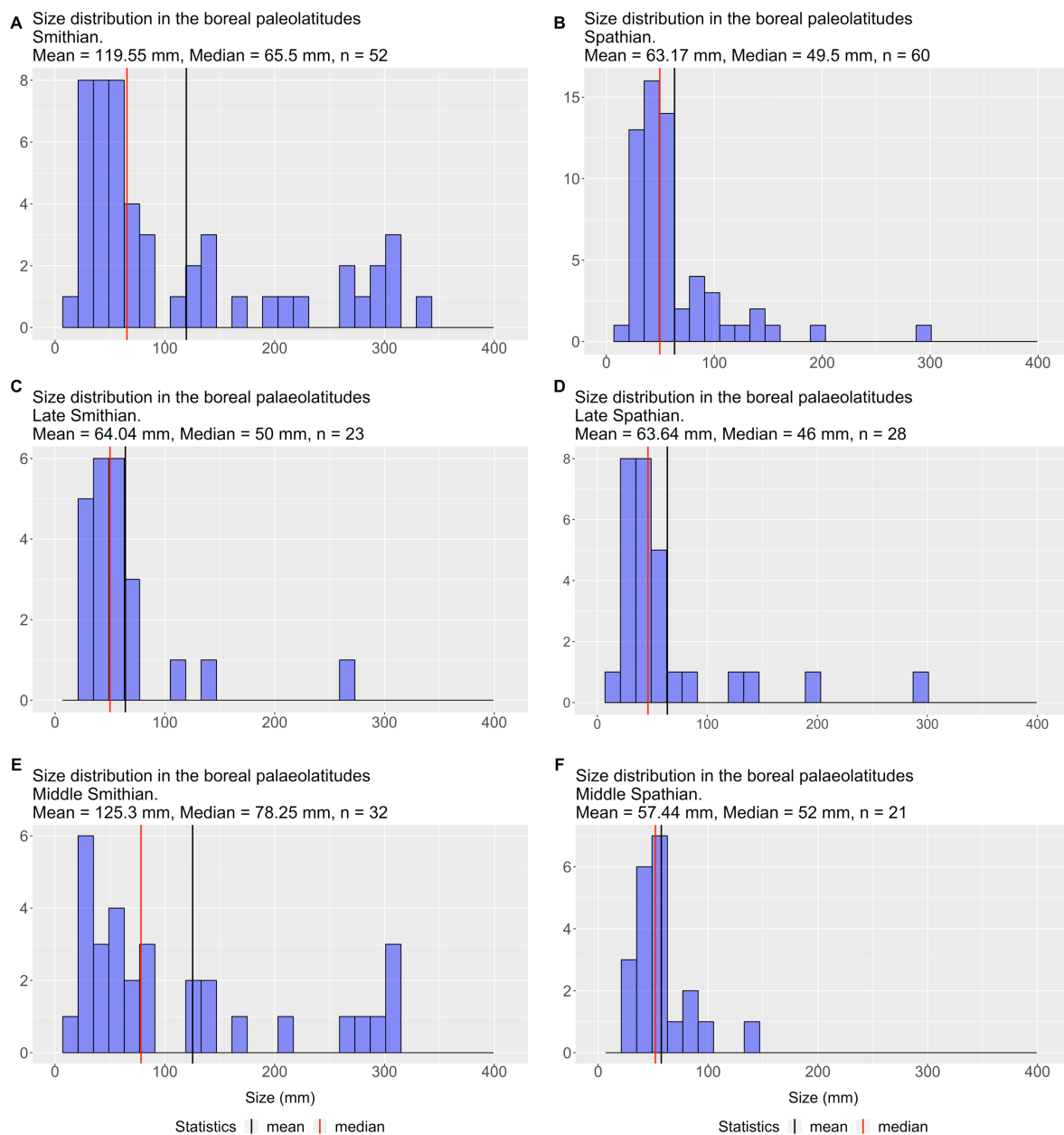


Figure 6: Size distribution of ammonoid species through time in the Boreal palaeolatitudes (including Arctic Canada, Spitzbergen and Siberia). All histograms are characterised by a positive skewness and all statistical populations present a non-normal distribution (except for the Early Spathian population, which was however not depicted here, as it contains less than 10 specimens).

Boreal Palaeolatitudes

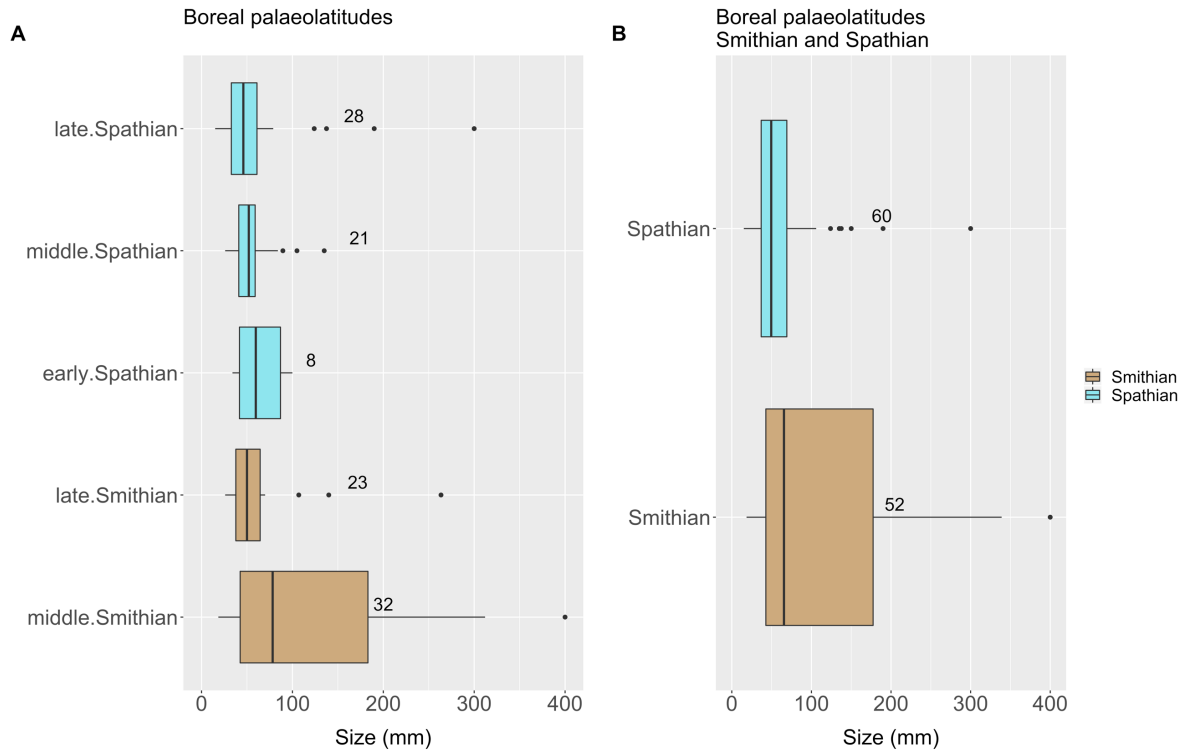


Figure 7: Boxplots of specimens collected in the Boreal palaeolatitudes (Arctic Canada, Spitzbergen, Siberia). Statistical tests revealed a significant size reduction between Smithian and Spathian only.

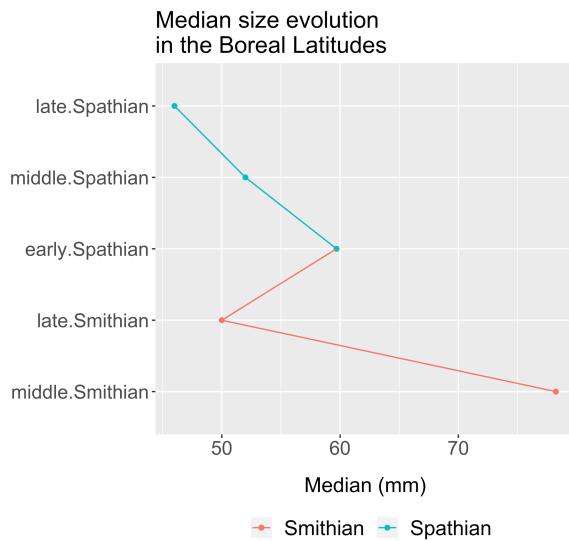


Figure 8: Evolution of the median size through time in the Boreal domain (Arctic Canada, Spitzbergen, Siberia)

Low Palaeolatitudes

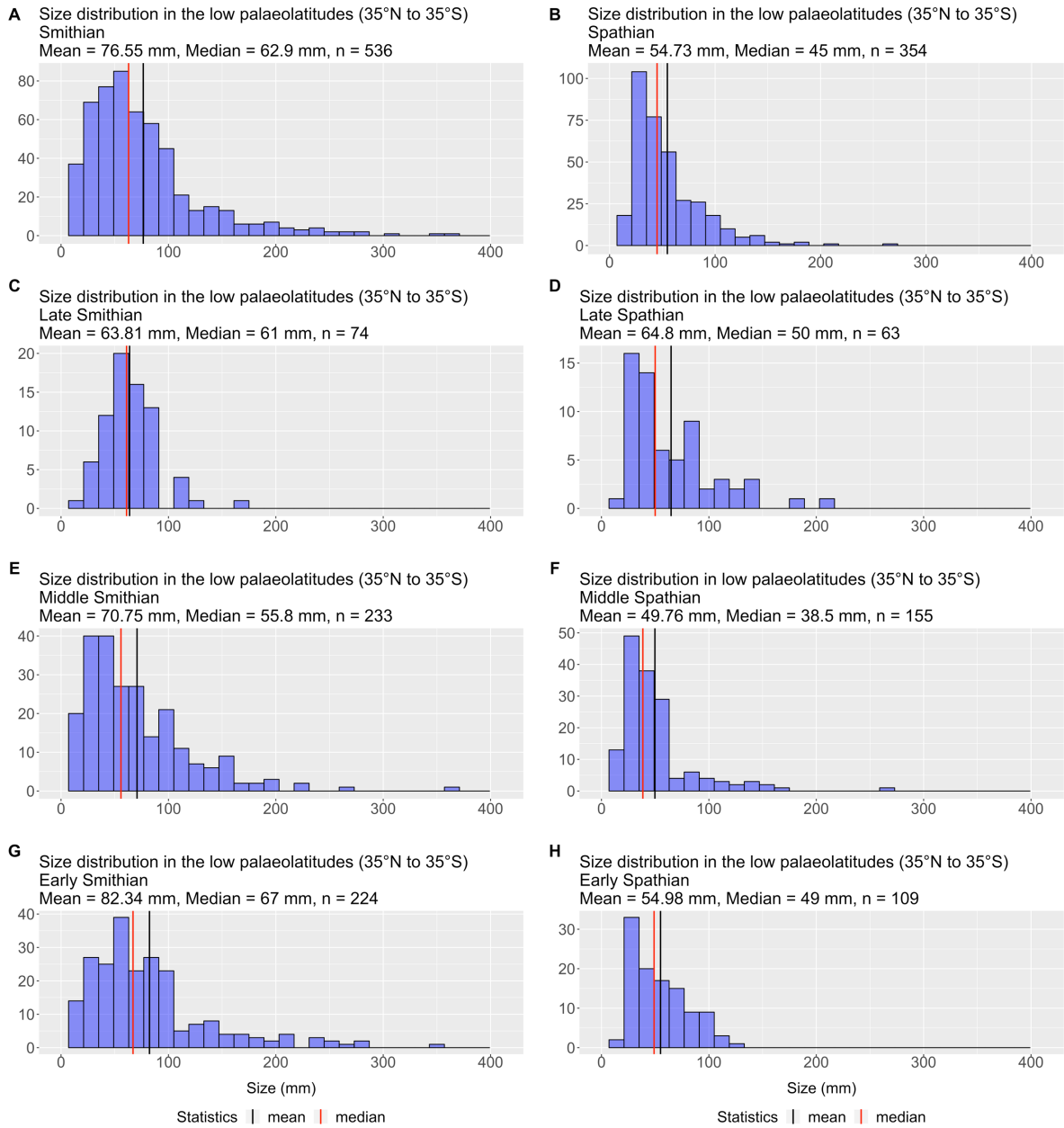


Figure 9: Size distribution of ammonoid species through time in the low palaeolatitudes (including all locations sampled between 35° N and 35° S). All histograms deviate from normality and are positively skewed.

Low Palaeolatitudes

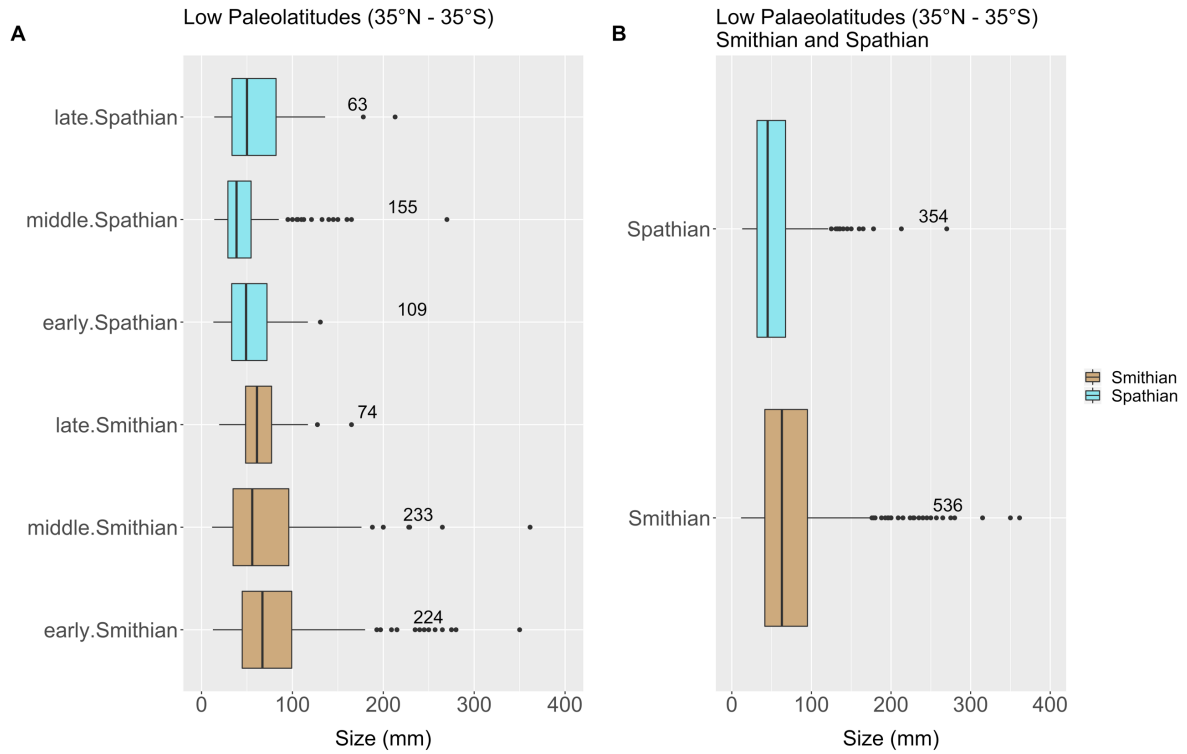


Figure 10: Boxplots of specimens collected in the low palaeolatitudes (including all locations sampled between 35° N and 35° S). Statistical tests reveal a significant size reduction between Smithian and Spathian, as well as between Early and Middle Smithian, Late Smithian and Early Spathian, Early and Middle Spathian. A significant size increase is detected between Middle and Late Spathian.

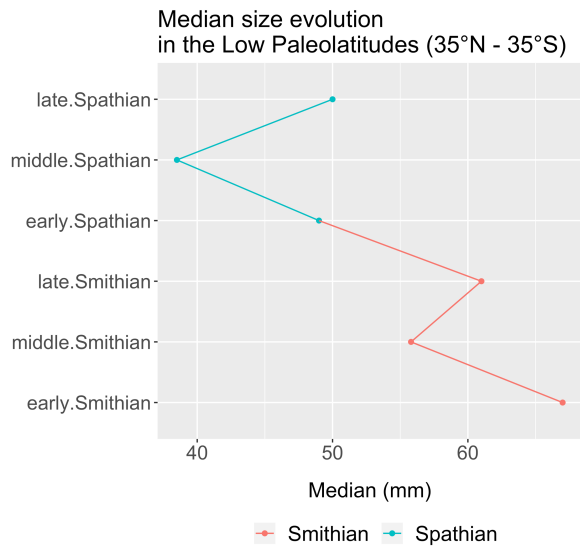


Figure 11: Evolution of the median size through time in the low palaeolatitudes (locations between 35° N and 35° S).

Palaeotethys

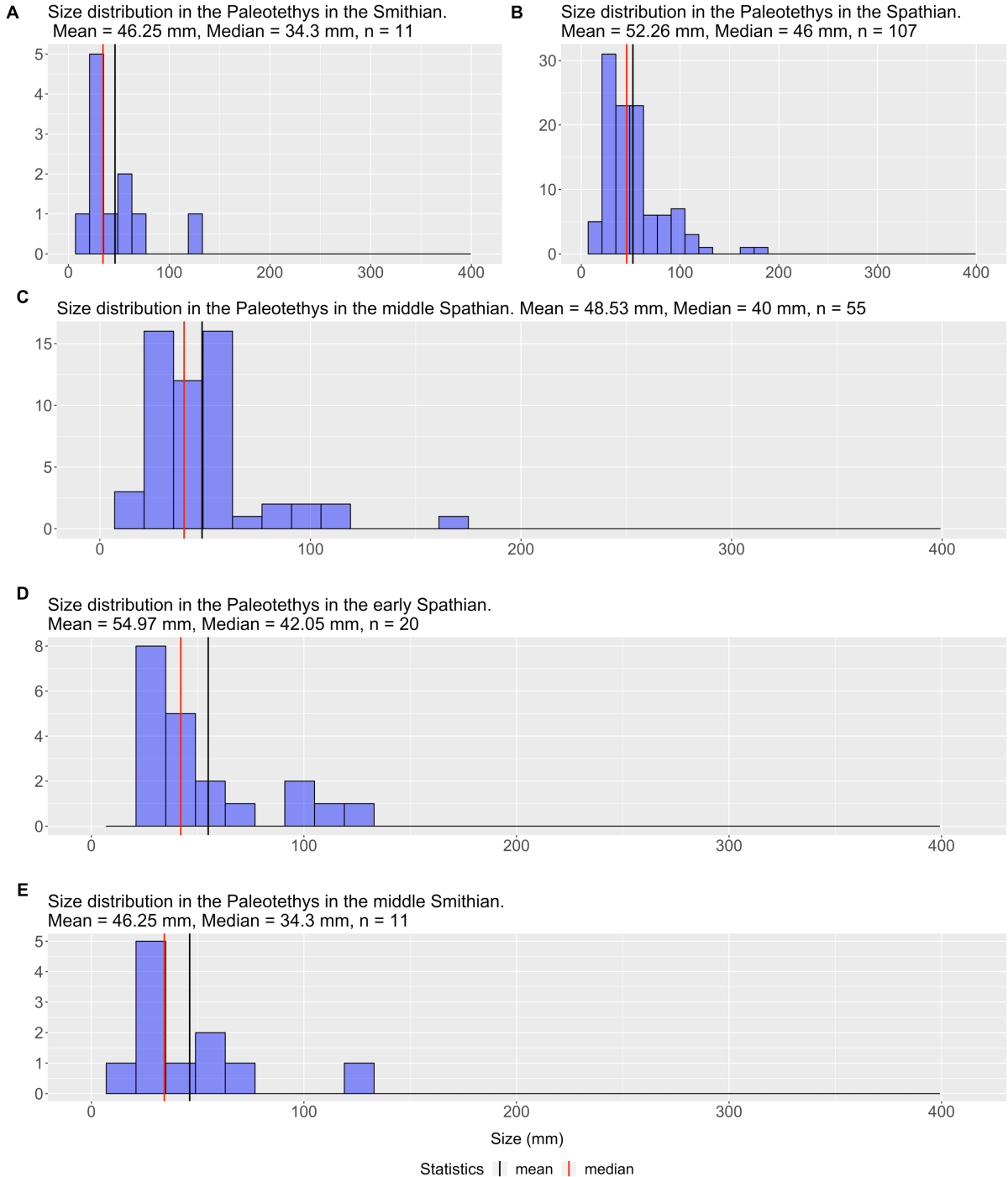


Figure 12: Size distribution of ammonoid species through time in the Palaeotethys domain (including Mangyshlak, Albania, Chios and North-West Caucasus). Only the Late Spathian subgroup is characterised by a normal distribution. All histograms are positively skewed.

Palaeotethys

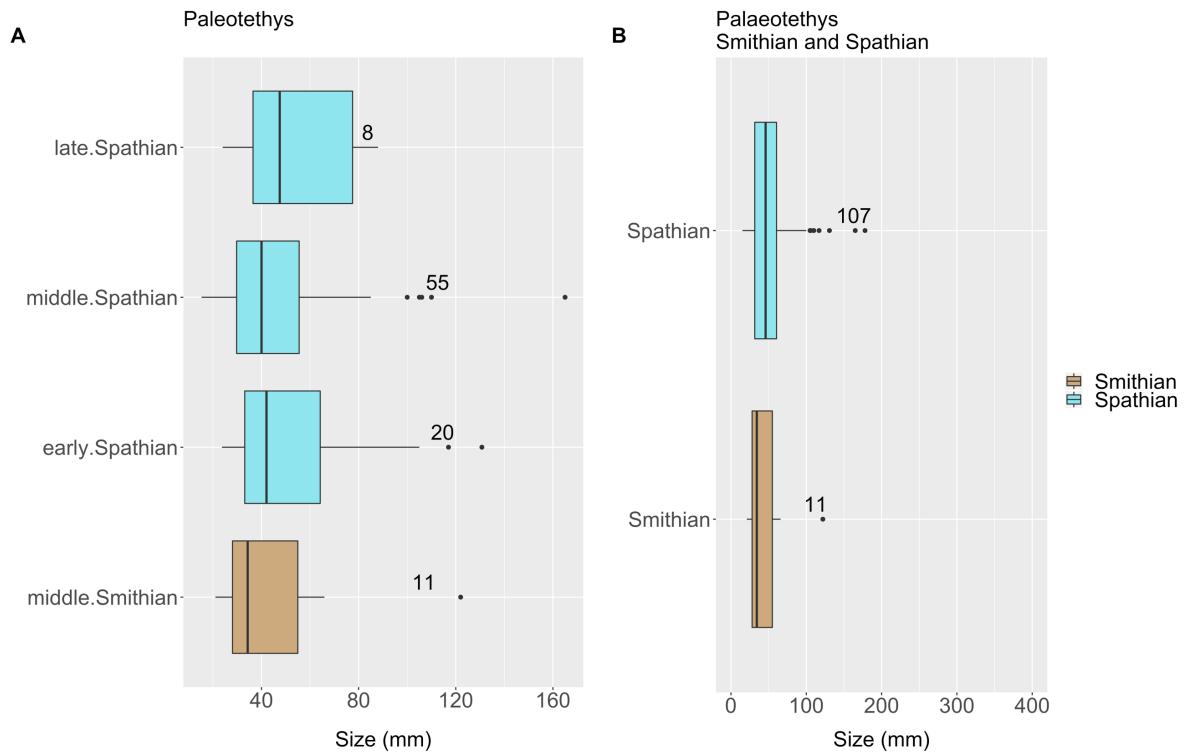


Figure 13: Boxplots of specimens collected in the Palaeotethys domain (Mangyshlak, Albania, Chios and North-West Caucasus). Statistical tests reveal the absence of any statistically significant size changes.

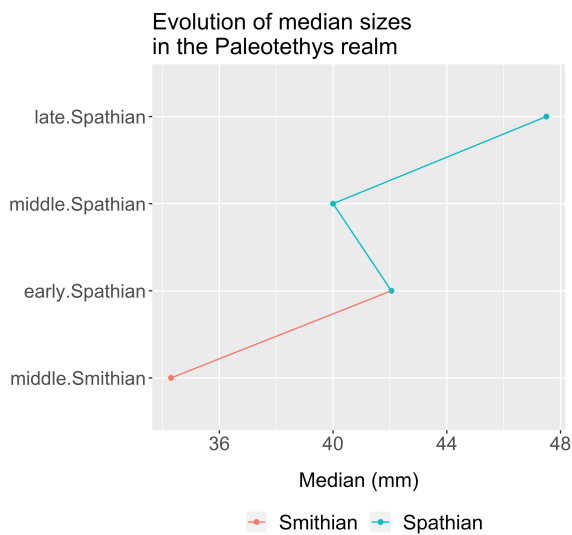


Figure 14: Evolution of the median size through time in the Palaeotethys domain (Mangyshlak, Albania, Chios and North-West Caucasus).

Neotethys

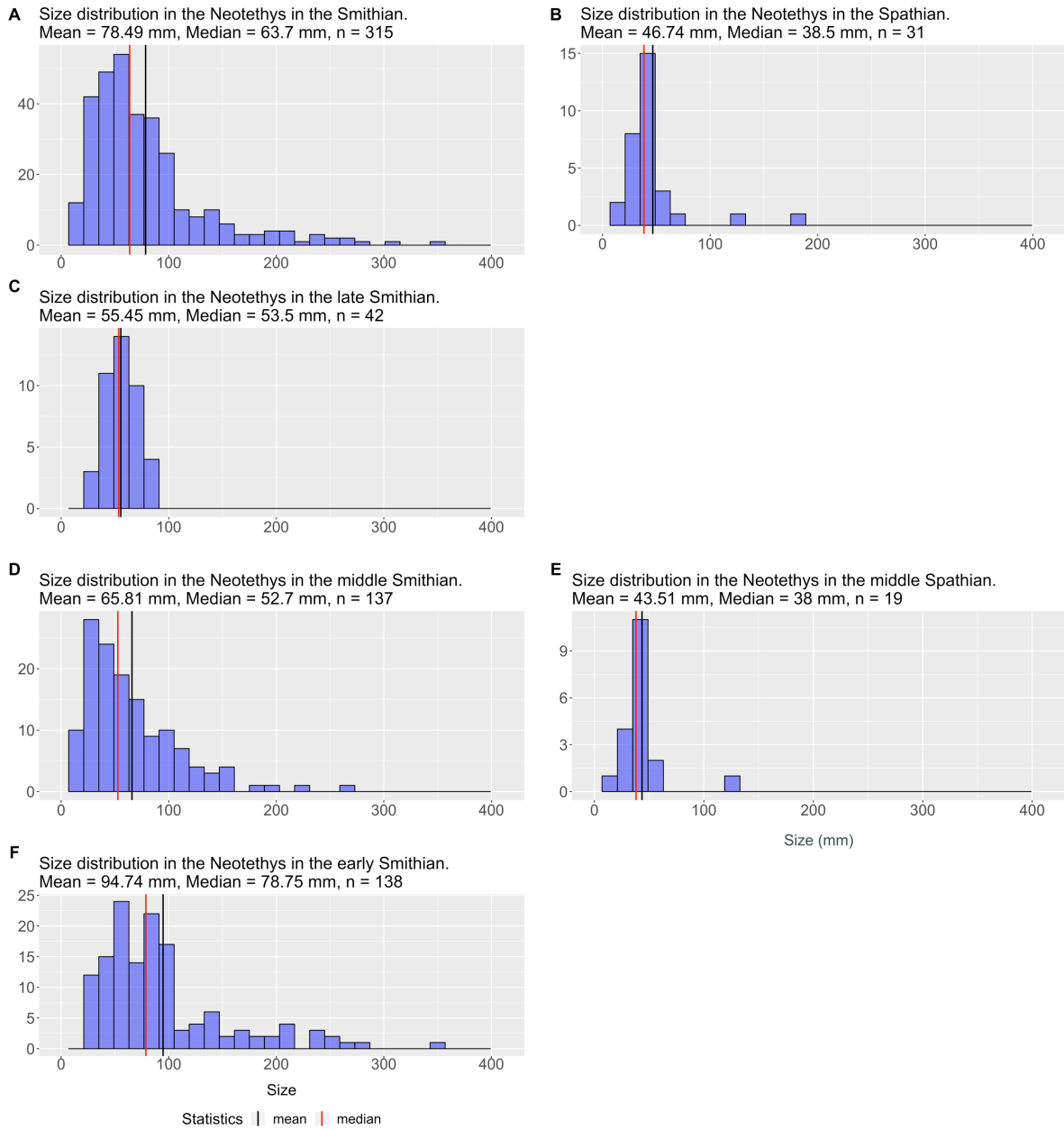


Figure 15: Size distribution of ammonoid species through time in the Neotethys domain (including Oman, Salt Range (Pakistan), Spiti, Timor, South Tibet and Afghanistan). All histograms deviate from normality except for Late Smithian, and all are positively skewed.

Neotethys

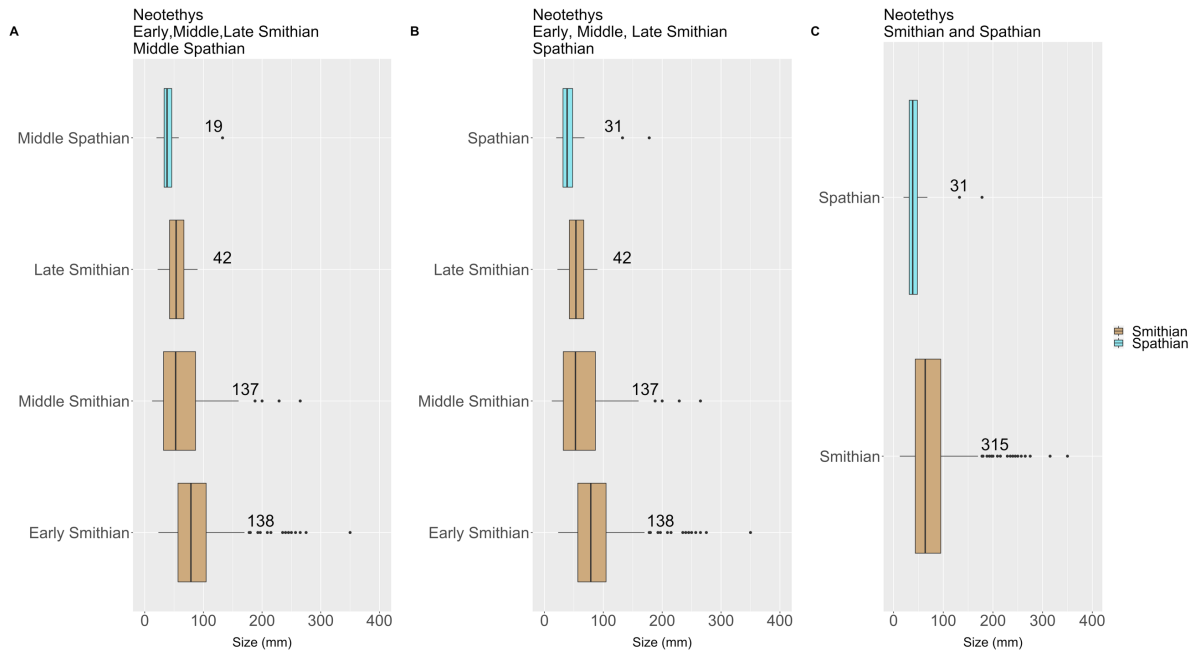


Figure 16: Boxplots of specimens collected in the Neotethys domain (including Oman, Salt Range (Pakistan), Spiti, Timor, South Tibet and Afghanistan). Statistical tests reveal a significant size reduction between Smithian and Spathian, as well as between Early and Middle Smithian and between Late Smithian and Middle Spathian, and Late Smithian and Spathian as a whole.

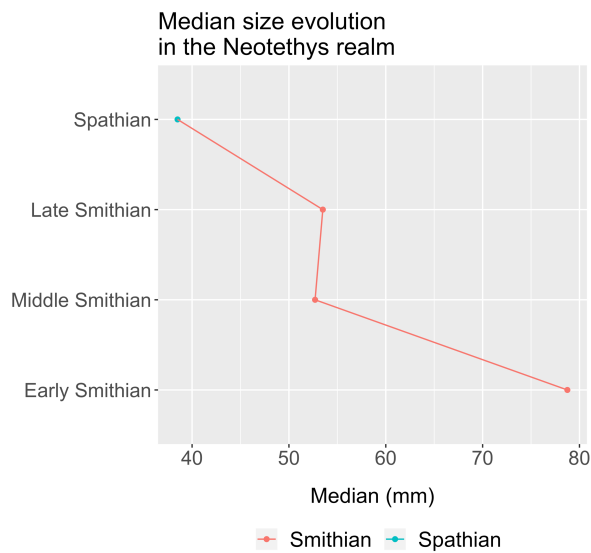


Figure 17: Evolution of the median size through time in the Neotethys domain (including Oman, Salt Range (Pakistan), Spiti, Timor, South Tibet and Afghanistan).

Neotethys seamounts

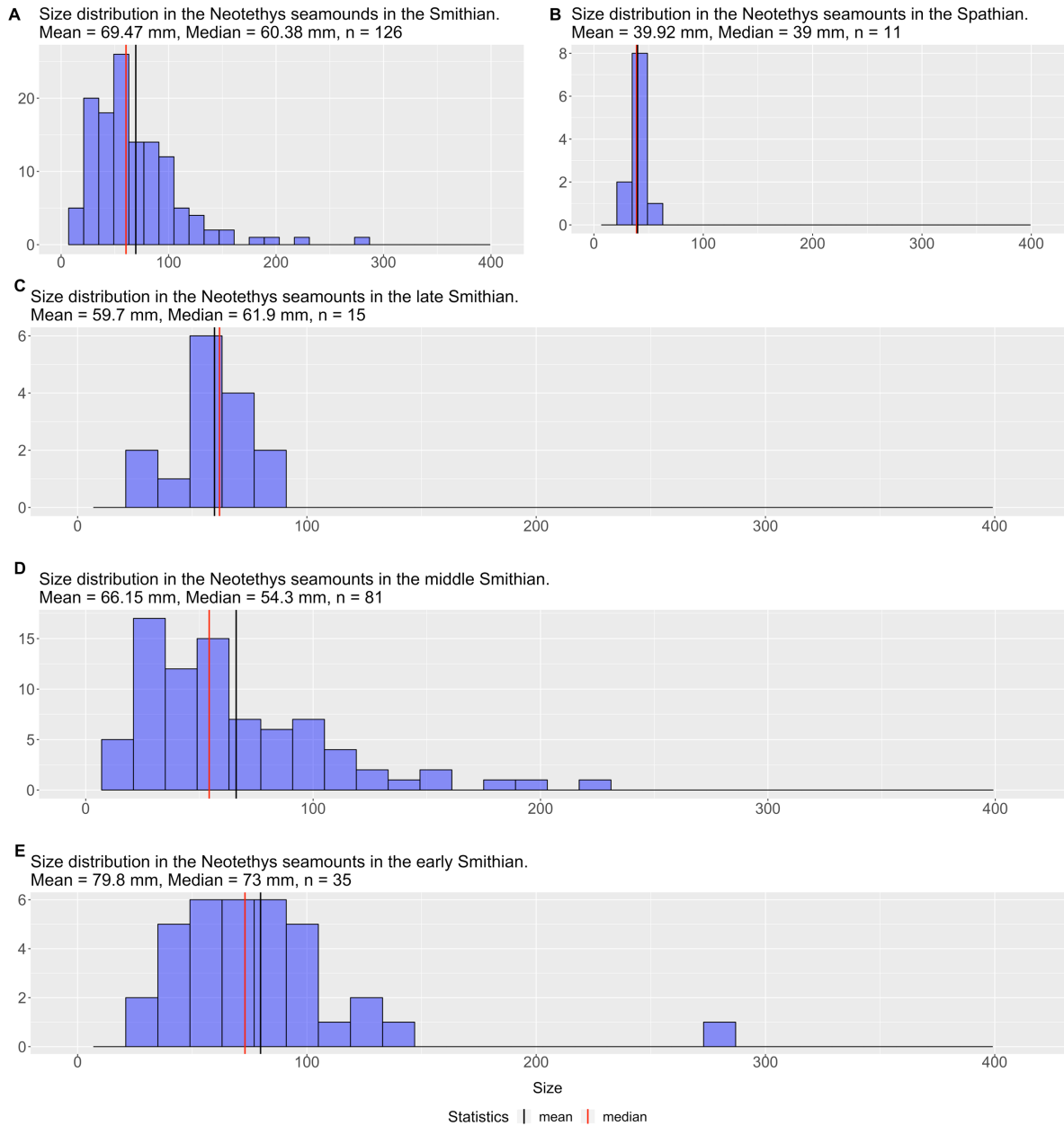


Figure 18: Size distribution of ammonoid species through time in the Neotethys seamounts (including Oman and Timor). All histograms positively skewed except for Late Smithian, for which a median > mean indicates a prevalence of sizes larger than the median. The Late Smithian and the whole Spathian are the only statistical populations with normal distribution.

Neotethys seamounts

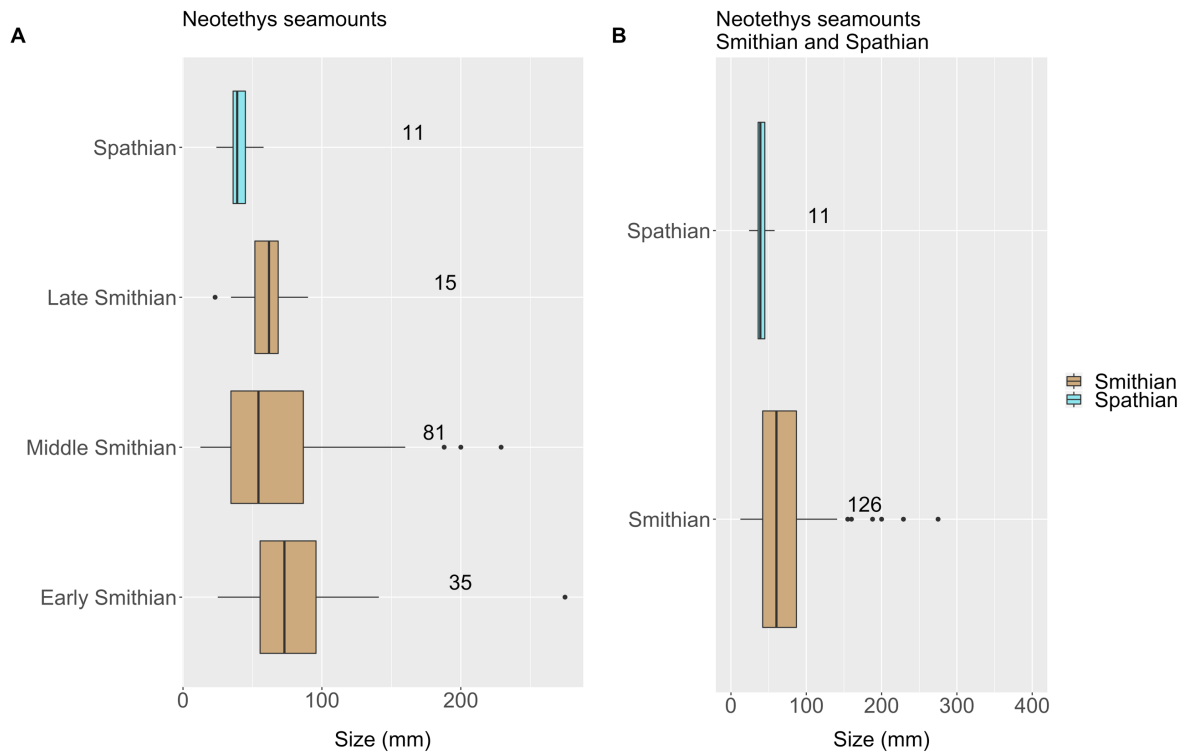


Figure 19: Boxplots of specimens collected in the Neotethys seamounts (including Oman and Timor). Statistical tests reveal a significant size reduction between Smithian and Spathian, as well as between Early and Middle Smithian and Late Smithian and Spathian.

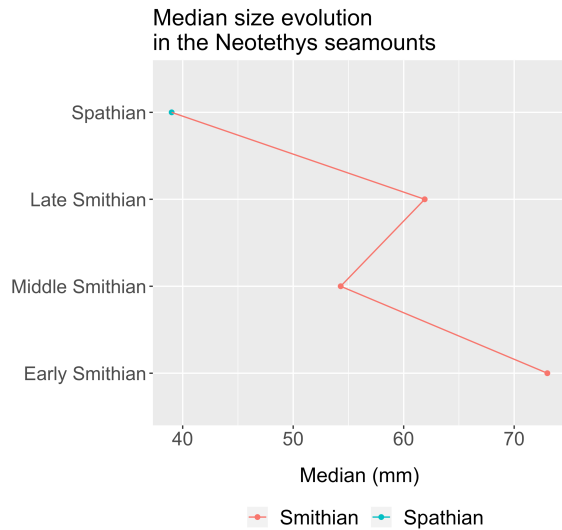


Figure 20: Evolution of the median maximal size through time in the Neotethys seamounts (including Oman and Timor).

Northern Indian Margin

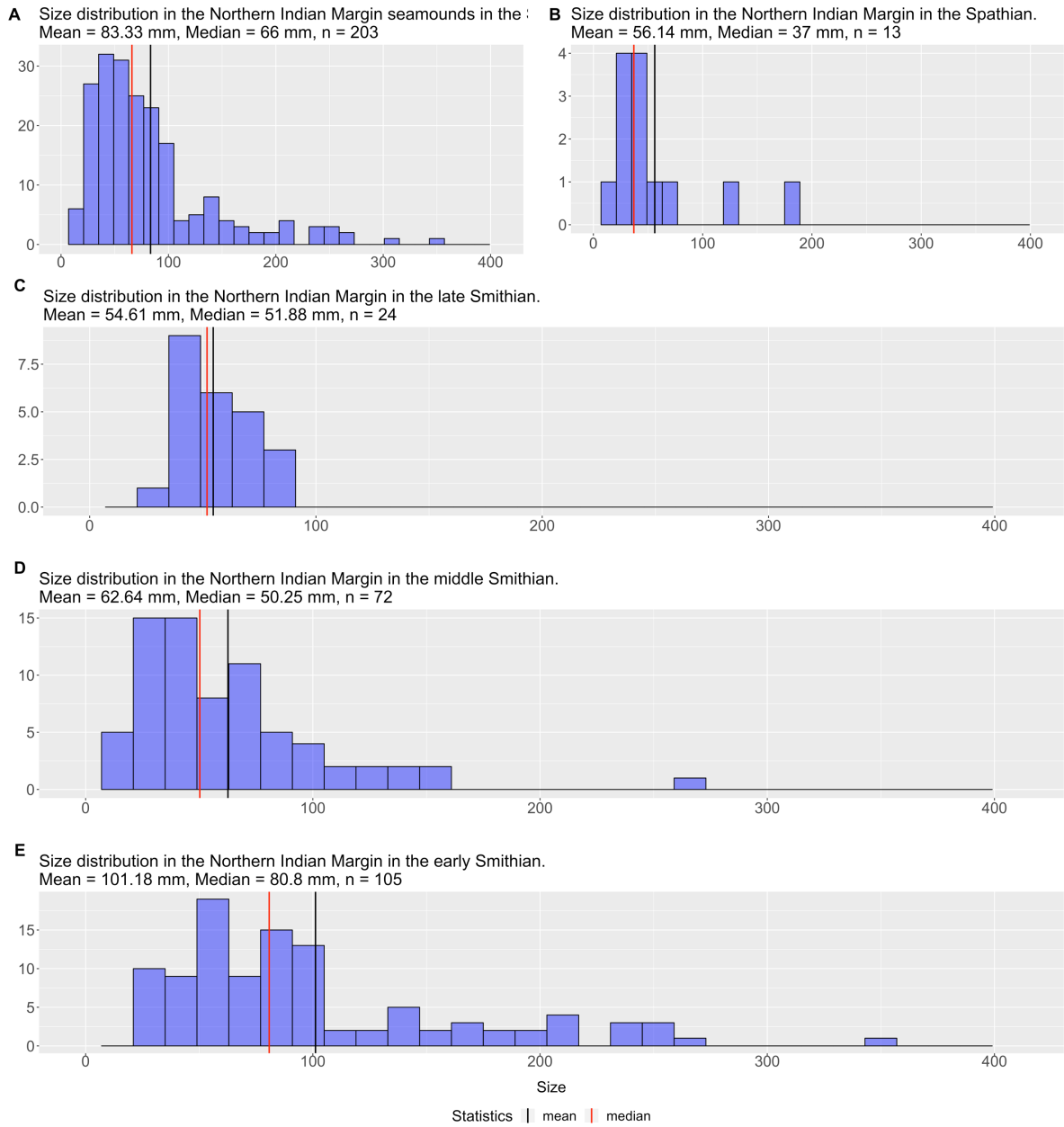


Figure 21: Size distribution of ammonoid species through time in the Northern Indian Margin (including Salt Range (Pakistan), Spiti and South Tibet). All histograms positively skewed and characterised by a non-normal distribution (with the exception of the Late Smithian).

Northern Indian Margin

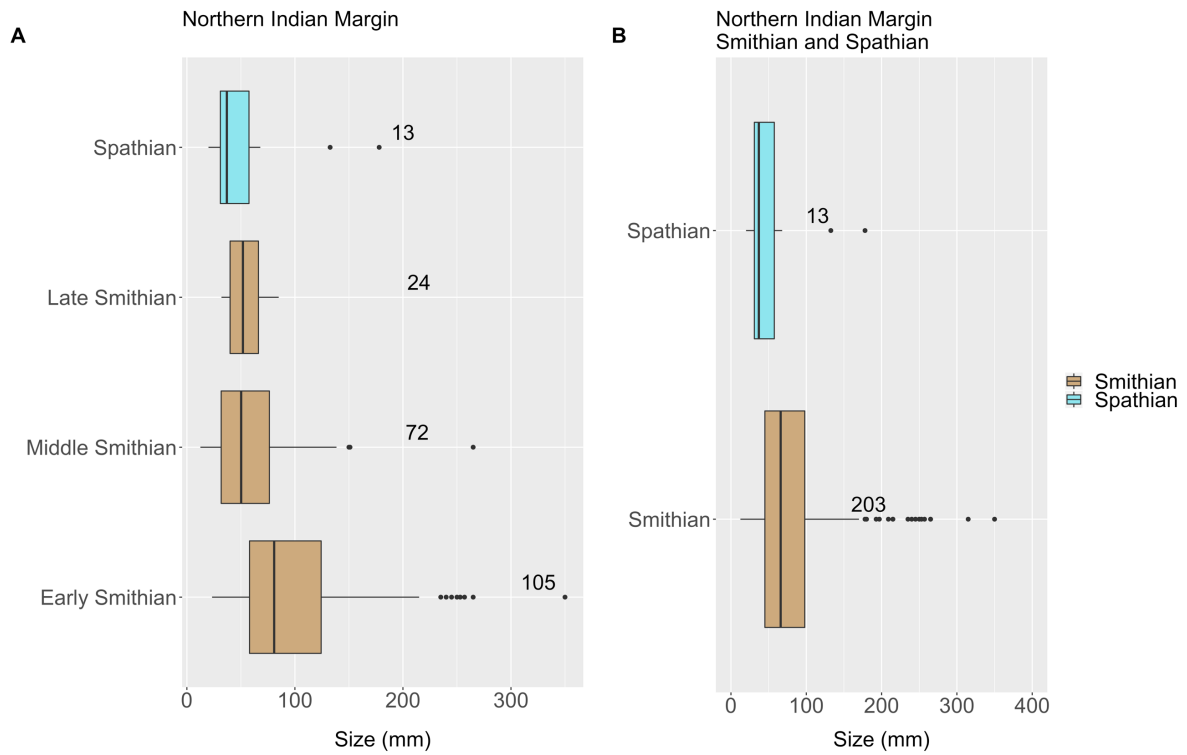


Figure 22: Boxplots of specimens collected in the Northern Indian Margin (including Salt Range (Pakistan), Spiti and South Tibet). Statistical tests reveal a significant size reduction between Smithian and Spathian, as well as between Early and Middle Smithian. A significant size change between Late Smithian and Spathian could however only be detected by the Kolmogorov-Smirnov test, as opposed to the Mann-Whitney-U test.

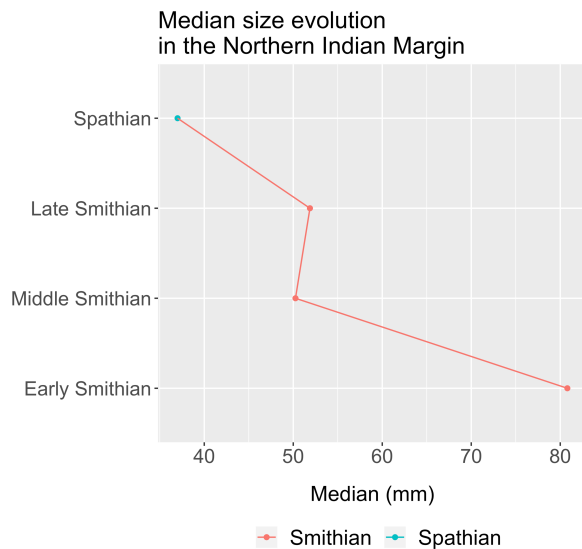


Figure 23: Evolution of the median size through time in the Northern Indian Margin (including Salt Range (Pakistan), Spiti and South Tibet).

South China

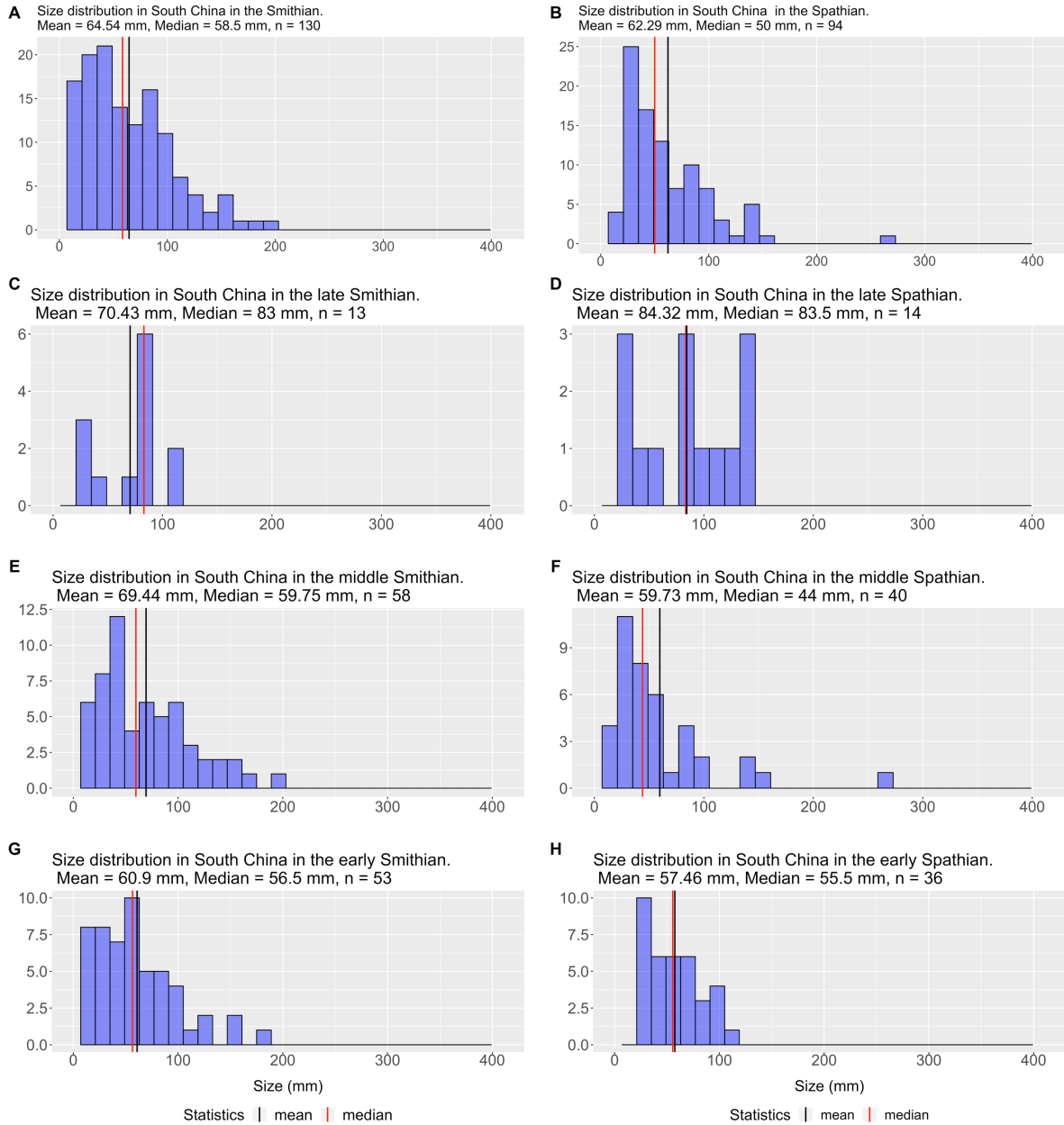


Figure 24: Size distribution of ammonoid species through time in the South China Block (including today's South China and North East Vietnam). Only Late Smithian and Late Spathian subsets are characterised by a normal distribution. A negative skewness can be observed in the histogram for Late Smithian.

South China

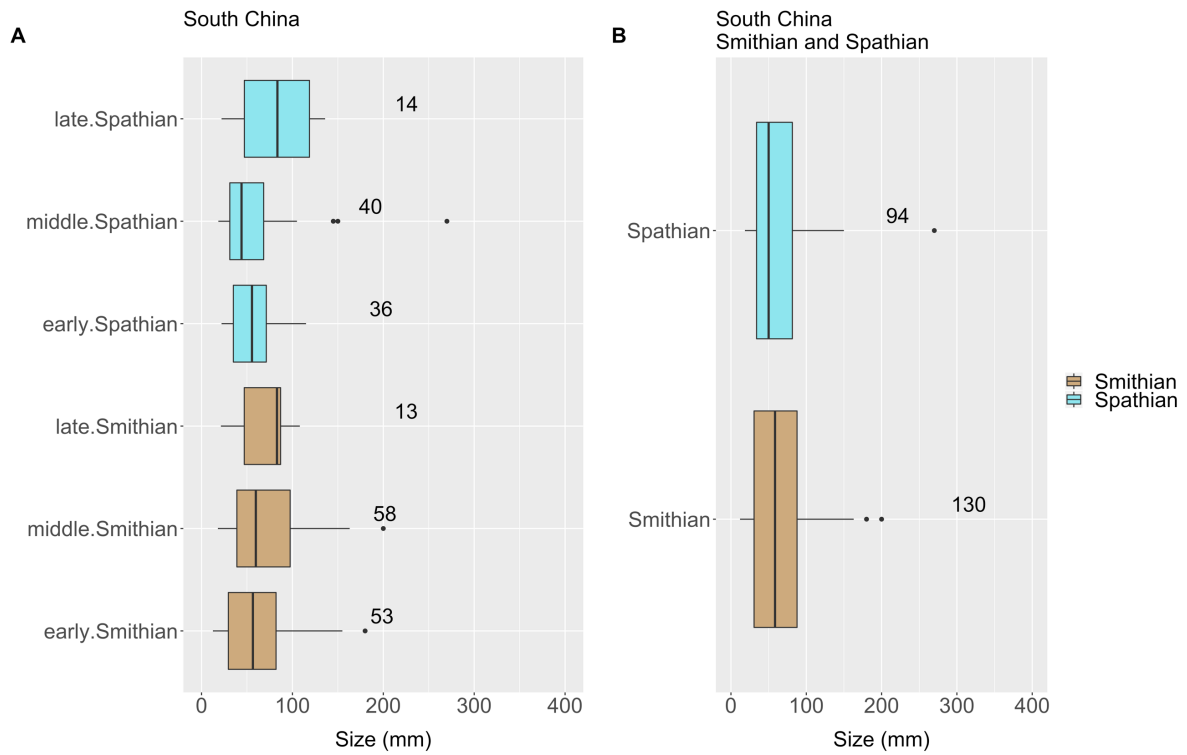


Figure 25: Boxplots of specimens collected in the South China Block (including today's South China and North East Vietnam). Statistical tests reveal the absence of any statistically significant size changes.

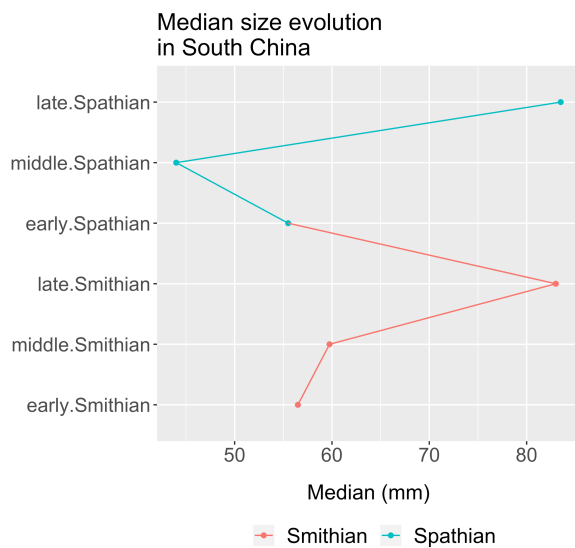


Figure 26: Evolution of the median maximal size through time in the South China Block (including today's South China and North East Vietnam).

Western USA

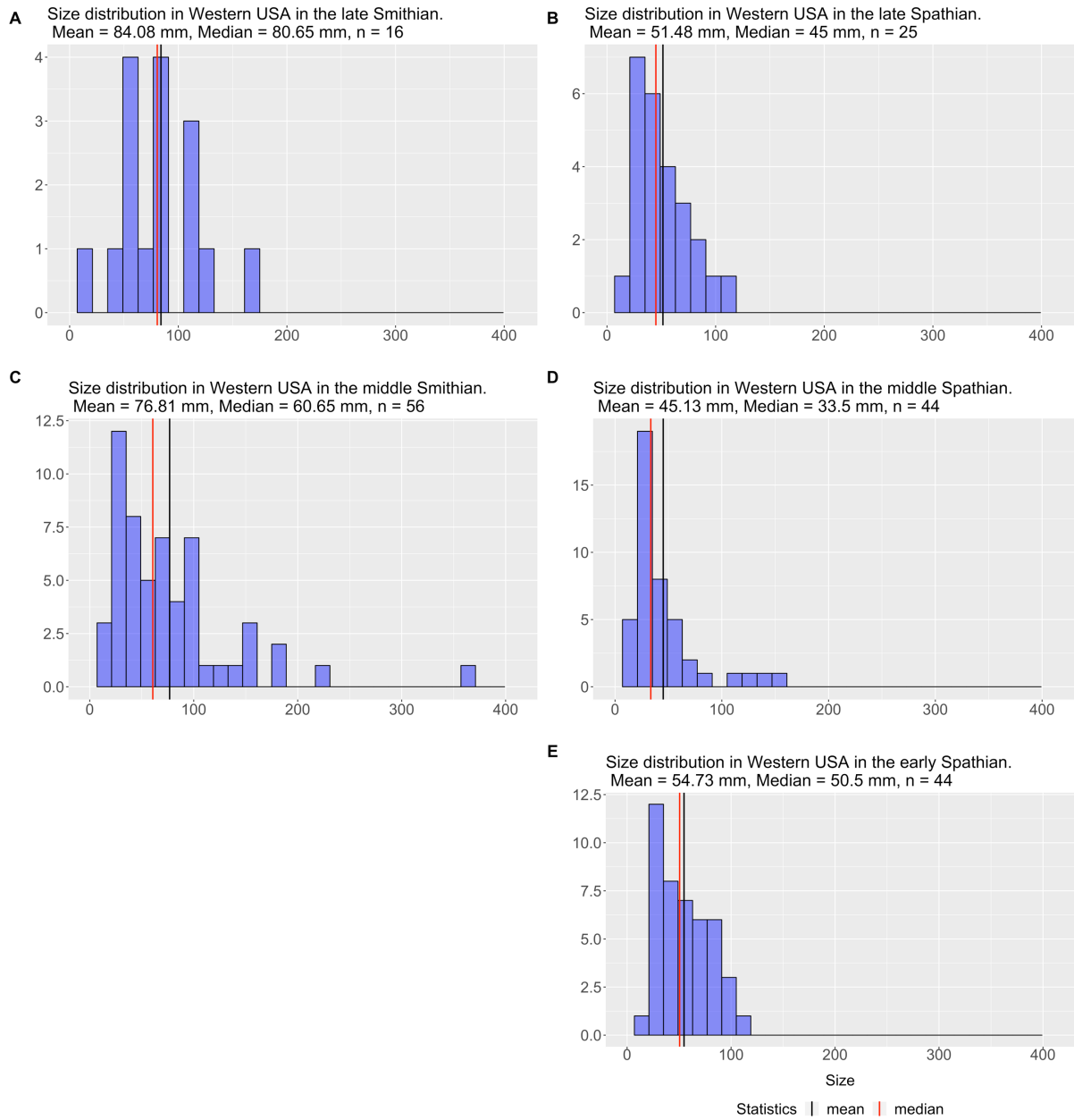


Figure 27: Size distribution of ammonoid species through time in the Western US basin (including Western U.S. Sonoma basin locations, California and Star Peak Group). The Late Smithian and the Late Spathian are the only statistical populations that conform to a normal distribution. All histograms are positively skewed. Palaeogeographic region considered:

Western USA

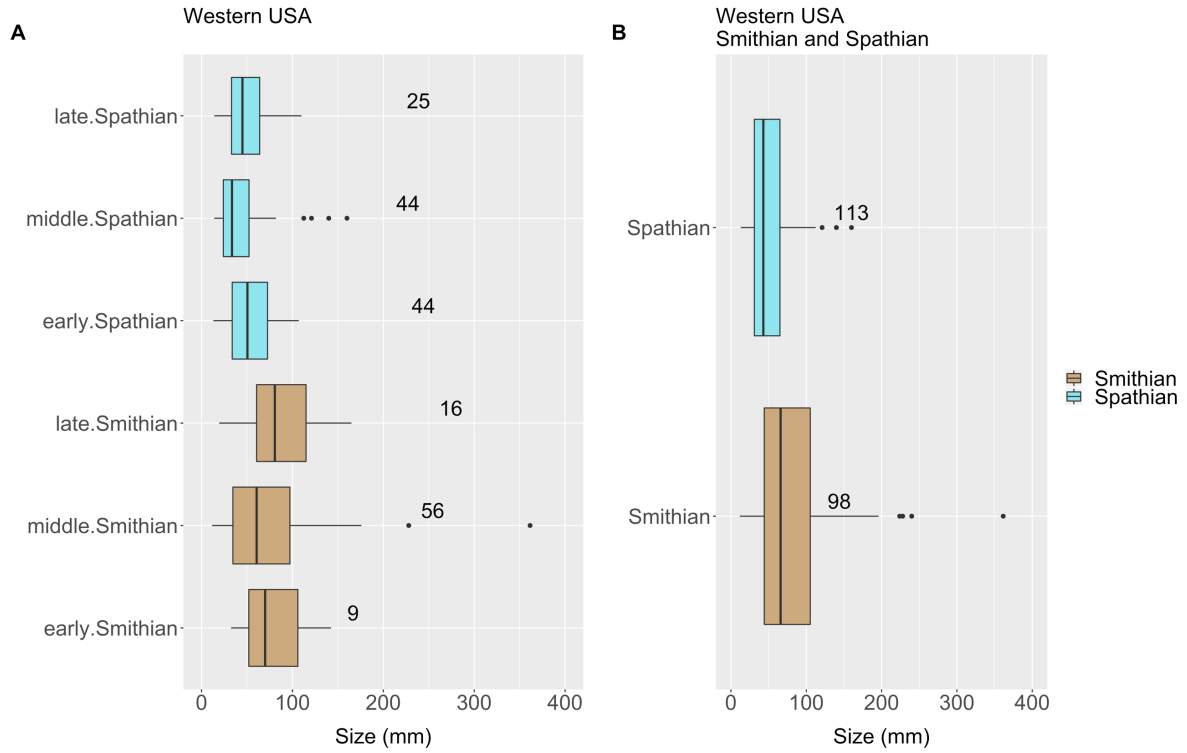


Figure 28: Boxplots of specimens collected in the Western US basin (including Western U.S. Sonoma basin locations, California and Star Peak Group). Statistical tests reveal a significant size reduction between Late Smithian and Early Spathian, Early and Middle Spathian and between Smithian and Spathian stages.

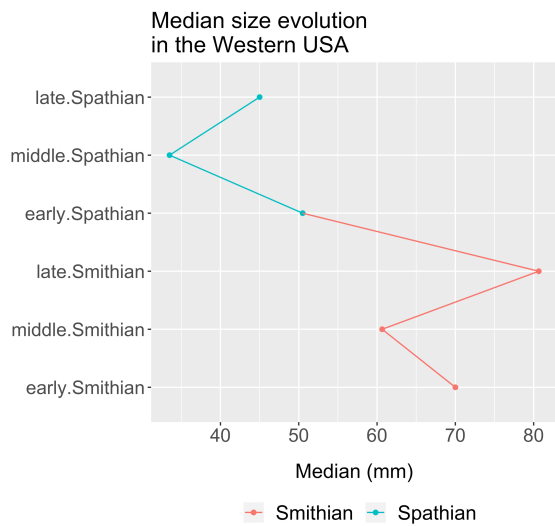


Figure 29: Evolution of the median maximal size through time in the Western US basin (including Western U.S. Sonoma basin locations, California and Star Peak Group).

4.2 Size patterns across space

Since the largest measured samples were found in the Boreal realm (from table 2 it can be seen that the boreal palaeolatitudes have the broadest size range) and since it is known from several studies (e.g. Atkinson and Sibyl 1997, Chapelle and Peck 1999) that organisms tend to be larger at higher latitudes, it seemed appropriate to investigate the presence of any latitudinal and/or longitudinal trends in size.

For the analysis the median size of the samples measured either at a specific palaeolatitudes or palaeolongitudes or at both coordinates at the same time was calculated. The analyses were implemented taking the Smithian and Spathian substages first together, then separately. On the basis of the outcomes of the statistical tests implemented on the larger timescale, the smaller time subdivisions, i.e. early, middle and late Smithian-Spathian, were not examined. This was also due to a lack of a sufficient diversity of palaeolocations for most of such small time partitions (which makes the implementation of linear models less and less feasible).

For the main outputs of the performed linear models and their detailed interpretations the reader is referred to the Appendix-Part 2 (pages VI to XXVII).

Fig. 30 shows the median size as a function of both palaeolatitude and palaeolongitudes for each hemisphere in different time subdivisions (both Smithian and Spathian together, figs. 30 A,B; Spathian figs. 30 C,D; and Smithian, figs. 30 E,F). The size and the colour of the dots show the position of the different sizes along the coordinates field.

A multiple linear regression was implemented on each of these time/space subdivision (see Appendix – Part 2, p. VII-XIV). Only very few points are present in the southern hemisphere, which represents an obvious bias when implementing a linear model (as the fewer the points, the easier a line can fit in). However, even with a few points, a trend of linear dependence could be found if present and strong enough, and it would be characterised by an excellent fit of a linear model. For this reason, multiple linear regressions were performed also in the southern hemisphere. It is however true that the graphic representation of the data itself already speaks against the presence of any noticeable size pattern.

Considering Smithian and Spathian together (fig. 30A,B; Appendix-part 2, pages VIII-IX), the R^2 values of the models of both northern and southern hemispheres indicate a very poor fit (resp. 26% and 25%) and the p-value of the F statistics indicates in both cases that the combination of the explanatory variables (palaeolongitude and palaeolatitude, also defined as *predictors*) may not necessarily be needed to explain the data. In other words, the size distribution that is observed in the graph may still be obtained (resp. in 14% and 57% of the times, according to the p-value of resp. the northern and southern hemisphere) even without the assumption of a linear dependence of size on latitude/longitude.

In the southern hemisphere the p-values of each independent variable (fig. 30A; Appendix-part 2, page IX) indicate that none of the predictors can explain the observed variance in size. Hence, no linear dependence can be established between size versus palaeolatitude and palaeolongitude.

On the other hand, in the northern hemisphere (fig. 30B; Appendix-part 2, page VIII) it would seem that (with a p-value of 0.05) the palaeolongitude might play a role into explaining the variance of size, while the

palaeolatitude still exhibit a p-value larger than 0.05, which argues against a linear dependence with size. A possible explanation for this is given later in this section.

Similar results are obtained when considering size patterns in Smithian times (fig. 30E,F; Appendix-part 2, pages X-XI). For both hemispheres R^2 indicates once again a very poor fit (18% in the northern hemisphere and 22% in the southern). Also the p-values of the F statistics, both $\gg 0.05$, reveals that the two predictors taken together are not a necessary and sufficient condition to explain the variance observed in size through space. In this case, the p-values of each explanatory variables are bigger than 0.05 for both hemispheres, which signifies that none of the variables plays a role into explaining the size variance and no linear relationship between the response (size) and the explanatory variables can thus be proposed.

Finally, size patterns in the two hemispheres throughout Spathian times (fig. 30C,D; Appendix-part 2, pages XII-XIII) still yields results that are almost identical to those obtained when taking both Smithian and Spathian as a whole. The fit of the models remains very poor (35% in the northern hemisphere and 27% in the southern).

Once more, the high p-value of the F statistic points to the two explanatory variables together as not necessary in order to reproduce the observable space distribution of size.

Lastly, in the southern hemisphere the p-values of each predictor (both > 0.05) indicate that none of the variables is decisive for explaining the size variation. On the other hand, in the northern hemisphere the palaeolongitude seems to be the predictor for which a slight linear dependence with the response variable can be suspected (p-value: 0.041). Therefore, just as was the case for the both stages taken together, palaeolongitudes would seem like the one explanatory variable that could potentially be considered relevant for explaining size variation.

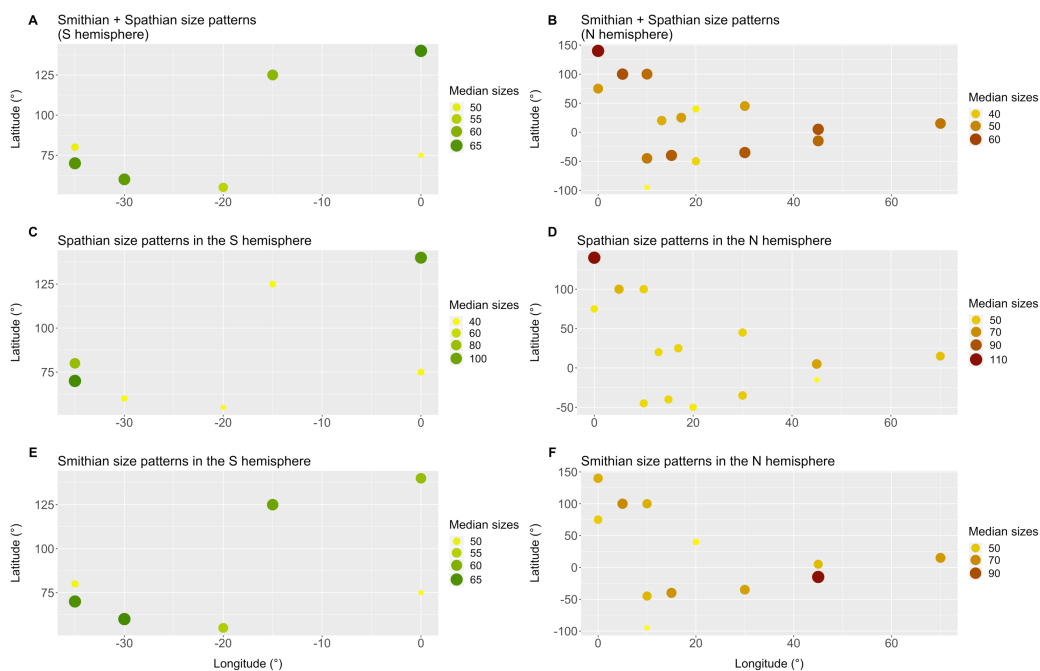


Figure 30: median size as a function of both palaeolatitude and palaeolongitudes for each hemisphere in different time's subdivisions. A,B: Smithian and Spathian stages taken together. C,D: Spathian; E,F: Smithian).

From these multiple linear regression, only one conclusion could potentially be drawn: while palaeolatitude never seems to play a role into the explanation of size change, palaeolongitude seems to hold a slight linear relationship with size, and to be somewhat relevant for promoting size variation in space. This was observed in case of the Spathian time and throughout Smithian and Spathian as a whole.

However, it still should be kept in mind that all these models are characterized by a very poor fit. A low R^2 value indicates that a linear model might not be the most appropriate model to describe observed size variation.

To corroborate any supposition, the effects of palaeolongitude and palaeolatitude are analysed separately through the aid of simple linear regressions (figs. 32, 34), to get a better view on the possible presence of trends. General graphs showing the amount of points found in each palaeolatitude (figs. 31, and Appendix-Part 2, fig. B1 page XXVI) and palaeolongitude (figs. 33, and Appendix-Part 2, fig. B2, page XXVII) and the fluctuations of the median size through space (in red) are given, both for the Smithian and Spathian substages as a whole, as well as separately and for their smaller time divisions (in the Appendix-Part 2, p. XXVI,XXVII). The latter (figs. B1 and B2 p. XXVI,XXVII, Appendix-Part 2) are given to illustrate any noteworthy difference with the higher ranking time subdivisions. However, the relative data subsets are not statistically analysed, because, as previously mentioned, too few locations are present for linear regressions of the two hemispheres. Given the absence of any major difference between the graphs of the smaller subdivisions and those of the bigger time spans, it can be asserted with confidence that the implemented analyses are sufficient in order to detect any significant size trend that might be present.

On a latitudinal scale, none of the linear models (fig. 32) reveals the presence of a linear relationship between palaeolatitude and size (see Appendix-Part 2, pages XV-XXI).

All models show a very poor fit, with R^2 values as low as 2% (e.g. Appendix-Part 2, page XVI and XX), large residual standard errors (high up to 2 cm in case of Spathian southern hemisphere, Appendix-Part 2, page XXI). All palaeolatitude p-values are much bigger than 0.05, pointing to a predictor unable to explain any observed variation in size. The southern hemisphere, as previously mentioned, includes too few data to discriminate between absence or presence of a latitudinal trend. The fact that no regression line can be fitted to such a small amount of data is remarkable, and argues against latitude playing any role for the observed size variation.

On a longitudinal scale (Appendix-Part 2, page XXII-XXV) similar results are obtained. All models (fig. 34) display a very poor fit (R value as low as 10^{-5} in case of Smithian stage, Appendix-Part 2, page XXIV), accompanied once again by rather large residual standard errors. The p-values (> 0.05) indicate that neither in Smithian nor in Spathian times can a linear relationship between size and palaeolongitude be recognized. A slight trend towards higher sizes for higher palaeolongitudes is detected when Smithian and Spathian are considered as a whole (p-value 0.02), though the model still displays a poor fit (R squared 0.25). However, a quick inspection of the relative scatterplot (fig. 33A) hints to the leftmost lowest extreme (palaeolongitude of -95°) to be an important driver of the fitted regression line. This point, however, is not only the median value of a smaller subsample of data but also lies in a very marginal position compared to the rest of the data (in other words, the gap between this point and the rest of the data is much bigger than for any other of the points). When this point is removed from the

test, no trend can be detected anymore (see Appendix-Part 2, page XXIII).

Based on these observations, the most reasonable conclusion seems to assume that, just as was the case for palaeolatitude, variation in palaeolongitude also does not have an effect on the observed size distribution.

Since all models have a very poor fit, according to the R squared values, it might be a reasonable claim that other type of trends should be investigated before concluding that there is no causal relation between latitude/longitude and size. However, the diagnostic plots of each model (in specific the plots of the residuals versus fitted values observable amongst them, see Appendix-part 2, page XIV and pages XVI-XXV) reveal no reason to suspect that the data might follow another trend (i.e. that they could be modelled through another mathematical function). The residuals appear in fact randomly distributed around the horizontal *residual = 0* line, and do not deviate all too strong from the normality line in the QQ-plot. All the considered diagnostic plots confirm the implicit assumption of linear regressions, i.e. that the residuals should be normally distributed, and hence give reason to believe that the implementation of a linear model is justified. The poor fit and the absence of a trend might therefore signify that the observed distribution of size is indeed independent of latitudinal and longitudinal variations.

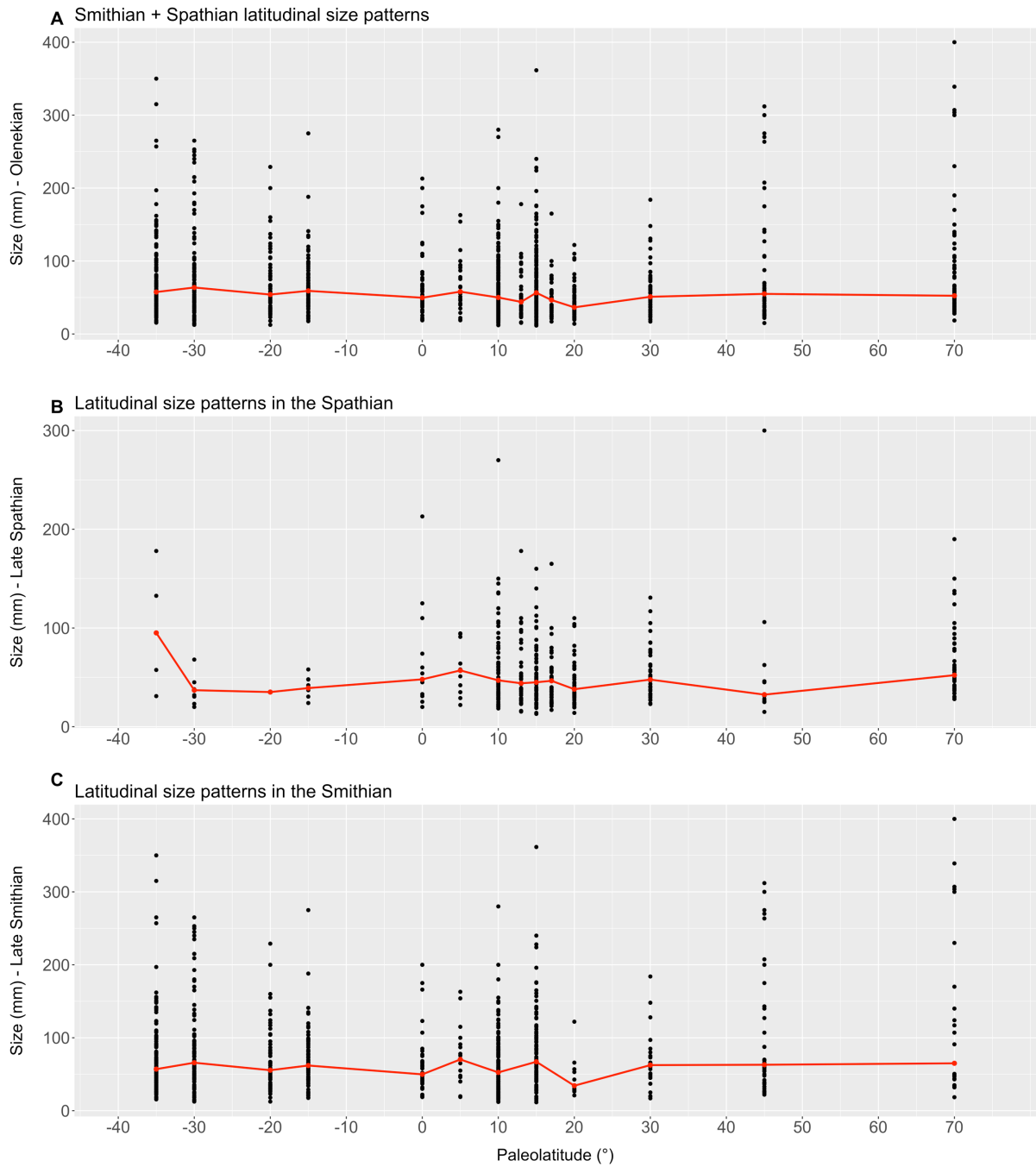


Figure 31: Graphs showing the amount of points found in each paleolatitude during A) both Smithian and Spathian times taken together B) Spathian and C) Smithian times and the fluctuations of the median size through space (in red).

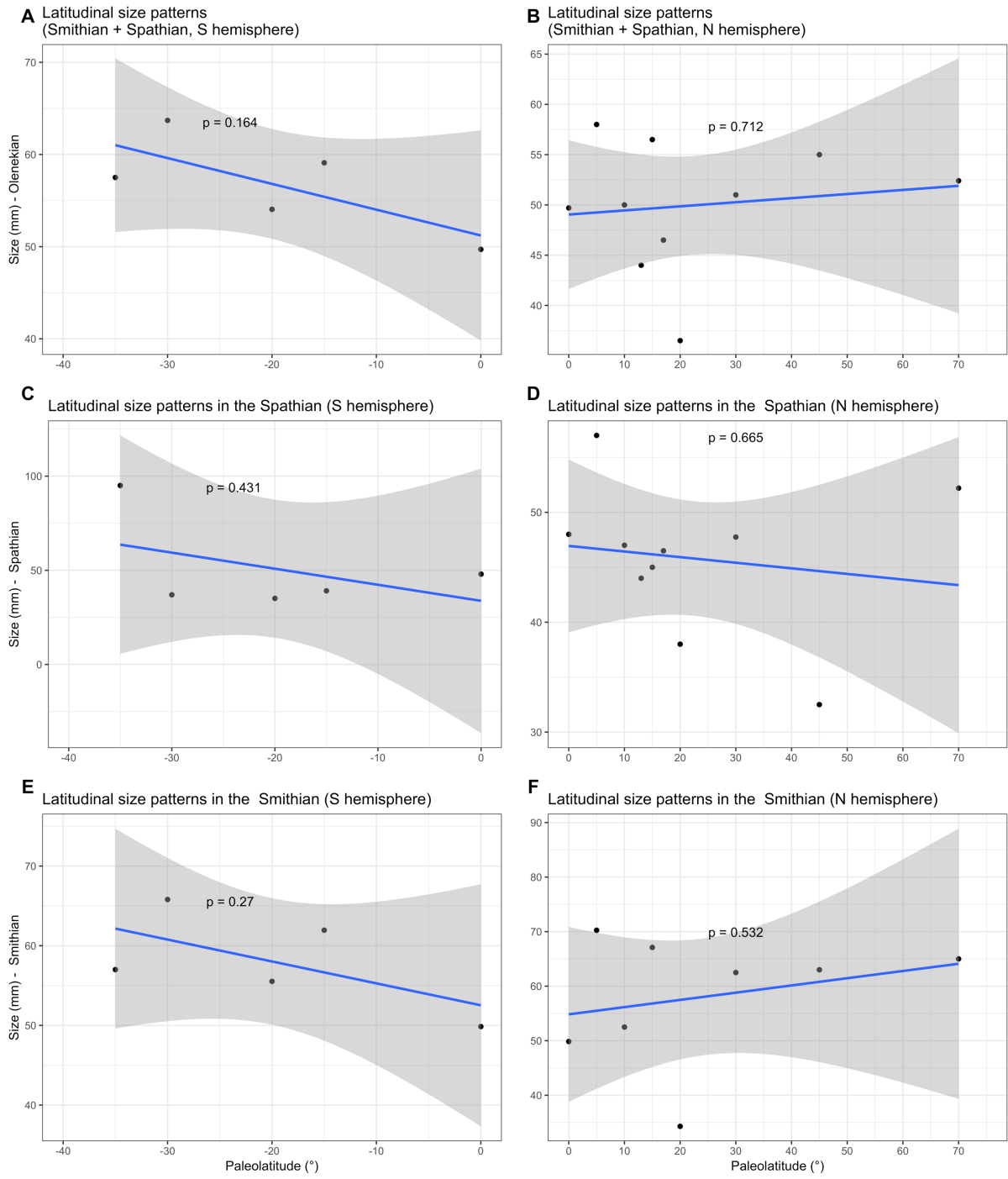


Figure 32: Simple linear regression model to observe the effect of palaeolatitude for A) both Smithian and Spathian times taken together; B) Spathian and C) Smithian times

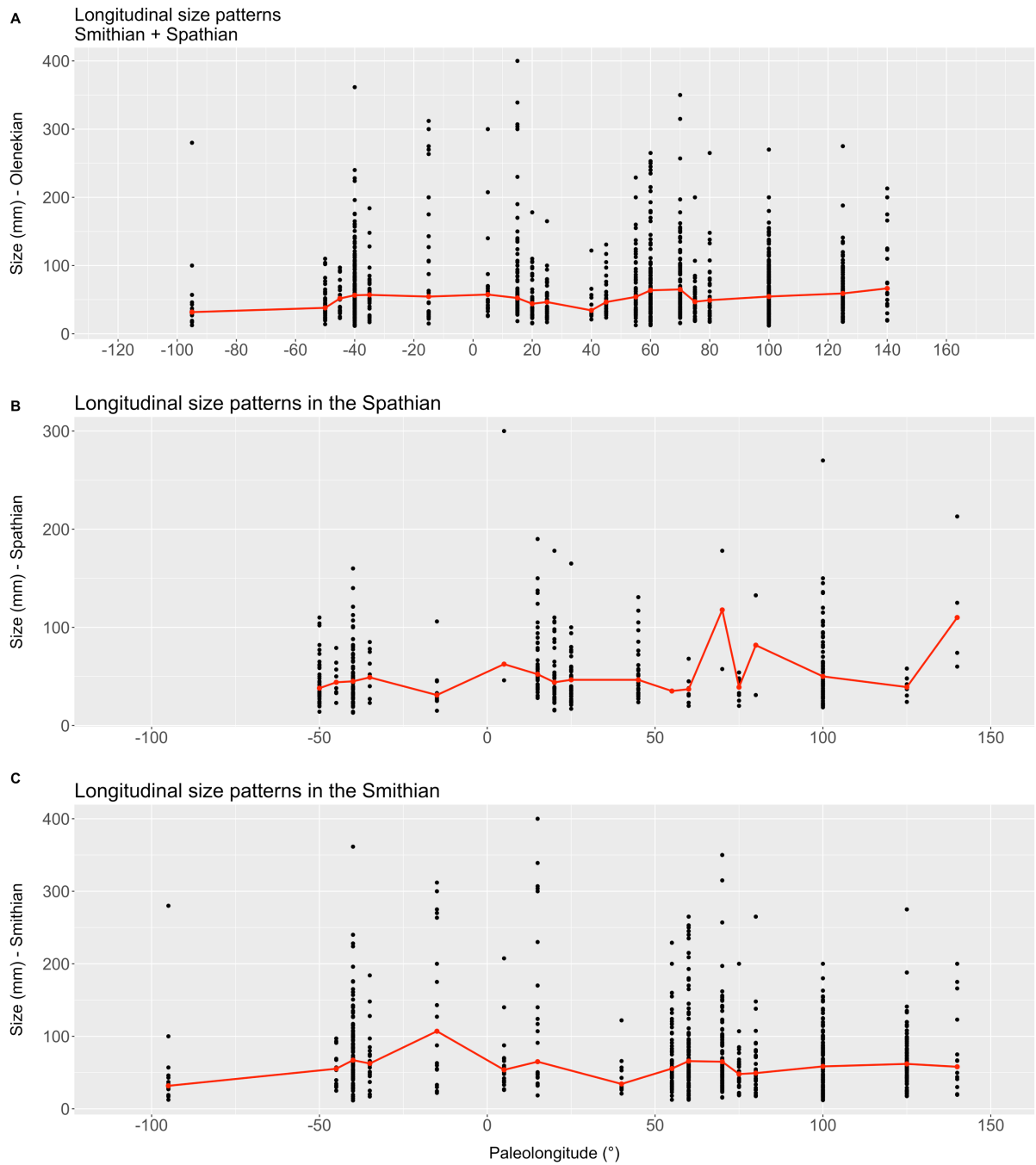
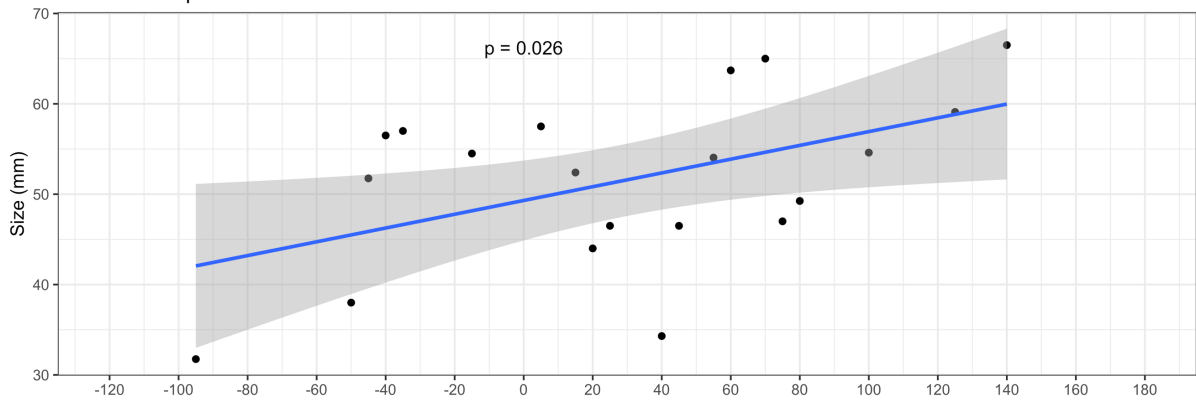
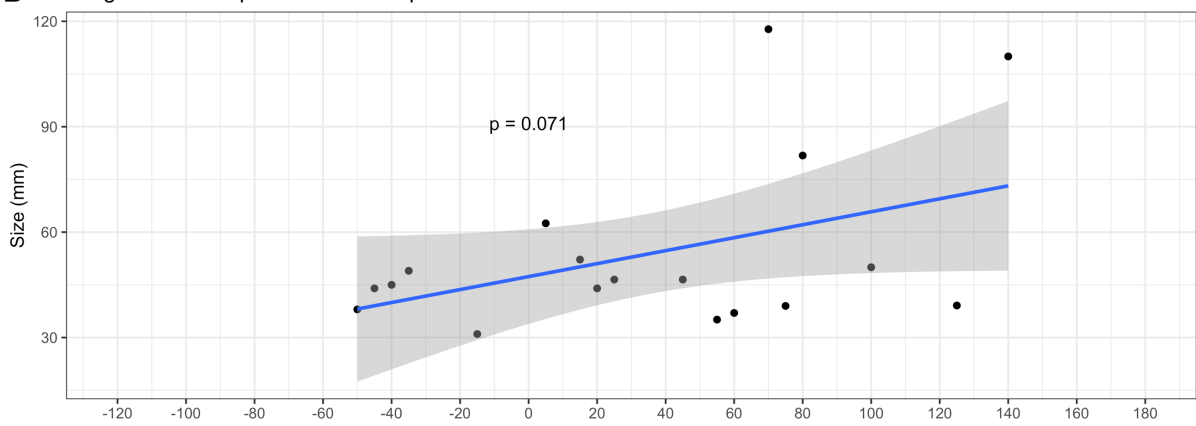


Figure 33: Graphs showing the amount of points found in each palaeolongitude during A) both Smithian and Spathian times taken together B) Spathian and C) Smithian times and the fluctuations of the median size through space (in red).

A Longitudinal size patterns
Smithian + Spathian



B Longitudinal size patterns in the Spathian



C Longitudinal size patterns in the Smithian

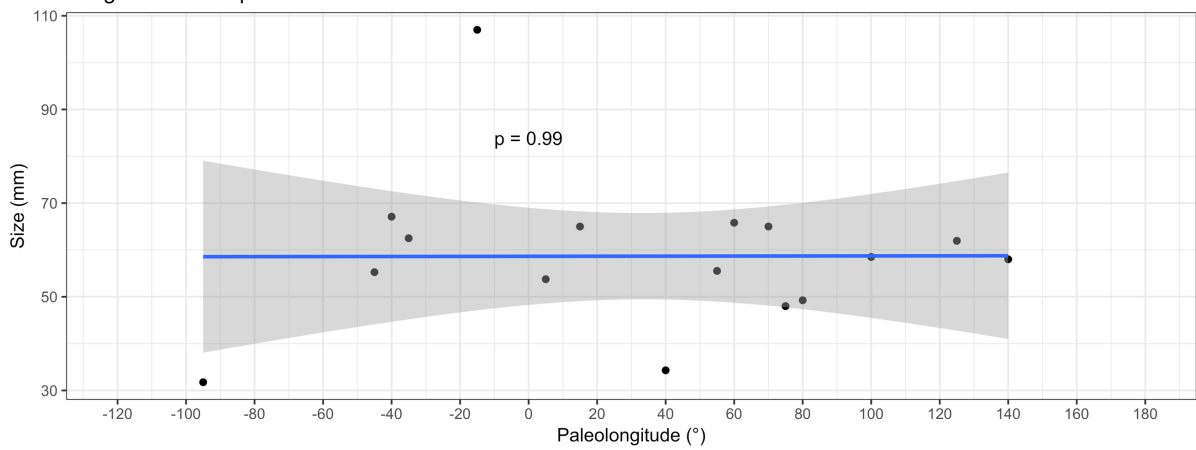


Figure 34: Simple linear regression model to observe the effect of palaeolongitude for A) both Smithian and Spathian times taken together; B) Spathian and C) Smithian times

5. Discussion

5.1 Interactions between environmental and ecological parameters and body size

Size is not a constant parameter within a species. It is affected by many factors, which can in turn impact the trophic interrelations within food webs (a thorough and more detailed description of the concepts discussed in this section, can be found in Locatelli's UZH Academic Internship Report, 2017).

5.1.1 Temperature

Among the most important parameters influencing body size, temperature has proven the most crucial for extant cephalopods. Rosa et al. (2012) observed a strong negative correlation between temperature and cephalopod body size, in agreement with Atkinson's (1994) "temperature-size rule", according to which lower temperatures result in lower growth rates and delayed maturation, but also in larger body sizes. Rosa et al. (2012) revealed that it is indeed SST to have the biggest impact on body size, while net primary productivity, resource availability, seasonality and competition only seem to play a limited role in comparison.

The negative correlation between temperature and size is observed also in other extant marine clades. Ansell (1968), compared the rate of growth of *Mercenaria mercenaria* throughout a broad geographical range, and observed that despite the clams displayed similar annual growth throughout the continuous geographic range, seasonal growth variations in the different areas were observed: in the northernmost areas growth was restricted to summer months, with little activity of the organism and no growth during the other months, while further south, the more extended growing season allowed extended growth.

Rosa et al. (2012) also observed a strong impact of latitude on body size, with an evident increase in body size towards the poles at the class (Cephalopoda) level. A latitudinal trend during Smithian and Spathian time intervals is clearly absent from our results, despite the biggest specimens have indeed been measured at high latitudes. This could relate to the geologically high amplitude changes that characterised Early Triassic climate or simply to insufficient data at latitudinal/longitudinal scale.

The impact of temperature on body size was also detected by Wood and O'Dor (2000), who observed that temperature influences growth rate and time of maturation and therefore maximal achievable body size of cephalopods (based on their assumption that a delayed maturity speaks for larger body sizes).

5.1.2 Nutrients

Another important parameter affecting body size in marine environments is food availability, despite not being the dominant factor for extant cephalopods (Rosa et al. 2012; Wood and O'Dor 2000). Ansell (1968) noted that even where temperatures remained constant, growth of the venus clams did not remain steady, but followed concentration of the particulate matter in water. The importance of food resources for population body size is

evident, for example, within r- and K-selection theories. Where resources are more prone to fluctuation, such as in unstable environments, populations must develop with the ability to adjust to rapid shifts in food availability (Valentine, 1971). It follows that in unstable environments, where unpredictable and variable mortality factors act indiscriminately on any population size and phenotype, organisms tend to concentrate most of their resources into generating as many offspring as possible (Adams 1980). These organisms (r-strategists) are then usually characterized by an early and single reproduction phase, a large number of offspring, quick development with rapid growth rates, and small body size (Pianka, 1970), the latter explained by the biological trade-off between small size and large reproductive rates (Southwood et al. 1974). On the other hand, in more stable environments, species (K-strategists) tend to utilize their resources into increasing their fitness, hence into competitive abilities rather than into productivity (Adams, 1980). Organisms are thus characterized by a delayed maturity, extended reproduction time, lower growth and mortality rates, longer life span and larger body size (Pianka, 1970), the latter resulting in an easier development of competitive abilities (Southwood et al. 1974). Despite the evident importance of food availability in organisms ecology, resources availability does not seem to be the main limiting factor for cephalopod maximal achievable body size, as previously mentioned. In fact, as pointed out by Westermann (1996), ammonoids must have exploited a broad variety of food sources, and, like extant cephalopods, they were characterised by a wide variety of feeding habitats. Similar to extant cephalopods they could have thus developed migratory behaviours to exploit seasonal resources (Rosa et al. 2012; Brayard et al. 2006). Predation seems to impact cephalopod size much more deeply than food (Wood and O’Dor 2000), considering the large amount of potential cephalopods predators (Rosa et al. 2012): the larger the predation risk, the smaller the size cephalopods tend to (Wood and O’Dor 2000; see section 5.1.5)

5.1.3 Oxygen availability

Other important factors impacting body size include oxygen availability and calcium carbonate saturation level. Chapelle and Peck (1999) have associated “polar gigantism” (i.e. the large body sizes characteristic of cold aquatic regions) with oxygen availability, which limits the maximal achievable size and which becomes relatively more important than other ecological factor as size increases. Similarly, Atkinson and Sibly (1997) state that, since in aquatic environment oxygen availability decreases with increasing water temperature, an initially fast growth for organisms living in high temperatures might be slowed down already at small body sizes as soon as oxygen supply becomes limiting. Aside from temperature, oxygen solubility is also controlled by salinity of water, with oxygen solubility increasing as salinity decreases, which stresses the importance of the latter factor in constraining body size as well (Chapelle and Peck 1999; O’Dea and Okamura 1999).

5.1.4 Calcium carbonate saturation level

Finally, the ability of marine organisms such as ammonoids to grow their calcareous shell also depends on the availability of carbonate ion in water as well as on pH (Fabry et al. 2008; Gazeau et al. 2007). Calcification rates decline with declining CO_3^{2-} concentrations (i.e. with declining calcium carbonate saturation and pH, i.e. with

ocean acidification), which decrease with increased oceanic uptake of CO₂ (according to the reaction: CO₂ + CO₃²⁻ + H₂O → 2HCO₃⁻) (Orr et al. 2005).

5.1.5 Body size and trophic relations

While body size is influenced by a large range of parameters it is also strongly related to many aspects of a species ecology that deeply influence trophic relations; for example, size is related to a species' energetic demands, to its spatial use of resources, its interaction with other components of the food web, its life history traits and longevity (Woodward et al. 2005). As such, *maximal* size measurements can be used as a proxy to observe changes of trophic levels through time within a clade. Trophic levels represent the positions that organisms occupy in the food web and are graphically expressed through the aid of *food pyramids* (Elton 1927). The connection between the position of organisms within the food pyramid and their body size mostly relies on the observations that predators usually become progressively larger with higher trophic level (Elton 1927; see also Trebilco et al. 2013) and, depending on its size, a predator can subsist neither on an organism above a certain size (due to morphological constraints) nor on one below a certain size (since it would become difficult to find a big enough amount of small organisms to satisfy its energy needs) (Elton, 1927). Commonly accepted paradigms supporting the size based hierarchical sequence of trophic interactions within a food web (Woodward et al. 2005, Arim et al. 2010) state that: i) predators are usually larger than their prey; ii) predator size increases with increasing prey size (Cohen et al. 1993; Wilson, 1975); iii) the higher up in the trophic chain the bigger the predator (Cohen et al. 1993; Elton, 1927; Warren and Lawton, 1987); iv) the range of prey sizes increases with increasing predator size and the smaller the prey, the more abundance of predators is to be expected (Cohen et al. 1993; Scharf et al. 2000; Wilson, 1975). For these reasons, statistically significant changes in maximal size of an organism can help us infer how it moved through the levels of its trophic chain through time, and speculate on the evolution of trophic conditions throughout that period.

From the prevailing maximal size, hypothesis can also be attempted regarding the predators related pressure during that time. It would be expected that a decreased risk of predation would lead not only to larger sizes of preys populations, (which are associated with smaller individuals; Pianka 1970; see section 5.1.2), but also to a reduced selection against smaller individuals. In fact, especially in marine realm, predation on large preys is often limited by morphological constraints such as gape size limitations (e.g. Labropoulou and Eleftheriou 1997; Scharf et al. 2000) and preys' mobility (Folkvord and Hunter, 1986). Bigger preys have a lower chance of fitting a predator's mouth apparatus and an increased chance of escaping predation due to a usually higher mobility. Predators would thus be expected to prefer smaller sized prey and a prevalence of larger sizes could therefore speak for high predation abundance. However, contrary to expectations, a study on extant cephalopods has demonstrated the existence of a trade-off in coleoids between maturing early at a smaller size, and maturing late at a larger size. The earlier coleoids mature, the more prone they are to avoid predation and thus increase their fitness (Wood and O'Dor 2000). The latter research thus states that maximal achievable size is highly impacted by predation, and, in case of coleoids, the lower the abundance of predators, the larger the size they can develop. Since phylogenetic studies have suggested that coleoids would be a more appropriate model than

the Nautilus to interpret ammonoids' mode of life (Jacobs and Landman 1993), it can be assumed for ammonoids as well that a larger size might speak for a relaxation of predators' induced stress. Considering, however, that prey vulnerability is impacted by many different variables that rely on the predator's predatory strategies as well as on preys' and predators' swimming abilities, this remains a generally simple but viable hypothesis.

5.2 Size changes throughout Smithian and Spathian – an overview on climate upheavals

The analysis outlined above have shown that statistically significant reduction or increase of ammonoid size occurred multiple times throughout the Smithian-Spathian substages, though not homogeneously throughout the Triassic ocean. Overall, the observed changes seem to correlate with the major climatic upheavals that characterised the Smithian-Spathian stages of the Early Triassic. Unstable and rapid climate changes have been observed on a global scale. Romano et al. (2013), through the aid of oxygen isotopes (see fig. 1), detected in the Salt Range record (Pakistan) a warming of seawater temperature of 4°C building up towards the late Smithian, characterised by low $\delta^{13}\text{C}_{\text{org}}$ and $\delta^{13}\text{C}_{\text{carb}}$ values (the latter detected in South China by Payne et al. 2004), and a cooling trend developing at the base of Spathian, accompanied by a positive excursion of $\delta^{13}\text{C}_{\text{org}}$ and $\delta^{13}\text{C}_{\text{carb}}$ at the SSB (once again, the latter observed by Payne et al. 2004, in South China). Due to short-termed depositional breaks in the area, the authors could not observe details of the $\delta^{18}\text{O}$ pattern during the very early Spathian. New insights on climatic disturbances around the Smithian-Spathian Boundary (SSB) could however be given by the recent work of Goudemand et al. (2019); oxygen isotopes measurements from the same area agree with the results of Romano et al. (2013), but reveal a clearer climatic pattern, characterised by 1) a cooling interval in the early Smithian; 2) a thermal maximum in the middle Smithian (contrary to Sun et al.'s (2012) assertion of a late Smithian Thermal Maximum) with warm temperatures persisting until the early late Smithian; 3) a second cooling interval in the late late Smithian-early Spathian; 4) mid-Spathian temperatures comparable with those of mid-Smithian time; 5) renewed cooling around the late Spathian, also observed by Song et al. (2014) through isotopic measurements from South China, and indicated by the evolution of oxygen isotopes in the Salt Range (Romano et al. 2013). Romano et al. (2013; fig. 1) observed that evolution of oxygen isotopes positively correlates with the carbon isotopes trend in the Salt Range, which, in turn, parallels the carbon isotopes curves of other localities both in the Tethyan and Boreal realm (e.g. Tian et al. 2014; Galfetti et al. 2007c; Hansen et al. 2018). For this reason, they infer oxygen isotopes from this Tethyan locality to parallel *global* climatic changes. Indeed, Horacek et al. (2007) found a similar carbon isotopic trend in Italy, i.e. in the Palaeotethys, specifically observing a steep rise of $\delta^{13}\text{C}_{\text{carb}}$ at the SSB, and the same carbon isotopes evolution was observed in South China by Tian et al. (2014) and Galfetti et al. (2007a), in the Arctic Canada by Grasby et al. (2013) as well as in the western US (Thomazo et al. 2016).

Isotopic measurements therefore confirm this positive late Smithian $\delta^{13}\text{C}_{\text{carb}}$ excursion to be associated with a cooling event, while the middle Smithian negative shift is associated with a warming event (Romano et al. 2013; Song et al. 2013, 2014).

Hermann et al. (2011) observed a prominent spore spike during the middle Smithian, and a shift from lycopod dominated vegetation to a gymnosperm dominated one during the late Smithian-early Spathian. Proliferation

of spores is usually associated with more humid conditions, while gymnosperms reflect a drier environment. Combined with oxygen isotopes data, this allows to infer a shift from prevailing warm-humid conditions from the middle Smithian, to cool arid conditions during the early Spathian (Galfetti et al. 2007c, Hochuli and Vigran 2010, Hermann et al. 2011, Romano et al. 2013, Hochuli et al. 2016). As previously mentioned (see section 2.4), the ammonoid extinction that took place at the end of the Smithian stage, might have been induced by the combination of sea level fall caused by the late late Smithian-early Spathian cooling, perhaps in combination with the ocean acidification (Galfetti et al. 2007c, H. Bucher ongoing work). The strong warming observed in the middle - early late Smithian, is assumed to have been caused by a massive release of volcanogenic CO₂ from the Siberian Traps (Galfetti et al. 2007a). The causes of the end Smithian extinction are still debated, but the appearance of the sedimentary gap associated with the extinction only at the end of the late Smithian suggests that diverse processes must have been at work, before the cooling would become strong enough to cause a glacio-eustatic sea level fall accompanied by such intense extinction. Possible mechanisms leading to the cooling may include silicate weathering and the biological pump as sinks for atmospheric CO₂. Alternatively, injection of sulphur-rich volcanic volatiles by the Siberian traps may conceivably have led to a volcanic winter (H. Bucher, ongoing work).

5.3 Size reduction from Smithian to Spathian

The above mentioned climatic observations can be compared to the observed size changes.

A statistically significant size change is to be observed between Smithian and Spathian taken as a whole, as well as between late Smithian and early Spathian (where the comparison was possible) in all considered palaeoregions except for South China and for the Palaeotethys region (and for the Afghanistan block), which will be specifically addressed in the next section. Such a change obviously correlates with the end Smithian extinction. In fact, extinctions have often been associated with a reduction of the size of faunal elements, a characteristic that is usually defined as “Lilliput effect”, (Harries and Knorr 2009; see also Academic Internship Report, Locatelli 2017). The Lilliput effect implies either *faunal stunting*, (i.e. a species sorting, which sees smaller taxa preferentially surviving over larger species), *dwarfing* of the fauna (after which selected smaller descendants of a certain lineage that show a morphological correspondence with their ancestral taxa remain) or *miniaturisation* of clades (i.e. the appearance of new lineages, during an extinction phase, which are usually characterized by a small size and considerable morphological changes relative to their ancestors) (Harries and Knorr 2009). The latter has been observed, for example, by Landman et al. (1991) in Mesozoic ammonites, whose progenetic species show small size at maturity as well as specific features typical of the juveniles of more primitive species, despite none of these progenetic species correspond entirely to the juvenile stage of their primitive ancestors. In short, the “Lilliput Effect” implies a temporary body-size reduction within survival clades (Brayard et al. 2015). At the SSB the biggest turnover of the Early Triassic ammonoids is recorded (Brayard et al. 2006), and the definition of “Lilliput effect” might therefore not be quite appropriate. The fact that ammonoid size decreases in Spathian time, i.e., in specific, during early Spathian, agrees with the empirical observation that new taxa tend to arise at relatively smaller body sizes (Stanley 1973).

Considering however the duration of the Spathian stage (ca. 2.5 to 3Myr, more than half of the duration of the entire Early Triassic; Ovtcharova et al. 2006) and the more stable environmental conditions that characterised it, the lack of a more pronounced size recovery during that time seems noteworthy and somewhat paradoxical. In fact, abiotic changes such as strong climatic upheavals are usually thought to be the main driver of evolutionary change (a concept referred to as the *Court Jester* hypothesis; see review of Voje et al. 2015), as it seems to be the case throughout the Smithian. According to the classical r-K selection theories, populations composed of larger individuals are then expected to prevail during times of stable environmental conditions (Pianka 1970, Adams 1980). This is however not what is observed during the Spathian: the prevailing smaller size detected throughout the time interval would seem to indicate that the more stable environmental conditions allowed biotic (i.e. increased predation pressure) rather than abiotic factors to play the preponderant control over ammonoid body size (*Red Queen* hypothesis; see review of Voje et al. 2015). In specific, it would seem that increased predation pressure could have affected ammonoid body size the most throughout the considered time interval, although the warm temperatures recorded in the middle Spathian might have certainly had an influence as well. Evidence of a potential increase of ammonoid predators during this time is in fact reported by Scheyer et al. (2014; see section 2.5). A radiation of marine reptiles is recorded from the Spathian stage, which includes taxa with high mobility and durophagous forms (Bardet 1994; Scheyer et al. 2014); moreover, as previously mentioned, evidence of food pyramids including the high trophic levels of large aquatic predators has been reported from the Spathian of North America (Brayard et al. 2017) and Japan (Nakajima and Izumi 2014), further confirming the presence of potentially varied ammonoid predators during that time. Assuming that the hypothesis advanced by Wood and O’Dor (2000) can be considered valid for ammonoids as well (i.e. the higher the abundance of predators, the smaller the size that cephalopods will tend to; see section 5.1), the larger amount of Spathian predators could indeed be one plausible reason for the prevailing smaller size of the entire Spathian stage.

While the relative contribution of abiotic and biotic factors as determinant drivers of ammonoid size still remains unresolved, it seems clear that, as far as ammonoids are concerned, body size cannot be read at face value as a dichotomy along a simple r-K axis.

5.4 The South China block and the Palaeotethys

No size change is observed throughout the Smithian and Spathian stages in the South China block, in the Palaeotethys semi-enclosed basin, or in the Afghanistan block (although for the latter, statistical tests could be biased by the limited amount of available specimens). The Kolmogorov-Smirnov and Mann-Whitney–U tests have revealed no statistically significant difference between populations size and distributions of these two palaeoregions throughout Smithian and Spathian times (see Appendix-Part 1, table 10B). However, when the regions are compared (by means of the two tests) to most other palaeoregions (Neotethys, Boreal domain and Western US; see Appendix - table 10A-C) a significant smaller size is observed in South China, in the Palaeotethys and in Afghanistan (Smithian median size: 48 mm; Spathian median size: 39 mm) during the Smithian stage, while very little significant change is observed during Spathian times (the only clearly significant difference is the

larger maximal size reached in South China, compared to the smaller median size measured within the Neotethys).

None of the regions in question were immune to the climatic upheavals that took place on a global scale during the Early Triassic.

Wei et al. (2015) observed how the early early Smithian of South China was characterised by cooler temperatures accompanied by a contraction of oceanic oxygen-minimum zones. This was followed by an expansion of the available ecospace, as well as an intensified marine productivity explained by increased terrestrial weathering fluxes and by an enhanced thermohaline circulation typical of colder intervals. The middle-late Smithian in the same area witnesses a shift to intensified anoxic conditions (i.e. expansion of the oxygen-minimum zone and following reduction of ecospace) probably due to enhanced water column stratification and increased riverine nutrient inputs from intensified terrestrial weathering fluxes typical of warmer climates. Productivity proxies in the deeper water sections of South China indicate an increased productivity but, according to Wei et al. (2015), this could be explained by enhanced preservation of organic matter due to the spreading of anoxia, rather than by actually higher productivity. However, if, as previously suggested, warmer temperatures and increased weathering did indeed enhance productivity (see section 5.2), this could also be connected to the absence of significant size changes (though not being the main driver): in fact, if primary productivity had been shut down, trophic relationships would have been impacted and a change in size change (which is usually closely related to changes in trophic level) would have probably been noticed. On the other hand, if we accept the hypothesis of Wood and O'Dor (2000), that the higher the predators pressure, the smaller is the size of cephalopods, an enhanced primary productivity that would logically be able to support higher trophic levels, should speak for a reduced ammonoid size. A probable hypothesis could therefore be that an increased nutrient recycling might have contributed to keeping marine productivity at a constant level throughout the Smithian, *enhancing* it relatively to what would be expected in stratified, anoxic conditions, so that trophic relationships and size also remained constant throughout the warmer intervals.

During the Spathian, Wei et al. (2015) observed in South China large declines in terrestrial weathering fluxes accompanied by a decline of marine anoxia and of the overall primary production (with the exception of a peak in the early Spathian), the latter suggested to be the consequence of the reduced weathering rates that characterise cold climate. It is assumed that cooling episodes such as those of early Smithian and early and late Spathian might steepen equator-to-pole sea surface temperature (SST) gradients, thus allowing a regeneration of ocean thermohaline circulation and of nutrients upwelling from deep water into the surface layer (Romano et al. 2013, Song et al. 2014, Stebbins et al. 2018). This could possibly sustain surface water productivity (as it was observed by Wei et al. - 2015 - in the Early Spathian) and organic carbon sinking flux. Improved ocean ventilation, reduced anoxic conditions and more stable environmental conditions (Wei et al. 2015), possibly combined with a slightly higher amount of oxygen that can be dissolved within colder waters (Atkinson and Sibly 1997), might thus contribute to explain the absence of a significant size reduction that is usually expected after an extinction.

All these climatic changes taken into account, the absence of any significant size change throughout both stages in the three localities remains striking, and a general attempted (and probably most reasonable) explanation

might be given by the palaeolocations of these regions. As previously mentioned, temperature is the parameter that most affects cephalopod body size (Rosa et al. 2012). All three regions were close to the equator during Early Triassic times and boreal latitudes usually suffer most of the consequences of climate warming relative to equatorial regions. The fact that most significant differences between the three regions and the others are mainly observed in Smithian times might support this hypothesis: indeed, the Smithian was characterised by a much more unstable climate than the Spathian, with the most significant climatic upheavals taking place throughout the Smithian and at the SSB. Warmer temperatures typical of equatorial regions might have damped the effects of such climatic upheavals on cephalopods during the unstable environmental conditions of the Smithian time interval. Moreover, the smaller amount of oxygen that can dissolve in warmer waters, might have kept Smithian ammonoids at a smaller size in these regions, so that no significant change could be detected when the cooler and more stable Spathian climate replaced the unstable previous environmental conditions. In the Palaeotethys region, of the two implemented statistical tests, only the Mann-Whitney-U test shows in all cases a significant difference between the Smithian of the Palaeotethys and of the other Palaeoregions. However, the tests could be biased by the poor amount of Smithian specimens measured within the semi enclosed basin, and, as a matter of fact, the same bias could explain the absence of a size reduction between Smithian and Spathian. Indeed, the specimens from Smithian that could be used for the analysis within this palaeoregion, are not only very limited (see section 4.1), but also all belong to the middle Smithian. No statistical differences have been observed between South China and the Palaeotethys when the available time intervals were compared, but the assumption that size within the Palaeotethys might differ from the other regions the same way as South China's (and Afghanistan's) median body size does is very speculative. Lastly, surface oceanic currents might also have played an important role, as suggested by Brayard et al. 2009b, when taking into consideration taxonomy patterns and dispersals. Their work proposes a strong reorganization of oceanic circulation between Smithian and Spathian, and, in specific, proposes a system of gyres to characterize Spathian times, the most prominent one being the North Tethyan gyre that possibly transported taxa to the western equatorial Tethys and then brought them back along the Cathaysian terranes. If this type of circulation was indeed present during Spathian times, the nutrients brought along with it in such a circular motion within the Palaeotethys and the Eastern Tethys (South China block), aside from sustaining trophic relations, might also be a further explanation for the size similarities observed within the three regions, at least during Spathian times.

5.5 The Neotethys

In the Neotethys region on the other hand, (both in the seamounts of Oman and Timor and in the rest of the NIM and both with and without Afghanistan), results show a negative correlation with sea surface temperatures, as would normally be expected.

During the colder period of the early Smithian, when more oxygen can be dissolved in waters (Atkinson and Sibly 1997) and thermohaline circulation is more active (Song et al. 2014), ammonoids are characterised by the largest size, and a significant size reduction is observed when the climate starts to warm toward the middle Smithian

thermal maximum and less oxygen can be dissolved in water.

No statistically significant size change is observed between the middle and late Smithian, and this observation is consistent for all considered palaeoregions. A possible explanation might be the fact that warm temperatures persisted until the early late Smithian while the cooling only started subsequently, in the late late Smithian.

In any case, the absence of size changes during this time might be interpreted as absence of changes within the trophic levels, which would oppose Sun et al. (2012) view of an “equatorial marine vertebrate eclipse” (EMVE) during the Late Smithian. No comparison between the late Smithian and the early Spathian could be made, but the statistical analyses show a significant reduction of size between the late Smithian and the middle Spathian. Aside from the size reduction associated with the end Smithian extinction, mid Spathian temperatures comparable to those of middle Smithian (Goudemand et al. 2019) could support the observed size reduction, in agreement with Atkinson’s (1994) “temperature-size rule”.

5.6 The Boreal domain

In the Boreal region the only observed change is the one between Smithian and Spathian taken as a whole, justifiable by the end Smithian extinction (and partially by a probable increase of predatory pressure), as previously discussed. The most striking observation is probably the absence of significant size changes between late Smithian and early Spathian as well as between the middle Spathian and the cooler intervals preceding and following it. In fact, boreal regions are the most sensitive to temperature changes and they would be expected to be highly impacted by them. In both cases, the late Smithian-early Spathian, as well as the early and middle Spathian, absence of size change could be explained by the small number of specimens that could be measured from the early Spathian.

Alternatively, the anoxic conditions documented, for example, in the Sverdrup Basin of the Canadian Arctic during the late Smithian, followed by an early Spathian reoxygenation (Grasby et al. 2013), might have contributed to smaller resp. larger size during the two time intervals. Similarly, increasing anoxic conditions observed during the early and middle Spathian (Hansen et al. 2018, Grasby et al. 2013) could contribute to the absence of a significant size change within the Spathian, since an oxygen depauperation could prevent size from recovering to larger values even during the Late Spathian cooling. This hypothesis would however imply that in the colder palaeolatitudes oxygen is a more limiting factor for ammonoid body size than temperature (as opposed to the lower palaeolatitudes, where temperature has been proven to play a larger role with respect to cephalopod size changes).

However, it should be noted that boreal record is globally characterised by a very low carbonate content, which induces a considerable preservation bias in the ammonoid record. It would be therefore reasonable to assume that such a discontinuous fossil record prevents us from confirming the validity of the obtained statistical results.

5.7 The pull-apart basinal area of the Western U.S.

The Western U.S basin shows once again the size reduction between Smithian and Spathian times that is expected in the aftermath of the extinction. In agreement with all other considered palaeoregions, no significant size change can be detected between the middle and the late Smithian (see section 5.5 for a possible explanation). Contrary to expectations, this palaeoregion is characterised by the absence of size changes between the early and the middle Smithian. This result is most likely related to the small number of specimens measured from the early Smithian compared to the middle Smithian. The early Smithian of the Western U.S. basin is in fact characterised by a very poor ammonoid record, and such preservation bias would undoubtedly impact any related statistical results.

The early Smithian poor ammonoid preservation might be explained by the progressive advance of the marine transgression phase within the complex and contrasted palaeogeography of the area which, as opposed to the other analysed palaeolocations, is part of an active margin. The epicontinental basin was characterised by irregular shorelines and very shallow environments in the earliest Smithian. The beginning of the Smithian transgression within the basin is recorded in central Utah, in the earliest Smithian. Subsequently, driven by regional tectonic subsidence, the transgression proceeded southward, following a central corridor, and did not expand in all directions from the basin *depocenter*. Maximal transgression levels and true open sea conditions in which ammonoid deposits could form were reached in the late Smithian (Brayard et al. 2015; in contrast to the regression phase recorded in this time in the other considered localities) and were only restricted to certain areas such as Central Utah. They never reached North-Eastern Nevada (Crittenden Springs) or the Northernmost (e.g. Wasatch Mountains) and Southernmost Utah (Brayard et al. 2013).

An expected significant size reduction can also be observed between late Smithian and early Spathian. Finally, the statistically significant size decrease that can be observed between the early and middle Spathian can be related to the warm middle Spathian temperatures that have been globally recorded.

Table 4 summarizes the main hypotheses that have been advanced throughout the last chapter (5) in attempt to explain the obtained results for the considered palaeoregions.

Table 4: Summary of the hypotheses that have been advanced throughout sections 5.4-5.7 in the attempt to explain the obtained results for the considered palaeoregions. In the brackets the stage is given to which the hypothesis is referred.

Palaeoregion	Advanced explanations for the observed size changes
South China Block	<ul style="list-style-type: none"> - Palaeolocation, i.e. warmer temperature, less oxygen solubility, higher weathering rates (Smithian - Spathian) - Stable primary productivity during warmer intervals (Smithian) - Improved ocean ventilation + reduced anoxic conditions + stable environmental conditions (Spathian)
Palaeotethys	<ul style="list-style-type: none"> - Palaeolocation, i.e. warmer temperature, less oxygen solubility, higher weathering rates (Smithian - Spathian) - Stable productivity during warmer intervals (Smithian) - Improved ocean ventilation + reduced anoxic conditions + stable environmental conditions (Spathian) - Poor Smithian ammonoid record
Neotethys	<ul style="list-style-type: none"> - Temperature (Smithian - Spathian)
Boreal domain	<ul style="list-style-type: none"> - Temperature (Smithian - Spathian) - Anoxia (Smithian - Spathian) - Preservation bias (lack of carbonate sedimentation)
Western U.S.	<ul style="list-style-type: none"> - Temperature (Smithian - Spathian) - Early Smithian poor ammonoid record (regional tectonics)

5.8 Size range and diversity gradients

Throughout the Early Triassic, diversity gradients of ammonoids have been impacted by climatic disturbances. Brayard et al. (2006) observe that during the early Smithian generic richness of ammonoids shifted from a short initial cosmopolitan phase to a progressively increasing endemism that characterises most of the early and middle Smithian in particular. This endemic character might explain the size span observed in the boxplots interquartile ranges of middle Smithian: in fact, of all the considered substages the middle Smithian seems to include the widest assortment of sizes, usually followed by early Smithian. During the late Smithian, a cosmopolitan distribution develops (Brayard et al. 2006), which seems to be reflected by the very small size range observed within the boxplots interquartile ranges and by the normal distribution that is often detected in this time bin. However, Brayard et al. (2006) associate the observed early-middle Smithian endemism with a steeper SST gradient and the late Smithian cosmopolitanism with a flat one. This, however, is at variance with the latest findings: the temperature maximum reached in the middle Smithian (Goudemand et al. 2019), should argue for a smaller temperature difference between the poles (which are more impacted by warmer temperatures) and the lower latitudes and hence imply a flatter gradient. On the other hand, the cooling that characterised the late Smithian (Goudemand et al. 2019) should imply a steeper gradient between poles and lower latitudes, instead of a flat one. Although the connection between such generic richness gradients and SST might still be open to dispute, the diversity trend observed by Brayard et al. (2006) does seem to agree with our findings. Brayard et al. (2006) further observed that the Spathian stage is characterised by a recovery of

endemism; this is more difficult to relate to our results, since, when comparing Spathian and Smithian boxplots, the Spathian generally presents a smaller size interquartile range as obvious consequence of the end Smithian extinction and its gradual recovery, combined with the probable increase of predatory pressure. In most of the palaeoregions, the middle Spathian is characterised by a smaller size spread compared to early or late Spathian, but the differences are not as striking as they are when middle and late Smithian are compared. This might support the hypothesis of more stable climatic conditions that possibly allowed a steadier diversity pattern throughout the Spathian.

6. Conclusion

Ammonoid size had contrasting responses to the climatic upheavals during of the Smithian-Spathian time interval. However, there seems to be an overall negative correlation between temperature evolution and body size, and some general conclusions can be made.

- For most of the considered palaeoregions the middle Smithian as well as the middle Spathian, are characterised by a significant size reduction, in association with the warmer temperatures and possibly with the related lower amount of oxygen that can be dissolved in warmer waters (Atkinson and Sibly 1997). This trend can be observed on a global level, as well as in the whole of the lower palaeolatitudes and in the included Neotethys seamounts, and the Northern Indian Margin region.
- With the exception of the Palaeotethys, the South China block and Afghanistan, a general statistically significant reduction in body size in Spathian times can be observed, in the aftermath of the end Smithian extinction. The extinction at the SSB is considered the most severe faunal setback that occurred within the Early Triassic, and it lead to a massive ammonoids turnover (Brayard and Bucher, 2015; Galfetti et al. 2007c; Brayard et al. 2006). A smaller body size is therefore expected for the new taxa that occupy the niches left vacant, as is generally empirically observed in the aftermath of extinction events (Stanley, 1973). An increased predation pressure might have also played a significant role in the continuous predominance of smaller sizes throughout the Spathian stage. The predominant role of biotic factors in shaping the evolution of ammonoid body size during the Spathian time appears paradoxical when considering the seemingly higher significance of abiotic factors as main drivers of size change during the Smithian.
- No significant size change is observed throughout the Smithian-Spathian time in the South China Block, nor in the Palaeotethys and in the Afghanistan block. Although the paucity of data could represent a likely explanation in case of the Palaeotethys and of the Afghanistan area, another tentative explanation might be given by the more equatorial palaeoposition of the three locations, which speaks for generally warmer temperatures and less oxygen availability. These features might have kept Smithian ammonoids to a generally smaller size, so that no significant size change would then be observed in Spathian. An enhanced primary productivity in Smithian times (Wei et al. 2015) could have also aided to keep size constant during the warmer intervals, at least in the South China block. A reinforced circulation between the two areas during the cooler Spathian interval might further explain the similar size observed in that time in both locations.
- Statistical results have likely been affected by preservation biases in the Boreal region, where carbonate sediments are overall scarce. Results were probably also influenced by the poor ammonoid record of the early Smithian of the Western U.S. basin. Such poor record is explained by the gradual advance of the marine transgression phase in combination with the local tectonics proper of an active (i.e. convergent) margin.

- No latitudinal or longitudinal trend in size could be observed, which might either indicate the global nature of the climatic upheavals, or simply an insufficient amount of sampled locations.

Further work is needed in order to confirm the observed trends and to better interpret the results. Additional sampling effort directed at the Smithian-Spathian time frame in already well studied areas as well as in new sites, might allow a better analysis on latitudinal/longitudinal size trends. Moreover, a refined taxonomy elucidating the nature of specimens in open nomenclature, would provide for a more accurate dataset, while further isotopic analysis of the considered locations would improve our understanding of the climate evolution in the different sampling localities, in the light of the most recent discoveries (Goudemand et al. 2019).

7. Outlook

While this work considerably helped in giving a general overview over ammonoid size variation throughout the Smithian and the Spathian, improved data analyses could be applied in order to further corroborate the obtained results. For example, converting the size measurements to a logarithmic scale, could not only allow a better visual representation of the smaller but significant size changes, but it would probably also normalise the considered statistical populations and thus allow the implementation of more robust parametric tests. Further space analyses could also be undertaken, in order to investigate whether the palaeogeographic location could be a predictor of body size. The concept has already been introduced in this work when South China, the Palaeotethys and Afghanistan were compared to the other palaeoregions, by means of the Mann-Whitney-U and the Kolmogorov Smirnov tests. If the size distributions can be normalised, the different locations could be analysed (in the available common time intervals) by means of an ANOVA procedure (analysis of variance) followed by a Tukey's range test. The first would help to investigate the equality of the mean size of all considered locations. The second would allow the actual identification of the groups of regions that differ from the others. Of great interest would also be the investigation of the relationship between size and taxonomic diversity on a basin scale through time and space. Moreover, an attempt could be made to quantify the impact of among-taxa versus within-taxa size variation across space, i.e. to understand whether the differences between the considered locations are given by the presence of different taxa with their own size range, or by the same taxa characterised by smaller/bigger size.

Furthermore, considering the global nature of the Early Triassic climatic upheavals, the analysis could be run on a smaller dataset in which only the biggest specimen for each of the species identified in each time bin would be taken into account. This (sub)-dataset could then lay the foundations for an analysis of the impact of origination and extinction rates on the evolution of body size through time, i.e. it could shed some light on whether size change is driven by the selection of larger/smaller species, or by origination of new ones and/or extinction of older ones.

For all the suggested analysis the dataset will surely need to be polished and updated, but it is clear to see that the compilation of such extensive dataset represents a potentially significant contribution to future research.

Acknowledgments

I would first like to give my warmest thanks to my supervisor, Prof. Dr. Bucher, of the University of Zurich. His confidence in me, his advice and patient guidance have accompanied me since the years of my Bachelor's degree. Thank you for giving me the opportunity to embark on this journey of discovery through many exciting research projects!

I would like to kindly thank PD Dr. Michael Hautmann, for taking the time and the patience not only to read my thesis, but also to make valuable comments and corrections that helped improve this work.

I also wish to acknowledge Prof. Dr. Øyvind Hammer for his help with the statistical procedures and astrophysics PhD student Tomas Tamfal (of the University of Zurich) for the technical support with the software R.

Special thanks to Dr. Thomas Brühwiler as well, for patiently helping with the taxonomic review of the older literature. The construction of such an extensive dataset would not have been possible without the knowledge and expertise of both him and my supervisor.

I also want to express my appreciation to all my old and new friends and colleagues of the PIM institute that made my time there so memorable. A special thanks to my now lifelong friends Morgane, Borhan, Romain and James: not only have I shared my most cherished moments of my staying in Switzerland with you, but your advice, your teachings and the sharing of your experience and knowledge with me have made my academic path so enjoyable and so less scary!

Last but not least, I wish to express my most profound gratitude to my family. My parents, for teaching me the value of hard work, for helping me become who I am now and for always giving me the strength and support to overcome all the (many) obstacles that came my way. My boyfriend, who walked through those obstacles right by my side without ever letting go of me. My grandfather, for always being my life inspiration and guardian angel. And the sisters that life allowed me to choose, Lucia and Giulia who never stopped believing in me, supporting me and teaching me about life.

Without the help of all these wonderful people it would not have been possible for me to have come this far!

Thank you to each and every one of you!

Bibliography

- Adams, P. B. (1980). Life history patterns in marine fishes and their consequences for fisheries management. *Fishery Bulletin*, 78(1), 1–12.
- Ansell, A. D. (1968). The Rate of Growth of the Hard Clam *Mercenaria mercenaria* L) throughout the Geographical Range. *ICES Journal of Marine Science*, 31(3), 364–409.
- Arim, M., Abades, S. R., Laufer, G., Loureiro, M., & Marquet, P. A. (2010). Food web structure and body size: trophic position and resource acquisition. *Oikos*, 119(1), 147–153.
- Arthaber, G. von (1911). Die Trias von Albanien. *Beiträge Zur Paläontologie Österreich-Ungarns*, 170–277.
- Atkinson, D. (1994). Temperature and organism size: a biological law for ectotherms? *Advances in Ecological Research*, 25, 1–58.
- Atkinson, D., & Sibly, R. M. (1997). Why are organisms usually bigger in colder environments? Making sense of a life history puzzle. *Trends in Ecology & Evolution*, 12(6), 235–239.
- Bardet, N. (1994). Extinction events among Mesozoic marine reptiles. *Historical Biology*, 7(4), 313–324.
- Bardet, N. (1995). Evolution et extinction des reptiles marins au cours du Mésozoïque. *Palaeovertebrata*, 24(3–4), 177–283.
- Beatty, T. W., Zonneveld, J. P., & Henderson, C. M. (2008). Anomalously diverse Early Triassic ichnofossil assemblages in northwest Pangea: A case for a shallow-marine habitable zone. *Geology*, 36(10), 771–774.
- Belasky, P., Stevens, C. H., & Hanger, R. A. (2002). Early Permian location of western North American terranes based on brachiopod, fusulinid, and coral biogeography. *Palaeogeography, Palaeoclimatology, Palaeoecology*, 179(3–4), 245–266.
- Benton, M. J., Zhang, Q., Hu, S., Chen, Z.-Q., Wen, W., Liu, J., ... Tong, J. (2013). Exceptional vertebrate biotas from the Triassic of China, and the expansion of marine ecosystems after the Permo-Triassic mass extinction. *Earth-Science Reviews*, 125, 199–243.
- Besse, J., Torcq, F., Gallet, Y., Ricou, L. E., Krystyn, L., & Saidi, A. (1998). Late Permian to late Triassic palaeomagnetic data from Iran: constraints on the migration of the Iranian block through the Tethyn Ocean and initial destruction of Pangea. *Geophysical Journal International*, 135, 77–92.
- Brayard, A., Bruehwiler, T., Bucher, H., & Jenks, J. (2009a). Guodunites, a low-palaeolatitude and trans-Panthalassic Smithian (Early Triassic) ammonoid genus. *Palaeontology*, 52(2), 471–481.
- Brayard, A., & Bucher, H. (2008). Smithian (Early Triassic) ammonoid faunas from northwestern Guangxi (South China): taxonomy and biochronology. *Fossils and Strata Monograph Series*, 55, 184.
- Brayard, A., & Bucher, H. (2015). Permian-Triassic extinctions and rediversifications. In C. Klug, D. Korn, K. De Baets, I. Kruta, & R. H. Mapes (Eds.), *Ammonoid Paleobiology: From macroevolution to paleogeography* (pp. 465–473). Springer.
- Brayard, A., Bucher, H., Bruehwiler, T., Galfetti, T., Goudemand, N., Guodun, K., ... Jenks, J. (2007a). Proharpoceras Chao: a new ammonoid lineage surviving the end-Permian mass extinction. *Lethaia*, 40(2), 175–181.
- Brayard, A., Bucher, H., Escarguel, G., Fluteau, F., Bourquin, S., & Galfetti, T. (2006). The Early Triassic ammonoid recovery: paleoclimatic significance of diversity gradients. *Palaeogeography, Palaeoclimatology, Palaeoecology*, 239(3–4), 374–395.
- Brayard, A., Bylund, K. G., Jenks, J. F., Stephen, D. A., Olivier, N., Escarguel, G., ... Vennin, E. (2013). Smithian ammonoid faunas from Utah: implications for Early Triassic biostratigraphy, correlation and basinal paleogeography. *Swiss*

- Journal of Palaeontology*, 132(2), 141–219.
- Brayard, A., Escarguel, G., & Bucher, H. (2007b). The biogeography of Early Triassic ammonoid faunas: clusters, gradients, and networks. *Geobios*, 40(6), 749–765.
- Brayard, A., Escarguel, G., Bucher, H., & Brühwiler, T. (2009b). Smithian and Spathian (Early Triassic) ammonoid assemblages from terranes: Paleooceanographic and paleogeographic implications. *Journal of Asian Earth Sciences*.
- Brayard, A., Escarguel, G., Bucher, H., Monnet, C., Brühwiler, T., Goudemand, N., ... Guex, J. (2009c). Good genes and good luck: ammonoid diversity and the end-Permian mass extinction. *Science*, 325(5944), 1118–1121.
- Brayard, A., Krumenacker, L. J., Botting, J. P., Jenks, J. F., Bylund, K. G., Fara, E., ... Escarguel, G. (2017). Unexpected Early Triassic marine ecosystem and the rise of the Modern evolutionary fauna. *Science Advances*, 3(2), e1602159.
- Brayard, A., Meier, M., Escarguel, G., Fara, E., Nuetzel, A., Olivier, N., ... Hautmann, M. (2015). Early Triassic Gulliver gastropods: Spatio-temporal distribution and significance for biotic recovery after the end-Permian mass extinction. *Earth-Science Reviews*, 146, 31–64.
- Brayard, A., Nützel, A., Stephen, D. A., Bylund, K. G., Jenks, J., & Bucher, H. (2010). Gastropod evidence against the Early Triassic Lilliput effect. *Geology*, 38(2), 147–150.
- Brosse, M., Brayard, A., Fara, E., & Neige, P. (2013). Ammonoid recovery after the Permian–Triassic mass extinction: a re-exploration of morphological and phylogenetic diversity patterns. *Journal of the Geological Society*.
- Brühwiler, T., Bucher, H., Brayard, A., & Goudemand, N. (2010a). High-resolution biochronology and diversity dynamics of the Early Triassic ammonoid recovery: the Smithian faunas of the Northern Indian Margin. *Palaeogeography, Palaeoclimatology, Palaeoecology*, 297(2), 491–501.
- Brühwiler, T., Bucher, H., & Goudemand, N. (2010b). Smithian (Early Triassic) ammonoids from Tulong, South Tibet. *Geobios*, 43(4), 403–431.
- Brühwiler, T., Bucher, H., Goudemand, N., & Galfetti, T. (2012a). Smithian (Early Triassic) ammonoid faunas from Exotic Blocks from Oman: taxonomy and biochronology. *Palaeontographica Abteilung A*, 296, 3–107.
- Brühwiler, T., Bucher, H., & Krystyn, L. (2012b). Middle and late Smithian (Early Triassic) ammonoids from Spiti, India. *Special Papers in Palaeontology*, (88), 119–174.
- Brühwiler, T., Bucher, H., Roohi, G., Yaseen, A., & Rehman, K. (2011). A new early Smithian ammonoid fauna from the Salt Range (Pakistan). *Swiss Journal of Palaeontology*, 130(2), 187–201.
- Brühwiler, T., Bucher, H., Ware, D., Schneebeili-Hermann, E., Hochuli, P. A., Roohi, G., ... Yaseen, A. (2012c). Smithian (Early Triassic) ammonoids from the Salt Range, Pakistan. *Special Papers in Palaeontology*, 88, 5–114.
- Brühwiler, T., Ware, D., Bucher, H., Krystyn, L., & Goudemand, N. (2010c). New Early Triassic ammonoid faunas from the Dienerian/Smithian boundary beds at the Induan/Olenekian GSSP candidate at Mud (Spiti, Northern India). *Journal of Asian Earth Sciences*, 39, 724–739.
- Buffrénil, V. de, Mazin, J. M., & De Ricqlès, A. (1987). Caractères structuraux et mode de croissance du femur d'Omphalosaurus nisseri, ichthyosaurien du Trias moyen de Spitsberg. In *Annales de Paléontologie* (Vol. 73, pp. 195–216).
- Burgess, S. D., Bowring, S., & Shen, S. (2014). High-precision timeline for Earth's most severe extinction. *Proceedings of the National Academy of Sciences*, 111(13).
- Chao, K. (1950). Some new ammonite genera of Lower Triassic from western Kwangsi. *Palaeontological Novitates*, 5, 1–11.
- Chao, K. (1959). Lower Triassic ammonoids from Western Kwangsi. *Palaeontologia Sinica*, 9, 155–355.
- Chapelle, G., & Peck, L. S. (1999). Polar gigantism dictated by oxygen availability. *Nature*, 399, 114–115.
- Chen, Y., Twitchett, R. J., Jiang, H., Richoz, S., Lai, X., Yan, C., ... Wang, L. (2013). Size variation of conodonts during the Smithian–Spathian (Early Triassic) global warming event. *Geology*, 41(8), 823–826.

- Cohen, J. E., Pimm, S. L., Yodzis, P., & Saldaña, J. (1993). Body sizes of animal predators and animal prey in food webs. *Journal of Animal Ecology*, 62, 67–78.
- Cohen, K. M., Finney, S. C., Gibbard, P. L., & Fan, J.-X. (2013). The ICS International Chronostratigraphic Chart. *Episodes*, 36(3), 199–204.
- Collignon, M. (1973). Ammonites du Trias inférieur et moyen d'Afghanistan. *Annales de Paléontologie Invertébrés*, 59(2), 8–39.
- Dagys, A. S., & Ermakova, S. P. (1988). Boreal Late Olenekian ammonoids (in Russian: Бореальные позднеоленьки аммоноидеи). *Institut Geologii i Geofiziki, Sibirskoe Otdelenie, Akademia Nauka SSSR*, 714, 1–133.
- Dagys, A. S., & Ermakova, S. P. (1990). Early Olenekian ammonoids of Siberia (in Russian: Раннеоленьки аммоноидеи Сибири). *Institut Geologii i Geofiziki, Sibirskoe Otdelenie, Akademia Nauka SSSR*, 737, 1–113.
- Daufresne, M., Lengfellner, K., & Sommer, U. (2009). Global warming benefits the small in aquatic ecosystems. *Proceedings of the National Academy of Sciences*, 106(31), 12788–12793.
- De Koninck, L. (1863a). Descriptions of some fossils from India, discovered by Dr. A. Fleming, of Edinburgh. *Quarterly Journal of the Geological Society*, 19(1–2), 1–19.
- De Koninck, L. (1863b). Notice sur les fossiles de l'Inde découverts par M. le Dr Fleming, d'Edimbourg. *Mémoires de La Société Royale Des Sciences de Liège*, 18, 553–579.
- Diener, C. (1897). Himálayan Fossils. Vol. II. *Palaeontologica Indica*, 2, 234.
- Elton, C. (1927). *Animal ecology*. New York, Macmillan Co.
- Erwin, D. H. (1994). The Permo-Triassic extinction. *Nature*, 367, 231–236.
- Fabry, V. J., Seibel, B. A., Feely, R. A., & Orr, J. C. (2008). Impacts of ocean acidification on marine fauna and ecosystem processes. *ICES Journal of Marine Science*, 65(3), 414–432.
- Folkvord, A., & Hunter, J. R. (1986). Size-specific vulnerability of northern anchovy, *Engraulis mordax*, larvae to predation by fishes. *Fishery Bulletin*, 84(4), 859–869.
- France, R., Chandler, M., & Peters, R. (1998). Mapping trophic continua of benthic foodwebs: body size- $\delta^{15}\text{N}$ relationships. *Marine Ecology Progress Series*, 174, 301–306.
- Frebold, H. (1930). Die altersstellung des fischhorizontes, des grippianiveaus und des unteren saurierhorizontes in Spitzbergen. *Skrifter Om Svalbard Og Ishavet*, 28.
- Frentzen, K. (1936). Fossilier Mageninhalt aus dem Lias Delta (Amaltheen Schichten) von Reichenbach, Aalen. *Beiträge Zur Naturkundlichen Forschung in Oberrheingebiet*, 1, 293–303.
- Gale, A. S., Kennedy, W. J., & Martill, D. (2017). Mosasauroid predation on an ammonite–Pseudaspidoceras–from the Early Turonian of south-eastern Morocco. *Acta Geologica Polonica*, 67(1), 31–46.
- Galfetti, T., Bucher, H., Brayard, A., Hochuli, P. A., Weissert, H., Guodun, K., ... Guex, J. (2007a). Late Early Triassic climate change: insights from carbonate carbon isotopes, sedimentary evolution and ammonoid paleobiogeography. *Palaeogeography, Palaeoclimatology, Palaeoecology*, 243(3–4), 394–411.
- Galfetti, T., Bucher, H., Ovtcharova, M., Schaltegger, U., Brayard, A., Brühwiler, T., ... Guodun, K. (2007b). Timing of the Early Triassic carbon cycle perturbations inferred from new U-Pb ages and ammonoid biochronozones. *Earth and Planetary Science Letters*.
- Galfetti, T., Hochuli, P. A., Brayard, A., Bucher, H., Weissert, H., & Vigran, J. O. (2007c). Smithian-Spathian boundary event: Evidence for global climatic change in the wake of the end-Permian biotic crisis. *Geology*, 35(4), 291–294.
- Gazeau, F., Quiblier, C., Jansen, J. M., Gattuso, J., Middelburg, J. J., & Heip, C. H. R. (2007). Impact of elevated CO₂ on shellfish calcification. *Geophysical Research Letters*, 34(7).
- Goudemand, N., Romano, C., Leu, M., Bucher, H., Trotter, J. A., & Williams, I. S. (n.d.). Dynamic interplay between climate

- and marine biodiversity upheavals during the Early Triassic Smithian-Spathian biotic crisis. *Earth-Science Reviews* (2019).
- Grasby, S. E., Beauchamp, B., Embry, A., & Sanei, H. (2013). Recurrent Early Triassic ocean anoxia. *Geology*, *41*(2), 175–178.
- Greene, C. H. (1986). Patterns of prey selection: implications of predator foraging tactics. *The American Naturalist*, *128*(6), 824–839.
- Guex, J. (1978). Le Trias inferieur des Salt Ranges (Pakistan). *Eclog. Geol. Helv.*, *71*(1), 105–141.
- Guex, J., Hungerbühler, A., Jenks, J. F., O'Dogherty, L., Atudorei, V., Taylor, D. G., ... Bartolini, A. (2010). Spathian (Lower Triassic) ammonoids from western USA (Idaho, California, Utah and Nevada). *Mémoires de Géologie (Lausanne)*, *49*, 1–203.
- Hallam, A. (1991). Why was there a delayed radiation after the end-Palaeozoic extinctions? *Historical Biology*, *5*(2–4), 257–262.
- Hammer, Ø., & Harper, D. A. T. (2006). *Paleontological data analysis*. (Ø. Hammer & D. A. T. Harper, Eds.). Blackwell Publishing.
- Hammer, W. R. (1987). Paleocology and phylogeny of the Trematosauridae. In G. D. McKenzie (Ed.), *Gondwana Six: Stratigraphy, Sedimentology, and Paleontology* (Vol. 41, pp. 73–83). Washington: American Geophysical Union.
- Hansen, B. B., Hammer, Ø., & Nakrem, H. A. (2018). Stratigraphy and age of the Grippia niveau bonebed, Lower Triassic Vikinghøgda Formation, Spitsbergen. *Norwegian Journal of Geology*, *98*(2), 175–187.
- Harries, P. J., & Knorr, P. O. (2009). What does the 'Lilliput Effect' mean? *Palaeogeography, Palaeoclimatology, Palaeoecology*, *284*(1–2), 4–10.
- Hautmann, M., Bagherpour, B., Brosse, M., Frisk, Å., Hofmann, R., Baud, A., ... Bucher, H. (2015). Competition in slow motion: the unusual case of benthic marine communities in the wake of the end-Permian mass extinction. *Palaeontology*, *58*(5), 871–901.
- Hautmann, M., Bucher, H., Brühwiler, T., Goudemand, N., Kaim, A., & Nützel, A. (2011). An unusually diverse mollusc fauna from the earliest Triassic of South China and its implications for benthic recovery after the end-Permian biotic crisis. *Geobios*, *44*(1), 71–85.
- He, W., Twitchett, R. J., Zhang, Y., Shi, G. R., Feng, Q., Yu, J., ... Peng, X. (2010). Controls on body size during the Late Permian mass extinction event. *Geobiology*, *8*(5), 391–402.
- Hermann, E., Hochuli, P. A., Bucher, H., Brühwiler, T., Hautmann, M., Ware, D., & Roohi, G. (2011). Terrestrial ecosystems on North Gondwana following the end-Permian mass extinction. *Gondwana Research*, *20*(2–3), 630–637.
- Hochuli, P. A., Sanson-Barrera, A., Schneebeil-Hermann, E., & Bucher, H. (2016). Severest crisis overlooked—Worst disruption of terrestrial environments postdates the Permian–Triassic mass extinction. *Scientific Reports*, *6*, 28372.
- Hochuli, P. A., & Vigran, J. O. (2010). Climate variations in the Boreal Triassic—inferred from palynological records from the Barents Sea. *Palaeogeography, Palaeoclimatology, Palaeoecology*, *290*(1–4), 20–42.
- Hofmann, R., Goudemand, N., Wasmer, M., Bucher, H., & Hautmann, M. (2011). New trace fossil evidence for an early recovery signal in the aftermath of the end-Permian mass extinction. *Palaeogeography, Palaeoclimatology, Palaeoecology*, *310*(3–4), 216–226.
- Hofmann, R., Hautmann, M., Brayard, A., Nuetzel, A., Bylund, K. G., Jenks, J. F., ... Bucher, H. (2014). Recovery of benthic marine communities from the end-Permian mass extinction at the low latitudes of eastern Panthalassa. *Palaeontology*, *57*(3), 547–589.
- Horacek, M., Brandner, R., & Abart, R. (2007). Carbon isotope record of the P/T boundary and the Lower Triassic in the Southern Alps: evidence for rapid changes in storage of organic carbon. *Palaeogeography, Palaeoclimatology, Palaeoecology*, *252*(1–2), 347–354.

- Jacobs, D. K., & Chamberlain, J. A. (1996). Buoyancy and hydrodynamics in ammonoids. In M. R. H. Klug Christian, Korn Dieter, De Baets Kenneth, Kruta Isabelle (Ed.), *Ammonoid paleobiology* (pp. 169–224). Springer.
- Jacobs, D. K., & Landman, N. H. (1993). Nautilus—a poor model for the function and behavior of ammonoids? *Lethaia*, 26(2), 101–111.
- Jattiot, R., Bucher, H., & Brayard, A. (2017). *The Smithian (Early Triassic) ammonoid diversification-extinction cycle - Smithian (Early Triassic) ammonoid faunas from Exotic Blocks from Timor: taxonomy and biochronology*. Universität Zürich (PhD Dissertation).
- Jattiot, R., Bucher, H., Brayard, A., Monnet, C., Jenks, J. F., & Hautmann, M. (2015). Revision of the genus *Anasibirites* Mojsisovics (Ammonoidea): an iconic and cosmopolitan taxon of the late Smithian (Early Triassic) extinction. *Papers in Palaeontology*, 1–34.
- Jattiot, R., Bucher, H., Brayard, A., Brosse, M., Jenks, J. F., & Bylund, K. G. (2017). Smithian ammonoid faunas from northeastern Nevada: implications for Early Triassic biostratigraphy and correlation within the western USA basin. *Palaeontographica Abteilung A*, 309(1–4), 1–89.
- Jenks, J., & Brayard, A. (2018). *Smithian (Early Triassic) ammonoids from Crittenden Springs, Elko County, Nevada: taxonomy, biostratigraphy and biogeography*. *New Mexico Museum of Natural History & Science Bulletin* (Vol. 78).
- Jenks, J. F. (2007). Smithian (Early Triassic) ammonoid biostratigraphy at Crittenden Springs, Elko County, Nevada, and a new ammonoid from the *Meekoceras Gracilitatis* zone. *New Mexico Museum of Natural History & Science Bulletin*, 40, 81.
- Jenks, J. F., Brayard, A., Brühwiller, T., & Bucher, H. (2010). New Smithian (Early Triassic) ammonoids from Crittenden Springs, Elko County, Nevada: Implications for taxonomy, biostratigraphy and biogeography: Bulletin 48. *New Mexico Museum of Natural History & Science Bulletin*, 48.
- Jenks, J., Guex, J., Hungerbühler, A., Taylor, D. G., & Bucher, H. (2013). Ammonoid biostratigraphy of the Early Spathian *Columbites Parisianus* zone (Early Triassic) at Bear Lake Hotsprings, Idaho. *New Mexico Museum of Natural History & Science Bulletin*, 61, 268–283.
- Jennings, S. (2005). Size-based analyses of aquatic food webs. In R. E. Belgrano, A., Scharler, U.M., Dunne, J. and Ulanowicz (Ed.), *Aquatic food webs: an ecosystem approach*. New York: Oxford University Press.
- Jennings, S., Pinnegar, J. K., Polunin, N. V. C., & Warr, K. J. (2002). Linking size-based and trophic analyses of benthic community structure. *Marine Ecology Progress Series*, 226, 77–85.
- Ji, C., Zhang, C., Jiang, D.-Y., Bucher, H., Motani, R., & Tintori, A. (2015). Ammonoid age control of the Early Triassic marine reptiles from Chaohu (South China). *Palaeoworld*, 24(3), 277–282.
- Kauffman, E. (1990). Mosasaur predation on ammonites during the Cretaceous-An evolutionary history. *Paleobiology of Behaviour and Coevolution.*, 184–189.
- Kauffman, E. G. (2004). Mosasaur predation on Upper Cretaceous nautiloids and ammonites from the United States Pacific Coast. *Palaios*, 19(1), 96–100.
- Kauffman, E. G., & Kesling, R. V. (1960). An Upper Cretaceous ammonite bitten by a mosasaur. *Contributions from the Museum of Paleontology*, 15(9), 193–248.
- Kennedy, W. J., & Cobban, W. A. (1976). Aspects of ammonite biology, biogeography, and biostratigraphy. *Special Papers in Palaeontology*, 17.
- Kiparisova, L.D. & Popov, J. N. (1956). Расчленение нижнего отдела триасовой системы на ярусы (Subdivision of the lower series of the Triassic System into stages). *Doklady Akademii Nauk SSSR*, 109(4), 842–845.
- Kojima, S. (1989). Mesozoic terrane accretion in northeast China, Sikhote-Alin and Japan regions. *Palaeogeography, Palaeoclimatology, Palaeoecology*, 69, 213–232.

- Krafft, A. v., & Diener, C. (1909). Lower triassic Cephalopoda from Spiti, Malla, Johar, and Byans. *Palaeontologica Indica*, 6(1), 1–186.
- Kruta, I., Landman, N., Rouget, I., Cecca, F., & Tafforeau, P. (2011). The role of ammonites in the Mesozoic marine food web revealed by jaw preservation. *Science*, 331, 70–72.
- Krystyn, L., Bhargava, O. N., & Richoz, S. (2007a). A candidate GSSP for the base of the Olenekian Stage: Mud at Pin Valley; district Lahul & Spiti, Himachal Pradesh (Western Himalaya), India. *Albertiana*, 35, 5–29.
- Krystyn, L., Richoz, S., & Bhargava, O. N. (2007b). The Induan-Olenekian Boundary (IOB) in Mud—an update of the candidate GSSP section M04. *Albertiana*, 36, 33–45.
- Kummel, B. (1961). The Spitzbergen Arctoceratids. *Bull. Mus. Comp. Zool.*, 123(9), 499–532.
- Kummel, B. (1966). The lower Triassic formations of the salt range and trans-Indus Ranges, West Pakistan. *Bulletin of the Museum of Comparative Zoology*, 134(10), 361–422.
- Kummel, B. (1968a). Additional Scythian ammonoids from Afghanistan. *Bull. Mus. Comp. Zool.*, 136(13), 483–509.
- Kummel, B. (1968b). Scythian ammonoids from Timor. *Breviora - Museum of Comparative Zoology*, 283, 1–21.
- Kummel, B., & Erben, H. K. (1968). Lower and middle triassic cephalopods from Afghanistan. *Palaeontographica Abteilung A*, 129(4–6), 95–148.
- Kummel, B., & Steele, G. (1962). Ammonites from the Meekoceras gracilitatus Zone at Crittenden Spring, Elko County, Nevada. *Journal of Paleontology*, 36(4), 638–703.
- Labropoulou, M., & Eleftheriou, A. (1997). The foraging ecology of two pairs of congeneric demersal fish species: importance of morphological characteristics in prey selection. *Journal of Fish Biology*, 50(2), 324–340.
- Landman, N. H., Dommergues, J. L., & Marchand, D. (1991). The complex nature of progenetic species - examples from Mesozoic ammonites. *Lethaia*, 24(4), 409–421.
- Lehmann, U. (1975). Über Nahrung und Ernährungsweise von Ammoniten. *Paläontologische Zeitschrift*, 49(3), 187–195.
- Lehmann, U., & Weitschat, W. (1973). Zur Anatomie und Ökologie von Ammoniten: Funde von Kropf und Kiemen. *Paläontologische Zeitschrift*, 47(1–2), 69–76.
- Leu, M., Bucher, H., & Goudemand, N. (2018). Clade-dependent size response of conodonts to environmental changes during the late Smithian extinction. *Earth-Science Reviews*.
- Locatelli, L. (2017). *Predator-prey and body size relationships in marine food webs*. Academic Internship Report, University of Zurich
- Lukeneder, A. (2015). Ammonoid habitats and life history. In C. Klug, D. Korn, K. De Baets, I. Kruta, & R. H. Mapes (Eds.), *Ammonoid Paleobiology: From anatomy to ecology* (pp. 689–791). Springer.
- Martill, D. M. (1990). Predation on Kosmoceras by Semionotid fish in the middle Jurassic Lower Oxford clay of England. *Palaeontology*, 33(3), 739–742.
- Massare, J. A. (1987). Tooth morphology and prey preference of Mesozoic marine reptiles. *Journal of Vertebrate Paleontology*, 7(2), 121–137.
- McKinney, M. L. (1997). Extinction vulnerability and selectivity: combining ecological and paleontological views. *Annual Review of Ecology and Systematics*, 28(1), 495–516.
- Metcalfe, B., Twitchett, R. J., & Price-Lloyd, N. (2011). Changes in size and growth rate of 'Lilliput' animals in the earliest Triassic. *Palaeogeography, Palaeoclimatology, Palaeoecology*, 308(1–2), 171–180.
- Metcalfe, I. (1996). Gondwanaland dispersion, Asian accretion and evolution of eastern Tethys. *Australian Journal of Earth Sciences*, 43, 605–623.
- Metcalfe, I. (1999). Gondwana dispersion and Asian accretion: an overview. In I. Metcalfe (Ed.), *Gondwana dispersion and Asian accretion* (pp. 9–28). A.A. Balkema.

- Mojsisovics, E., Waagen, W. H., & Diener, C. (1895). *Entwurf einer Gliederung der pelagischen Sedimente des Trias-Systems*. in Commiss. bei Gerold's Sohn.
- Monnet, C., Bucher, H., Brayard, A., & Jenks, J. F. (2013). Globacorchordiceras gen. nov. (Acrochordiceratidae, late Early Triassic) and its significance for stress-induced evolutionary jumps in ammonoid lineages (cephalopods). *Fossil Record*, 16(2), 197–215.
- Mørk, A., Elvebakk, G., Forsberg, A. W., Hounslow, M. W., Nakrem, H. A., Vigran, J. O., & Weitschat, W. (1999). The type section of the Vikinghogda Formation: a new Lower Triassic unit in central and eastern Svalbard. *Polar Research*, 18(1), 51–82.
- Motani, R. (1997). Redescription of the dentition of Grippia longirostris (Ichthyosauria) with a comparison with Utatusaurus hataii. *Journal of Vertebrate Paleontology*, 17(1), 39–44.
- Nakajima, Y., Houssaye, A., & Endo, H. (2014). Osteohistology of the Early Triassic ichthyopterygian reptile Utatusaurus hataii: Implications for early ichthyosaur biology. *Acta Palaeontologica Polonica*, 59(2), 343–352.
- Nakajima, Y., & Izumi, K. (2014). Coprolites from the upper Osawa Formation (upper Spathian), northeastern Japan: Evidence for predation in a marine ecosystem 5 Myr after the end-Permian mass extinction. *Palaeogeography, Palaeoclimatology, Palaeoecology*, 414, 225–232.
- Nakazawa, K., & Bando, Y. (1968). Lower and Middle Triassic ammonites from Portuguese Timor (Palaeontological study of Portuguese Timor, 4). *Memoirs of the Faculty of Science, Kyoto University. Series of Geology and Mineralogy*, 34(2), 83–114.
- Natal'in, B. (1993). History and modes of Mesozoic accretion in southeastern Russia. *Island Arc*, 2(1), 15–34.
- Nichols, K. M., & Silberling, N. J. (1979). Early Triassic (Smithian) ammonites of paleoequatorial affinity from the Chulitna terrane, south-central Alaska. *Geological Survey Professional Paper*, 1121(B).
- Noetling, F. (1905). Die Asiatische Trias. In *Das Mesozoicum. Lethaea Geognostica I, Trias*. (pp. 107–221). Stuttgart: E. Schweizerbart'sche Verlagsbuchhandlung.
- O'Dea, A., & Okamura, B. (1999). Influence of seasonal variation in temperature, salinity and food availability on module size and colony growth of the estuarine bryozoan *Conopeum seurati*. *Marine Biology*, 135(4), 581–588.
- Orchard, M. J. (2007). Conodont diversity and evolution through the latest Permian and Early Triassic upheavals. *Palaeogeography, Palaeoclimatology, Palaeoecology*, 252(1–2), 93–117.
- Orr, J. C., Fabry, V. J., Aumont, O., Bopp, L., Doney, S. C., Feely, R. A., ... Joos, F. (2005). Anthropogenic ocean acidification over the twenty-first century and its impact on calcifying organisms. *Nature*, 437, 681–686.
- Ovtcharova, M., Bucher, H., Schaltegger, U., Galfetti, T., Brayard, A., & Guex, J. (2006). New Early to Middle Triassic U–Pb ages from South China: calibration with ammonoid biochronozones and implications for the timing of the Triassic biotic recovery. *Earth and Planetary Science Letters*, 243(3–4), 463–475.
- Pakistanian-Japanese Research Group. (1985). Permian and Triassic system in the Salt Range and Surghar Range, Pakistan. In K. Nakazawa & J. M. Dickins (Eds.), *The Thetys: her paleogeography and paleobiogeography from paleozoic to Mesozoic* (pp. 221–312). Tokyo: Tokai University Press.
- Parfenov, L. M., Natapov, L. M., Sokolov, S. D., & Tsukanov, N. V. (1993). Terrane analysis and accretion in North-East Asia. *Island Arc*, 2(1), 35–54.
- Payne, J. L., Lehrmann, D. J., Wei, J., Orchard, M. J., Schrag, D. P., & Knoll, A. H. (2004). Large perturbations of the carbon cycle during recovery from the end-Permian extinction. *Science*, 305, 506–509.
- Payne, J. L., Summers, M., Rego, B. L., Altiner, D., Wei, J., Yu, M., & Lehrmann, D. J. (2011). Early and Middle Triassic trends in diversity, evenness, and size of foraminifers on a carbonate platform in south China: implications for tempo and mode of biotic recovery from the end-Permian mass extinction. *Paleobiology*, 37(3), 409–425.

- Pianka, E. R. (1970). On r-and K-selection. *The American Naturalist*, 104(940), 592–597.
- Piazza, V. (2015). *Late Smithian (Early Triassic) ammonoids from the uppermost Lusitaniadalen Member (Vikingshøgda Formation), Svalbard*. University of Oslo (Master Thesis).
- Piazza, V., Hammer, Ø., & Jattiot, R. (2017). New late Smithian (Early Triassic) ammonoids from the Lusitaniadalen Member, Vikingshøgda Formation, Svalbard. *Norwegian Journal of Geology*, 97(2), 105–117.
- Raup, D. M. (1979). Size of the Permo-Triassic bottleneck and its evolutionary implications. *Science*, 206(4415), 217–218.
- Renz, C., & Renz, O. (1948). Eine untertriadische Ammonitenfauna von der griechischen Insel Chios. *Schweizerische Palaeontologischen Abhandlungen*, 66.
- Retallack, G. J., Sheldon, N. D., Carr, P. F., Fanning, M., Thompson, C. A., Williams, M. L., ... Hutton, A. (2011). Multiple Early Triassic greenhouse crises impeded recovery from Late Permian mass extinction. *Palaeogeography, Palaeoclimatology, Palaeoecology*, 308(1–2), 233–251.
- Romano, C., Goudemand, N., Vennemann, T. W., Ware, D., Schneebeli-Hermann, E., Hochuli, P. A., ... Bucher, H. (2013). Climatic and biotic upheavals following the end-Permian mass extinction. *Nature Geoscience*, 6(1), 57–60.
- Romano, C., Koot, M. B., Kogan, I., Brayard, A., Minikh, A. V., Brinkmann, W., ... Kriwet, J. (2016). Permian–Triassic Osteichthyes (bony fishes): diversity dynamics and body size evolution. *Biological Reviews*, 91(1), 106–147.
- Rosa, R., Gonzalez, L., Dierssen, H. M., & Seibel, B. A. (2012). Environmental determinants of latitudinal size-trends in cephalopods. *Marine Ecology Progress Series*, 464, 153–165.
- Sander, P. M., & Faber, C. (2003). The Triassic marine reptile *Omphalosaurus*: osteology, jaw anatomy, and evidence for ichthyosaurian affinities. *Journal of Vertebrate Paleontology*, 23(4), 799–816.
- Schaal, E. K., Clapham, M. E., Rego, B. L., Wang, S. C., & Payne, J. L. (2016). Comparative size evolution of marine clades from the Late Permian through Middle Triassic. *Paleobiology*, 42(1), 127–142.
- Scharf, F. S., Juanes, F., & Rountree, R. A. (2000). Predator size-prey size relationships of marine fish predators: interspecific variation and effects of ontogeny and body size on trophic-niche breadth. *Marine Ecology Progress Series*, 208, 229–248.
- Scheyer, T. M., Romano, C., Jenks, J., & Bucher, H. (2014). Early Triassic marine biotic recovery: the predators' perspective. *PLOS ONE*, 9(3), e88987.
- Schmidt-Nielsen, K. (1984). *Scaling: why is animal size so important?* Cambridge University Press.
- Scotese, C. R., & McKerrow, W. S. (1990). Revised world maps and introduction. *Palaeozoic Palaeogeography and Biogeography - Geological Society Memoirs*, 12(1), 1–21.
- Scotese, C. R., & Schettino, A. (2017). Late Permian-Early Jurassic Paleogeography of Western Tethys and the World. In *Permo-Triassic Salt Provinces of Europe, North Africa and the Atlantic Margins* (pp. 57–95). Elsevier.
- Şengör, A. M. C. (1979). Mid-Mesozoic closure of Permo-Triassic Tethys and its implications. *Nature*, 279, 590–593.
- Şengör, A. M. C. (1984). The Cimmeride orogenic system and the tectonics of Eurasia. *Geological Society of America Special Paper*, 195, 82.
- Sengör, A. M. C. (1987). Tectonics of the Tethysides: orogenic collage development in a collisional setting. *Annual Review of Earth and Planetary Sciences*, 15(1), 213–244.
- Shevyrev, A. (1995). Triassic ammoniten of northwestern Caucasus (in Russian: Триасовые аммониты Северо-Западного Кавказа). *Nauka*, 264, 174.
- Shevyrev, A. A. (1968). Triassic Ammonoidea from the Southern Part of the USSR. *USSR Academy of Sciences; Transactions of the Paleontological Institute (English Translation)*, 119, 471.
- Shigeta, Y. (2014). *Olenekian (Early Triassic) stratigraphy and fossil assemblages in northeastern Vietnam*. (Y. Shigeta, T. Komatsu, T. Maekawa, & H. D. Tran, Eds.). Tokyo: National Museum of Nature and Science Monographs.

- Shigeta, Y., & Kumagae, T. (2016). Spathian (late Olenekian, Early Triassic) ammonoids from the Artyom area, South Primorye, Russian Far East and implications for the timing of the recovery of the oceanic environment. *Paleontological Research*, 20(1), 48–60.
- Shigeta, Y., Zaharov, J. D., Maeda, H., & Popov, A. M. (2009). *The Lower Triassic System in the Abrek Bay Area, South Primorye, Russia*. (Y. Shigeta, Y. D. Zakharov, H. Maeda, & A. M. Popov, Eds.). Tokyo: National Museum of Nature and Science Monographs.
- Sholto-Douglas, A. D., Field, J. G., James, A. G., & Van der Merwe, N. J. (1991). $^{13}\text{C}/^{12}\text{C}$ and $^{15}\text{N}/^{14}\text{N}$ isotope ratios in the Southern Benguela Ecosystem: indicators of food web relationships among different size-classes of plankton and pelagic fish; differences between fish muscle and bone collagen tissues. *Marine Ecology Progress Series*, 78, 23–31.
- Silberling, N. J., & Wallace, R. E. (1969). Stratigraphy of the Star Peak Group (Triassic) and overlying lower Mesozoic rocks, Humboldt Range, Nevada. *Geological Survey Professional Paper*, 592, 1–50.
- Silberling, N. J., & Nichols, K. M. (1982). *Middle Triassic molluscan fossils of biostratigraphic significance from the Humboldt Range, northwestern Nevada*. *Geological Survey Professional Paper*, 1207. US Government Printing Office.
- Smith, J. P. (1932). *Lower Triassic ammonoids of North America*. Washington: US Government Printing Office.
- Song, H., Tong, J., Algeo, T. J., Horacek, M., Qiu, H., Song, H., ... Chen, Z.-Q. (2013). Large vertical $\delta^{13}\text{C}_{\text{DIC}}$ gradients in Early Triassic seas of the South China craton: Implications for oceanographic changes related to Siberian Traps volcanism. *Global and Planetary Change*, 105, 7–20.
- Song, H., Tong, J., Algeo, T. J., Song, H., Qiu, H., Zhu, Y., ... Luo, G. (2014). Early Triassic seawater sulfate drawdown. *Geochimica et Cosmochimica Acta*, 128, 95–113.
- Song, H., Tong, J., & Chen, Z. Q. (2011a). Evolutionary dynamics of the Permian–Triassic foraminifer size: evidence for Lilliput effect in the end-Permian mass extinction and its aftermath. *Palaeogeography, Palaeoclimatology, Palaeoecology*, 308(1–2), 98–110.
- Song, H., Wignall, P. B., Chen, Z.-Q., Tong, J., Bond, D. P. G., Lai, X., ... Niu, Z. (2011b). Recovery tempo and pattern of marine ecosystems after the end-Permian mass extinction. *Geology*, 39(8), 739–742.
- Southwood, T. R. E., May, R. M., Hassell, M. P., & Conway, G. R. (1974). Ecological strategies and population parameters. *The American Naturalist*, 108(964), 791–804.
- Spath, L. F. (1934). *Part 4: the ammonoidea of the Trias, Catalogue of the fossil cephalopoda in the British Museum (Natural History)*. London: The Trustees of the British Museum.
- Stampfli, G. M., & Borel, G. D. (2002). A plate tectonic model for the Paleozoic and Mesozoic constrained by dynamic plate boundaries and restored synthetic oceanic isochrons. *Earth and Planetary Science Letters*, 196, 17–33.
- Stampfli, G., Marcoux, J., & Baud, A. (1991). Tethyan margins in space and time. *Palaeogeography, Palaeoclimatology, Palaeoecology*, 87, 373–409.
- Stanley, S. M. (1973). An explanation for Cope's rule. *Evolution*, 27(1), 1–26.
- Stebbins, A., Algeo, T. J., Krystyn, L., Rowe, H., Brookfield, M., Williams, J., ... Hannigan, R. (2018). Marine sulfur cycle evidence for upwelling and eutrophic stresses during early triassic cooling events. *Earth-Science Reviews*.
- Stephen, D. A., Bylund, K. G., Bybee, P. J., & Ream, W. J. (2010). Ammonoid beds in the Lower Triassic Thaynes Formation of western Utah, USA. *Cephalopods—Present and Past*, 243–252.
- Storrs, G. W. (1991). Anatomy and relationships of *Corosaurus alcovensis* (Diapsida: Sauropterygia) and the Triassic Alcova Limestone of Wyoming. *Bulletin of the Peabody Museum of Natural History*, 44, 1–151.
- Sun, Y., Joachimski, M. M., Wignall, P. B., Yan, C., Chen, Y., Jiang, H., ... Lai, X. (2012). Lethally hot temperatures during the Early Triassic greenhouse. *Science*, 338, 366–370.
- Thomazo, C., Vennin, E., Brayard, A., Bour, I., Mathieu, O., Elmeknassi, S., ... Jenks, J. (2016). A diagenetic control on the Early

- Triassic Smithian–Spathian carbon isotopic excursions recorded in the marine settings of the Thaynes Group (Utah, USA). *Geobiology*, 14(3), 220–236.
- Tian, L., Tong, J., Algeo, T. J., Song, H., Song, H., Chu, D., ... Bottjer, D. J. (2014). Reconstruction of Early Triassic ocean redox conditions based on framboidal pyrite from the Nanpanjiang Basin, South China. *Palaeogeography, Palaeoclimatology, Palaeoecology*, 412, 68–79.
- Tong, J., Zakharov, D. Y., & Wu, S. (2004). Early Triassic ammonoid succession in Chaohu, Anhui Province. *Acta Palaeontologica Sinica*, 43(2), 192–204.
- Tong, J., & Zakharov, Y. D. (2004). Lower Triassic ammonoid zonation in Chaohu, Anhui Province, China. *Albertiana*, 31, 65–69.
- Tozer, E. T. (1961). Triassic stratigraphy and faunas, Queen Elizabeth Islands, Arctic Archipelago. *Geological Survey of Canada Memoir*, 316.
- Tozer, E. T. (1962). Illustrations of Canadian fossils: Triassic of Western and Arctic Canada. *Geological Survey of Canada Paper*, 62–19, 1–27.
- Tozer, E. T. (1963). Lower Triassic ammonoids from Tuchodi Lakes and Halfway River areas, northeastern British Columbia. *Geol. Surv. Canada, Bull.*, 96, 1–28.
- Tozer, E. T. (1965). Latest Lower Triassic ammonoids from Ellesmere Island and northeastern British Columbia. *Geol. Surv. Canada, Bull.*, 123, 1–45.
- Tozer, E. T. (1967). A standard for Triassic time. *Geol. Surv. Canada, Bull.*, 156, 1–103.
- Tozer, E. T. (1974). Definitions and limits of Triassic stages and substages: suggestions prompted by comparisons between North America and the Alpine-Mediterranean region. *Schriftenreihe Erdwissenschaftlichen Kommissionen Osterreichische Akademie Der Wissenschaften*, 2, 195–206.
- Tozer, E. T. (1981). Triassic Ammonoidea: classification, evolution and relationship with Permian and Jurassic forms. In M. R. S. J. R. House (Ed.), *The ammonoidea: The evolution, classification, mode of life and geological usefulness of a major fossil group* (pp. 65–100). Academic Press.
- Tozer, E. T. (1982). Marine Triassic faunas of North America: their significance for assessing plate and terrane movements. *Geologische Rundschau*, 71(3), 1077–1104.
- Tozer, E. T. (1984). The Trias and its ammonoids: the evolution of a time scale. *Geological Survey of Canada Miscellaneous Report*, 35, 1–171.
- Tozer, E. T. (1994). *Canadian Triassic ammonoid faunas*. Ottawa (Ont.): Geological Survey of Canada Bulletin.
- Trebilco, R., Baum, J. K., Salomon, A. K., & Dulvy, N. K. (2013). Ecosystem ecology: size-based constraints on the pyramids of life. *Trends in Ecology & Evolution*, 28(7), 423–431.
- Tsujita, C. J., & Westermann, G. E. G. (2001). Were limpets or mosasaurs responsible for the perforations in the ammonite *Placenticaseras*? *Palaeogeography, Palaeoclimatology, Palaeoecology*, 169(3–4), 245–270.
- Twitchett, R. J. (2006). The palaeoclimatology, palaeoecology and palaeoenvironmental analysis of mass extinction events. *Palaeogeography, Palaeoclimatology, Palaeoecology*, 232(2), 190–213.
- Twitchett, R. J. (2007). The Lilliput effect in the aftermath of the end-Permian extinction event. *Palaeogeography, Palaeoclimatology, Palaeoecology*, 252(1–2), 132–144.
- Valentine, J. W. (1971). Resource supply and species diversity patterns. *Lethaia*, 4(1), 51–61.
- Voje, K. L., Holen, Ø. H., Liow, L. H., & Stenseth, N. C. (2015). The role of biotic forces in driving macroevolution: beyond the Red Queen. *Proceedings of the Royal Society B: Biological Sciences*, 282: 20150186.
- Waagen, W. H. (1895). Salt-range Fossils. Vol.II. Fossils from the Ceratite Formation. *Paleontologica Indica*, 1–323.
- Wanner, J. (1911). Triascephalopoden von Timor und Rotti. *Neues Jahrbuch Für Geologie Und Paläontologie*, 32, 177–196.

- Ward, D. J., & Hollingworth, N. T. J. (1990). The first record of a bitten ammonite from the Middle Oxford Clay (Callovian, Middle Jurassic) of Bletchley, Buckinghamshire. *Mesozoic Research*, 2(4), 153–161.
- Warren, P. H., de Ruiter, P. C., Wolters, V., & Moore, J. C. (2005). Wearing Elton's wellingtons: why body size still matters in food webs. In *Dynamics food webs: multispecies assemblages, ecosystem development and environmental change. Volume 3*. (pp. 128–136).
- Warren, P. H., & Lawton, J. H. (1987). Invertebrate predator-prey body size relationships: an explanation for upper triangular food webs and patterns in food web structure? *Oecologia*, 74(2), 231–235.
- Wei, H., Shen, J., Schoepfer, S. D., Krystyn, L., Richoz, S., & Algeo, T. J. (2015). Environmental controls on marine ecosystem recovery following mass extinctions, with an example from the Early Triassic. *Earth-Science Reviews*, 149, 108–135.
- Weitschat, W. (2008). Intraspecific variation of *Svalbardiceras spitzbergensis* (Frebald) from the Early Triassic (Spathian) of Spitsbergen. *Polar Research*, 27(3), 292–297.
- Weitschat, W., & Lehmann, U. (1978). Biostratigraphy of the uppermost part of the Smithian Stage (Lower Triassic) at the Botneheia, W-Spitsbergen. *Mitteilungen Geologisch-Paläontologischen Institut Universität Hamburg*, 48, 85–100.
- Welter, O. A. (1922). *Die Ammoniten der unteren Trias von Timor*. Stuttgart: Schweizerbart'sche Verlagsbuchhandlung(E. Nägele).
- Westermann, G. E. G. (1996). Ammonoid life and habitat. In N. H. Landman, T. Kazushige, & R. A. Davis (Eds.), *Ammonoid paleobiology* (pp. 607–707). Springer.
- Wilson, D. S. (1975). The adequacy of body size as a niche difference. *The American Naturalist*, 109(970), 769–784.
- Wood, J. B., & O'dor, R. K. (2000). Do larger cephalopods live longer? Effects of temperature and phylogeny on interspecific comparisons of age and size at maturity. *Marine Biology*, 136(1), 91–99.
- Woodward, G., Ebenman, B., Emmerson, M. C., Montoya, J. M., Olesen, J. M., Valido, A., & Warren, P. H. (2005). Body-size determinants of the structure and dynamics of ecological networks: Scaling from the individual to the ecosystem. In *Dynamics food webs: multispecies assemblages, ecosystem development and environmental change. Volume 3*. (pp. 179–197). Elsevier.
- Xu, Z., Dilek, Y., Cao, H., Yang, J., Robinson, P., Ma, C., ... Chen, X. (2015). Paleo-Tethyan evolution of Tibet as recorded in the East Cimmerides and West Cathaysides. *Journal of Asian Earth Sciences*, 105, 320–337.
- Yancey, T., Stanley, G., Piller, W., & Woods, M. (2005). Biogeography of the Late Triassic wallowaconchid megalodontoid bivalves. *Lethaia*, 38(4), 351–365

Appendix – Part 1

Tables reporting the outcomes (p-values) of the Mann-Whitney-U and the Kolmogorov-Smirnov test are here listed.

Table 1A

Global	Mann-Whitney-U p-value	Kolmogorov-Smirnov p-value
Early to Middle Smithian	0.03793 (significant)	0.00833 (significant)
Middle to Late Smithian	0.9292 (not significant)	0.01283 (significant)
Late Smithian to Early Spathian	0.02728 (significant)	0.03467 (significant)
Early to Middle Spathian	0.005481 (significant)	0.005178 (significant)
Middle to Late Spathian	0.01302 (significant)	0.03417 (significant)
Smithian vs Spathian	7.462e-13 (significant)	2.101e-12 (significant)

Table 2A

Boreal Palaeolatitudes	Mann-Whitney-U p-value	Kolmogorov-Smirnov p-value
Middle to Late Smithian	0.09112 (not significant)	0.0517 (?)
Late Smithian to Early Spathian	0.4982 (not significant)	0.8698 (not significant)
Early to Middle Spathian	0.4493 (not significant)	0.8217 (not significant)
Middle to Late Spathian	0.2888 (not significant)	0.2812 (not significant)
Smithian vs Spathian	0.009583 (significant)	0.02272 (significant)

Table 3A

Low Palaeolatitudes	Mann-Whitney-U p-value	Kolmogorov-Smirnov p-value
Early to Middle Smithian	0.01037 (significant)	0.00549 (significant)
Middle to Late Smithian	0.5903 (not significant)	0.02581 (significant)
Late Smithian to Early Spathian	0.009898 (significant)	0.008207 (significant)
Early to Middle Spathian	0.004028 (significant)	0.006406 (significant)
Middle to Late Spathian	0.002435 (significant)	0.006073 (significant)
Smithian vs Spathian	8.329e-12 (significant)	4.045e-11 (significant)

Table 4A

Palaeotethys	Mann-Whitney-U p-value	Kolmogorov-Smirnov p-value
Middle Smithian to Early Spathian	0.3529 (not significant)	0.5259 (not significant)
Early to Middle Spathian	0.598 (not significant)	0.6883 (not significant)
Middle to Late Spathian	0.4635 (not significant)	0.7847 (not significant)
Smithian vs Spathian	0.4562 (not significant)	0.7285 (not significant)

Table 5A: The second line indicates the values of the tests performed on the Neotethys region after removal of the Cimmerian block of Afghanistan.

Neotethys Neotethys without Afghanistan	Mann-Whitney-U p-value	Kolmogorov-Smirnov p-value
Early to Middle Smithian	1.056e-06 (significant) 2.915e-06 (significant)	1.411e-05 (significant) 9.014e-06 (significant)
Middle to Late Smithian	0.9254 (not significant) 0.9608 (not significant)	0.02518 (significant) 0.0337 (significant)
Late Smithian to Middle Spathian	0.0005437 (significant) 0.001276 (significant)	0.00229 (significant) 0.002916 (significant)
Late Smithian to Spathian	0.0002859 (significant) 0.0008811 (significant)	0.0006813 (significant) 0.002669 (significant)
Smithian vs Spathian	1.083e-05 (significant) 9.757e-05 (significant)	2.751e-06 (significant) 4.911e-05 (significant)

Afghanistan Smithian vs Spathian	0.1663 (not significant)	0.2332 (not significant)
---	--------------------------	--------------------------

Table 6A

Neotethys seamounts	Mann-Whitney-U p-value	Kolmogorov-Smirnov p-value
Early to Middle Smithian	0.02545 (significant)	0.04537 (significant)
Middle to Late Smithian	0.7277 (not significant)	0.436 (not significant)
Late Smithian to Spathian	0.002006 (significant)	0.001501 (significant)
Smithian vs Spathian	0.005431 (significant)	0.002936 (significant)

Table 7A

NIM	Mann-Whitney-U p-value	Kolmogorov-Smirnov p-value
Early to Middle Smithian	3.548e-06 (significant)	0.0001259 (significant)
Middle to Late Smithian	0.8957 (not significant)	0.1629 (not significant)
Late Smithian to Spathian	0.06044 (not significant)	0.01689 (significant)
Smithian vs Spathian	0.0146 (significant)	0.02043 (significant)

Table 8A

SOUTH CHINA	Mann-Whitney-U p-value	Kolmogorov-Smirnov p-value
Early to Middle Smithian	0.3418 (not significant)	0.6592 (not significant)
Middle to Late Smithian	0.6236 (not significant)	0.4631 (not significant)
Late Smithian to Early Spathian	0.1966 (not significant)	0.07507 (not significant)
Early to Middle Spathian	0.3357 (not significant)	0.4 (not significant)
Middle to Late Spathian	0.03632 (significant)	0.07681 (not significant)
Smithian vs Spathian	0.8053 (NOT significant)	0.2378 (NOT significant)

Table 9A

W_USA	Mann-Whitney-U p-value	Kolmogorov-Smirnov p-value
Early to Middle Smithian	0.3569 (not significant)	0.4895 (not significant)
Middle to Late Smithian	0.1713 (not significant)	0.1322 (not significant)
Late Smithian to Early Spathian	0.003001 (significant)	0.01769 (significant)
Early to Middle Spathian	0.005948 (significant)	0.02325 (significant)
Middle to Late Spathian	0.04917 (significant)	0.06329 (not significant)
Smithian vs Spathian	6.361e-07 (significant)	4.01e-05 (significant)

Table 10A: Comparison of Afghanistan block with the other palaeoregions in the different time bins. Numbers indicate p values of MWU: Mann-Whitney-U test and KS = Kolmogorov Smirnov test; S: Significant; NS: non-significant. Smithian median size= 48 mm; Spathian median size= 39 mm

Afghanista n	Boreal	Neot.	NIM	Sea- mounts	W U.S	S. China	Palaeot.
Smithian							
Mwu:	0.00840	0.00361	0.00398	0.03745	0.00488	0.2544	0.3797
Ks:	0.01114	0.01827	0.02046	0.186	0.02203	0.1714	0.6081
Spathian							
MWu:	0.0582	0.7112	0.7169	0.8043	0.3165	0.07812	0.2041
Ks	0.1723	0.957	0.7365	0.7364	0.3668	0.0914	0.3477

Table 10B: Comparison of South China with the other palaeoregions in the different time bins. Numbers indicate p values of MWU: Mann-Whitney-U test and KS = Kolmogorov Smirnov test; S: Significant; NS: non-significant

South China	Palaeotethys	Boreal	Neotethys	NIM	Seamounts	W US
Early Smithian MWU: KS:	- -	- -	7.102e-05 S 0.006629 S	3.398e-05 S 0.005264 S	0.01904 S 0.06918 NS	0.1419 NS 0.399 NS
Middle Smithian MWU: KS:	0.1273 0.1884	0.06186 NS 0.08882 NS	0.6222 NS 0.7369 NS	0.4369 NS 0.3548 NS	0.6991 NS 0.7867 NS	0.6978 NS 0.8158 NS
Late Smithian MWU: KS:	- -	0.1716 NS 0.04022 S	0.03933 S 0.009292 S	0.0722 NS 0.03114 S	0.1423 NS 0.05414 NS	0.4559 NS 0.4854 NS
Early Spathian MWU: KS:	0.4778 0.649	0.5732 NS 0.9655 NS	- -	- -	- -	0.6952 NS 0.8844 NS
Middle Spathian MWU: KS:	0.5119 0.5828	0.3237 NS 0.3223 NS	0.3592 NS 0.2949 NS	- -	- -	0.04244 S 0.06436 NS
Late Spathian MWU: KS:	0.0943 0.1303	0.06751 NS 0.01881 S	- -	- -	- -	0.01767 S 0.01479 S
SMITHIAN MWU: KS:	0.1676 0.2131	0.006214 S 0.007857 S	0.01989 S 0.0169 S	0.007155 S 0.02047 S	0.2995 NS 0.223 NS	0.01279 S 0.0308 S
SPATHIAN MWU: KS:	0.08331 0.1305	0.9852 NS 0.5965 NS	0.03248 S 0.01786 S	0.279 NS 0.3093 NS	0.09822 NS 0.06225 NS	0.02862 S 0.2146 NS

Table 10C: Comparison of Palaeotethys with the other palaeoregions in the different time bins. MWU: Mann-Whitney-U test; KS = Kolmogorov Smirnov test; S: Significant; NS: non-significant

Palaeotethys	Boreal	Neotethys	NIM	Seamounts	W US
Early Smithian MWU: KS:	- -	- -	- -	- -	- -
Middle Smithian MWU: KS:	0.01866 S 0.08362 NS	0.1274 NS 0.3643 NS	0.6991 NS 0.4244 NS	0.1055 NS 0.3494 NS	0.07279 NS 0.1956 NS
Late Smithian MWU: KS:	- -	- -	- -	- -	- -
Early Spathian MWU: KS:	0.1946 NS 0.32 NS	- -	- -	- -	0.6121 NS 0.6697 NS
Middle Spathian MWU: KS:	0.0575 ? 0.3223 NS	0.454 NS 0.1217 NS	- -	- -	0.09225 NS 0.1949 NS
Late Spathian MWU: KS:	0.8046 NS 0.9888 NS	- -	- -	- -	0.8336 NS 0.9924 NS
SMITHIAN MWU: KS:	0.008427 S 0.0933 NS	0.01093 S 0.0514 ?	0.006385 S 0.03929 S	0.02738 S 0.02738 S	0.01124 S 0.06083 NS
SPATHIAN MWU: KS:	0.09533 NS 0.4268 NS	0.2531 NS 0.05452 ?	0.6393 NS 0.7193 NS	0.3618 NS 0.1185 NS	0.5999 NS 0.9271 NS

Appendix – Part 2

MULTIPLE AND SIMPLE LINEAR REGRESSIONS

The output and the detailed interpretation of the multiple linear regression performed in order to test for the presence of palaeolongitudinal and/or palaeolatitudinal trends are here displayed.

MAIN OUTPUT COMPONENTS OF MULTIPLE LINEAR REGRESSION

- (Multiple) R squared: indicates the percentage of variation of the response variable (size) that can be explained by a model that includes the explanatory variables in question.
- Adjusted R squared: it keeps into consideration how many explanatory variables have been used to build the model and how crucial these variables are for it. If this value is much lower than the R squared value, it is a clear indication that one of the independent variables that has been introduced in the model is statistically insignificant i.e. plays no role into explaining the variance of the response variable (i.e. the size could possibly have been explained by only one of the predictors).
- The p- value of the F statistic tests the null hypothesis that the model's coefficients are all equal 0 (i.e. that the slope of palaeolatitude and palaeolongitude equal 0). This hypothesis cannot be rejected, if the p value is bigger than 0.05. This case would signify that the combination of the explanatory variables may not be necessarily needed to explain the data. The p-value indicates the probability of the data to still be reproduced as they are observed without a linear dependence of the response to the explanatory variables being present.
- The residual standard error gives an idea of how far the observed size deviates from the fitted size values; it means that using the model to predict the size from palaeolatitude and palaeolongitude data, results 68.3 % of the times in an error smaller than \pm such error.
- The slope (*estimate*) of each explanatory variable indicates the effect of that predictor on the response variable, while the other explanatory variable is fixed. In our case, the slope denotes that an increase of 1° of palaeolatitude or palaeolongitude is associated with an increase in size equal to the slope value.
- If the p-value of the explanatory variable is bigger than 0.05, it implies that the null hypothesis (i.e. that slope of the predictor = 0, or simply put, that the predictor cannot explain the variance of response variable) cannot be rejected.

SMITHIAN + SPATHIAN (NORTHERN HEMISPHERE)

Call:

```
lm(formula = dd_m_N_H$medians ~ dd_m_N_H$Palaeolatitude + dd_m_N_H$Palaeolongitude)
```

Coefficients:

	Estimate	Std. Error	t value	Pr(> t)	
(Intercept)	45.97365	3.61781	12.71	1.05e-08	***
dd_m_N_H\$Palaeolatitude	0.11430	0.12418	0.92	0.3741	
dd_m_N_H\$Palaeolongitude	0.07635	0.03652	2.09	0.0568	.

Residual standard error: 8.692 on 13 degrees of freedom

Multiple R-squared: 0.2565, Adjusted R-squared: 0.1421

F-statistic: 2.242 on 2 and 13 DF, p-value: 0.1457

INTERPRETATION

- R squared: indicates that approximately only 26% of variation in size can be explained by the model (i.e. by palaeolatitude and palaeolongitude as explanatory variables).
- Adjusted R squared = 0.14: it is much lower than the R squared value. Hence one of the independent variables that has been introduced in the model is statistically insignificant i.e. plays no role into explaining the variance of the response variable (in other words, the size could possibly have been explained by only one of the predictors).
- The p- value of the F statistics is bigger than 0.05. It indicates that the null hypothesis (i.e. that the slope of palaeolatitude and palaeolongitude equals 0) cannot be rejected. Hence the combination of the explanatory variables palaeolongitude and palaeolatitude may not be necessarily needed to explain the data, since, as defined by the p-value, in almost 14% of the cases the data could still be reproduced without a linear dependence of the size to the two explanatory variables.
- The residual standard error indicates that using the model to predict the size from palaeolatitude and palaeolongitude data, results 68.3 % of the times in an error smaller than ± 9 mm.
- The slope (*estimate*) of the palaeolatitude equals 0.11 and indicates that an increase of 1° palaeolatitude is associated with an increase of 0.1 mm in size.
- The p-value of the palaeolatitude, equals 0.37. Being it bigger than 0.05, the null hypothesis (i.e. that slope of latitude = 0, or simply put, that latitude cannot explain the variance of response variable) cannot be rejected.
- The slope of the palaeolongitude equals 0.08: an increase of 1° longitude is associated with an increase of 0.08 mm in size.
- The p-value of the palaeolongitude equals 0.056. Being close to the threshold 0.05, it could indicate that the null hypothesis (i.e. that slope for longitude equals 0, or in other words, that the longitude cannot explain the variance in size) could be rejected. This would tell us that only this term would actually be needed for the model, i.e. that of the two explanatory variables, only longitude could play a role in explaining variance of the response variable.

SMITHIAN + SPATHIAN (SOUTHERN HEMISPHERE)

Call:

```
lm(formula = dd_m_S_H$medians ~ dd_m_S_H$Palaeolatitude + dd_m_S_H$Palaeolongitude)
```

Coefficients:

	Estimate	Std. Error	t value	Pr(> t)
(Intercept)	41.5496	14.5730	2.851	0.0463 *
dd_m_S_H\$Palaeolatitude	-0.2204	0.2691	-0.819	0.4587
dd_m_S_H\$Palaeolongitude	0.1388	0.1238	1.122	0.3247

Residual standard error: 8.318 on 4 degrees of freedom

Multiple R-squared: 0.2476, Adjusted R-squared: -0.1285

F-statistic: 0.6583 on 2 and 4 DF, p-value: 0.566

INTERPRETATION

- R squared = 0.25: approximately only 25% of variation in size can be explained by the model.
- Adjusted R squared = -0.13: this value is lower than the R squared value, which indicates that one of the independent variables that has been introduced in the model is statistically insignificant (i.e. the size could possibly have been explained by only one of the predictors).
- The p-value of the F statistics is bigger than 0.05, and indicates that in 57% of the cases the data could still be reproduced without a linear dependence of the size to the two explanatory variables. Therefore, the combination of both the explanatory variables may not be necessarily needed to explain the data.
- The residual standard error shows that using the model to predict the size from palaeolatitude and palaeolongitude data, results 68.3% of the times in an error smaller than ± 8 mm.
- The slope (*estimate*) of the palaeolatitude explanatory variable equals -0.22 and indicates that an increase of 1° palaeolatitude is associated with a decrease of 0.22 mm in size.
- The p-value of the palaeolatitude, equals 0.46. Hence the null hypothesis (i.e. that slope of palaeolatitude = 0) cannot be rejected.
- The slope of the palaeolongitude equals 0.14: an increase of 1° palaeolongitude is associated with an increase of 0.14 mm in size.
- The p-value of the palaeolongitude equals 0.33. In this case too, the null hypothesis (i.e. that slope for palaeolongitude equals 0) cannot be rejected.

SMITHIAN - NORTHERN HEMISPHERE

Call:

```
lm(formula = dd_SM_m_N_H$medians ~ dd_SM_m_N_H$Palaeolatitude +  
  dd_SM_m_N_H$Palaeolongitude)
```

Coefficients:

	Estimate	Std. Error	t value	Pr(> t)	
(Intercept)	49.68691	8.86310	5.606	0.000332	***
dd_SM_m_N_H\$Palaeolatitude	0.39201	0.28311	1.385	0.199509	
dd_SM_m_N_H\$Palaeolongitude	0.04891	0.08586	0.570	0.582829	

Residual standard error: 19.28 on 9 degrees of freedom

Multiple R-squared: 0.177, Adjusted R-squared: -0.005938

F-statistic: 0.9675 on 2 and 9 DF, p-value: 0.4163

INTERPRETATION

- R squared = 0.18: approximately 18% of variation in size can be explained by the model.
- Adjusted R squared = - 0.005: being it much lower than the R squared value, it is a clear indication that one of the independent variables that has been introduced in the model is statistically insignificant and the size could possibly have been explained by only one of the predictors.
- The p-value of the F statistics rejects the null hypothesis that the slope of both palaeolatitude and palaeolongitude both equal 0 and indicates that in 42% of the cases the data could still be reproduced without a linear dependence of the size to the two explanatory variables
- The residual standard error indicates that using the model to predict the size from palaeolatitude and palaeolongitude data, results 68.3% of the times in an error smaller than ± 19 mm.
- The slope (*estimate*) of the palaeolatitude equals 0.39: an increase of 1° palaeolatitude is associated with an increase of 0.39 mm in size.
- The p-value of the palaeolatitude, equals 0.20. Being it bigger than 0.05 the null hypothesis (i.e. that slope of palaeolatitude = 0) cannot be rejected.
- The slope of the palaeolongitude equals 0.05 and implicates that an increase of 1° palaeolongitude is associated with an increase of 0.05 mm in size.
- The p-value of the palaeolongitude equals 0.58 and indicates that the null hypothesis (i.e. that slope for palaeolongitude equals 0) cannot be rejected.

SMITHIAN - SOUTHERN HEMISPHERE

Call:

```
lm(formula = dd_SM_m_S_H$medians ~ dd_SM_m_S_H$Palaeolatitude +  
    dd_SM_m_S_H$Palaeolongitude)
```

Coefficients:

	Estimate	Std. Error	t value	Pr(> t)
(Intercept)	45.79375	13.58976	3.370	0.0281 *
dd_SM_m_S_H\$Palaeolatitude	-0.26210	0.25096	-1.044	0.3553
dd_SM_m_S_H\$Palaeolongitude	0.07865	0.11540	0.682	0.5329

Residual standard error: 7.757 on 4 degrees of freedom

Multiple R-squared: 0.2168, Adjusted R-squared: -0.1749

F-statistic: 0.5535 on 2 and 4 DF, p-value: 0.6135

INTERPRETATION

- R squared = 0.22: approximately only 22% of variation in size can be explained by a model that has palaeolatitude and palaeolongitude as explanatory variables.
- Adjusted R squared = -0.17: being much lower than the R squared value, it is a clear indication that one of the independent variables that has been introduced in the plays no role into explaining the variance of the response variable (one predictor could be enough to explain the observed size).
- The p-value of the F statistics is bigger than 0.05. In 61% of the cases the data could still be reproduced without a linear dependence of the size to the two explanatory variables. This indicates that the combination of the explanatory variables palaeolongitude and palaeolatitude may not be necessarily needed to explain the data.
- The residual standard error indicates that using the model to predict the size from palaeolatitude and palaeolongitude data, results 68.3% of the times in an error smaller than ± 8 mm.
- The slope (*estimate*) of the palaeolatitude equals -0.26; hence, an increase of 1° palaeolatitude is associated with a decrease of 0.26 mm in size.
- The p-value of the palaeolatitude, equals 0.35 and therefore implies that the null hypothesis (i.e. that the slope of palaeolatitude = 0) cannot be rejected.
- The slope of the palaeolongitude equals 0.08: 1° palaeolongitude is therefore associated with an increase of 0.08 mm in size.
- The p-value of the palaeolongitude equals 0.53: the null hypothesis (i.e. the slope for palaeolongitude equals 0) cannot be rejected.

SPATHIAN - NORTHERN HEMISPHERE

Call:

```
lm(formula = dd_SP_m_N_H$medians ~ dd_SP_m_N_H$Palaeolatitude +  
    dd_SP_m_N_H$Palaeolongitude)
```

Coefficients:

	Estimate	Std. Error	t value	Pr(> t)	
(Intercept)	45.44346	7.89106	5.759	0.000127	***
dd_SP_m_N_H\$Palaeolatitude	0.03614	0.24850	0.145	0.886988	
dd_SP_m_N_H\$Palaeolongitude	0.18908	0.08188	2.309	0.041350	*

Residual standard error: 16.32 on 11 degrees of freedom
Multiple R-squared: 0.3573, Adjusted R-squared: 0.2404
F-statistic: 3.057 on 2 and 11 DF, p-value: 0.08792

INTERPRETATION

- R squared = 0.35: approximately 35% of variation in size can be explained by the model.
- Adjusted R squared = 0.24: it is lower than the R squared value, which indicates that one of the independent variables that has been introduced in the model is statistically insignificant (i.e. only one predictor could potentially suffice to explain the observed size distribution).
- The p-value of the F statistics is bigger than 0.05 and therefore indicates that the combination of the explanatory variables palaeolongitude and palaeolatitude may not be necessarily needed to explain the data. In fact, in 8% of the cases the data could still be reproduced without a linear dependence of the size to the two explanatory variables.
- The residual standard error indicates that using the model to predict the size from palaeolatitude and palaeolongitude data, results 68.3% of the times in an error smaller than ± 16 mm.
- The slope (*estimate*) of the palaeolatitude explanatory variable equals 0.03: 1° palaeolatitude is associated with an increase of 0.03 mm in size.
- The p-value of the palaeolatitude, equals 0.88 and implies that the null hypothesis (i.e. that slope of palaeolatitude = 0) cannot be rejected.
- The slope of the palaeolongitude equals 0.18: an increase of 1° palaeolongitude is associated with an increase of 0.05 mm in size.
- The p-value of the palaeolongitude equals 0.041. being it smaller than 0.05 indicates that the null hypothesis (i.e. that slope for palaeolongitude equals 0) can be rejected.

SPATHIAN - SOUTHERN HEMISPHERE

Call:

```
lm(formula = dd_SP_m_S_H$medians ~ dd_SP_m_S_H$Palaeolatitude + dd_SP_m_S_H$Palaeolongitude)
```

Coefficients:

	Estimate	Std. Error	t value	Pr(> t)
(Intercept)	-15.1116	67.1715	-0.225	0.833
dd_SP_m_S_H\$Palaeolatitude	-1.1805	1.2404	-0.952	0.395
dd_SP_m_S_H\$Palaeolongitude	0.6714	0.5704	1.177	0.304

Residual standard error: 38.34 on 4 degrees of freedom

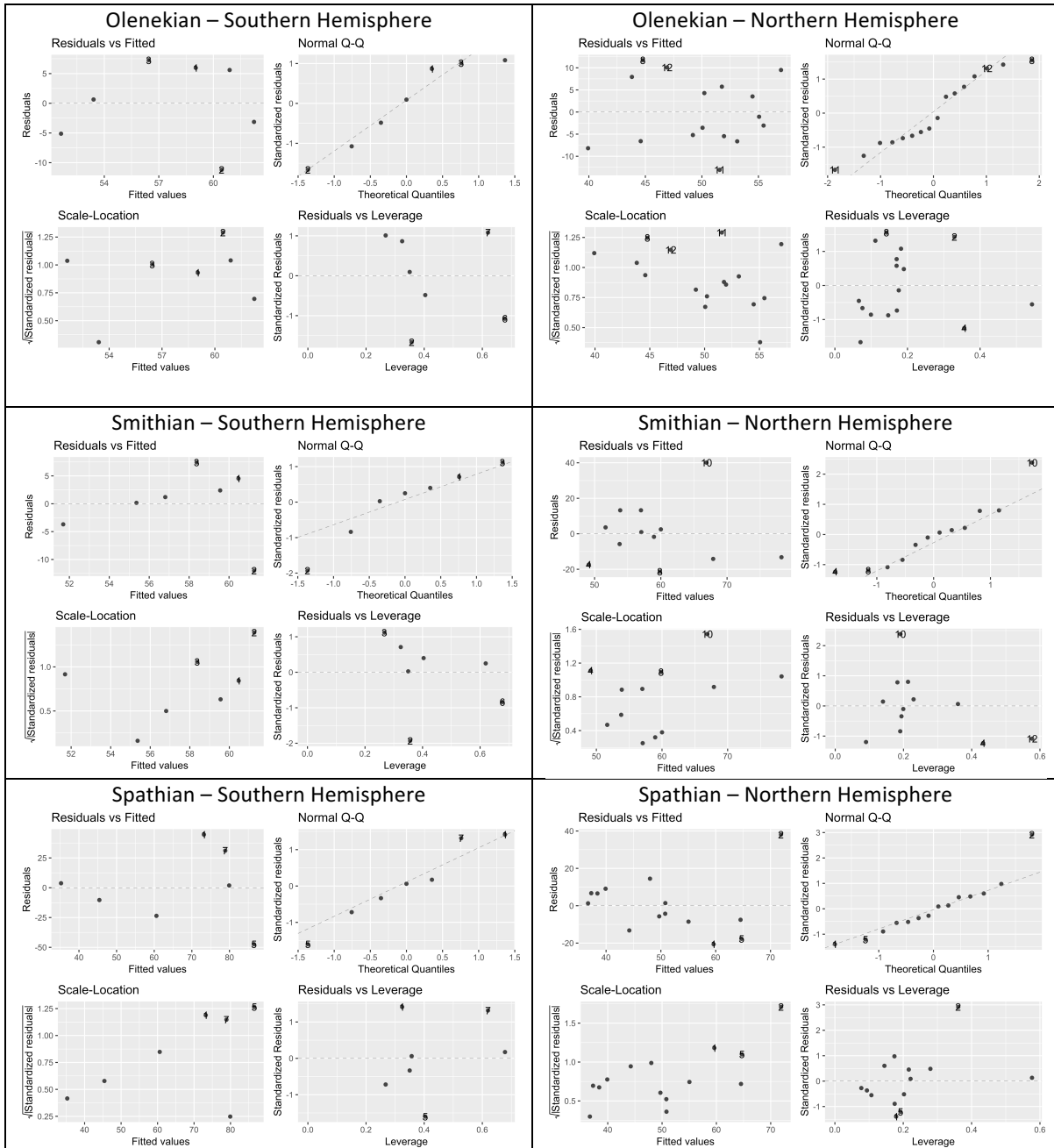
Multiple R-squared: 0.275, Adjusted R-squared: -0.08745

F-statistic: 0.7587 on 2 and 4 DF, p-value: 0.5256

INTERPRETATION

- R squared = 0.27: approximately 27% of variation in size can be explained by a model including palaeolatitude and palaeolongitude as explanatory variables.
- Adjusted R squared = -0.08: this value is much lower than the R squared value, signifying that one of the independent variables that has been introduced in the model is statistically insignificant i.e. plays no role into explaining the variance of the response.
- The p-value of the F statistics claims that the hypothesis that all model's coefficients are equal 0 cannot be rejected, since it is bigger than 0.05. This indicates that the combination of the explanatory variables palaeolongitude and palaeolatitude may not be necessarily needed to explain the data. In 52% of the cases the data could indeed still be reproduced without a linear dependence of the size to the two explanatory variables.
- The residual standard error indicates that using the model to predict the size from palaeolatitude and palaeolongitude data, results 68.3% of the times in an error smaller than ± 38 mm.
- The slope (*estimate*) of the palaeolatitude equals -1.18, which indicates that an increase of 1° palaeolatitude is associated with a decrease of 1.18 mm in size.
- The p-value of the palaeolatitude, equals 0.39, and thus implies that the null hypothesis (i.e. that slope of palaeolatitude = 0) cannot be rejected.
- The slope of the palaeolongitude explanatory variable equals 0.67: an increase of 1° palaeolongitude is thus associated with an increase of 0.67 mm in size.
- The p-value of the palaeolongitude equals 0.30, and also indicates that the null hypothesis (i.e. that slope for palaeolongitude equals 0) cannot be rejected.

DIAGNOSTIC PLOTS OF MULTIPLE LINEAR REGRESSIONS



MAIN OUTPUT COMPONENTS OF SIMPLE LINEAR REGRESSION

- (Multiple) R squared indicates the percentage of variation in size that can be explained by a model that includes, in this case, either palaeolatitude OR palaeolongitude as explanatory variable.
- The residual standard error gives an idea of how far the observed size deviates from the fitted size; using the model to predict the size from palaeolatitude and palaeolongitude data, results 68.3% of the times in an error smaller than \pm the residual standard error.
- The slope (*estimate*) of the explanatory variable indicates that an increase of, in our case, 1° palaeolatitude/palaeolongitude is associated with an increase in size equal to the slope itself.
- If the p-value of the explanatory variable is bigger than 0.05, it implies that the null hypothesis (i.e. that slope of the predictor = 0, or simply put, that the predictor cannot explain the variance of the response variable) cannot be rejected.
- The F statistics are meant to explain the overall significance of the whole model. The p-value of the F statistics tests the null hypothesis that the model's coefficients are all equal 0. Since in a simple linear regression model only one predictor is present, the p value of the the F statistic agrees with the p value of the slope of the predictor.

SMITHIAN + SPATHIAN (NORTHERN HEMISPHERE): SIZE VS PALAEOLATITUDE

Call:

```
lm(formula = medians ~ Palaeolatitude, data = dd_m_lat_Nh)
```

Coefficients:

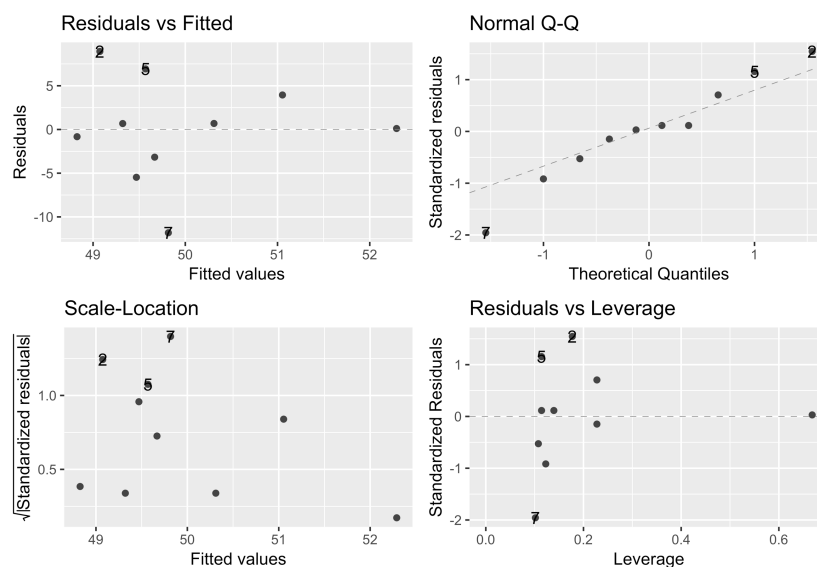
	Estimate	Std. Error	t value	Pr(> t)
(Intercept)	49.0420	3.2084	15.286	3.33e-07 ***
Palaeolatitude	0.0408	0.1067	0.382	0.712

Residual standard error: 6.727 on 8 degrees of freedom
Multiple R-squared: 0.01793, Adjusted R-squared: -0.1048
F-statistic: 0.1461 on 1 and 8 DF, p-value: 0.7123

INTERPRETATION

- R squared = 0.02: it indicates that approximately 2% of variation in size can be explained by the model (i.e. by the variation in palaeolatitude).
- The residual standard error shows that using the model to predict the size from palaeolatitude values results 68.3% of the times in an error smaller than ± 7 mm.
- The slope (*estimate*) of the palaeolatitude equals 0.04: an increase of 1° palaeolatitude is therefore associated with an increase of 0.04 mm in size.
- The p-value of the palaeolatitude, equals 0.71 and thus implies that the null hypothesis (i.e. that slope of palaeolatitude = 0) cannot be rejected.

DIAGNOSTIC PLOTS



SMITHIAN + SPATHIAN (SOUTHERN HEMISPHERE): SIZE VS PALAEOLATITUDE

Call:

```
lm(formula = medians ~ Palaeolatitude, data = dd_m_lat_Sh)
```

Coefficients:

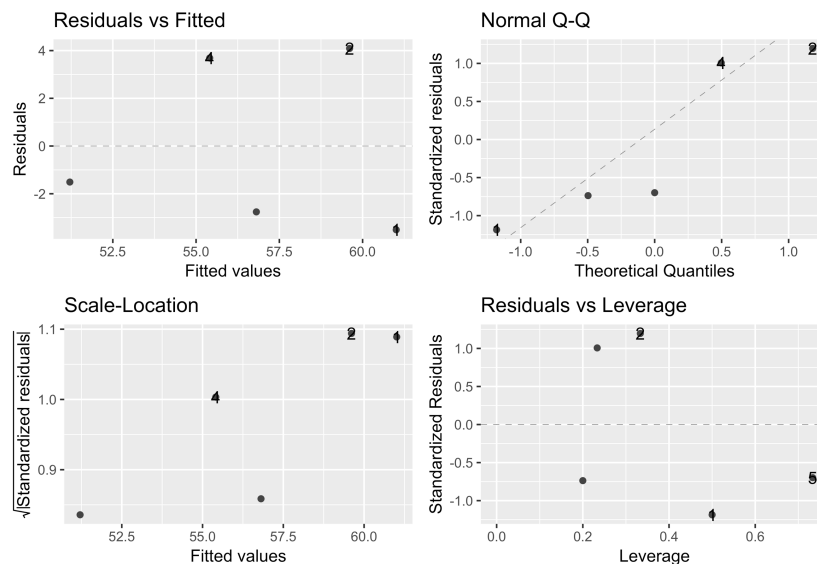
	Estimate	Std. Error	t value	Pr(> t)	
(Intercept)	51.2100	3.5845	14.287	0.000743	***
Palaeolatitude	-0.2800	0.1528	-1.832	0.164350	

Residual standard error: 4.186 on 3 degrees of freedom
Multiple R-squared: 0.528, Adjusted R-squared: 0.3707
F-statistic: 3.356 on 1 and 3 DF, p-value: 0.1644

INTERPRETATION

- R squared = 0.53: it indicates that approximately 53% of variation in size can be explained by the model.
- The residual standard error shows that using the model to predict the size from palaeolatitude values, results 68.3% of the times in an error smaller than ± 4 mm.
- The slope (*estimate*) of the palaeolatitude equals -0.28 and thus indicates that an increase of 1° palaeolatitude is associated with a decrease of 0.28 mm in size.
- The p-value of the palaeolatitude, equals 0.16. It implies that the Null Hypothesis (i.e. that slope of palaeolatitude = 0) cannot be rejected.

DIAGNOSTIC PLOTS



SMITHIAN (NORTHERN HEMISPHERE): SIZE VS PALAEO LATITUDE

Call:

```
lm(formula = medians ~ Palaeolatitude, data = dd_SM_lat_Nh)
```

Coefficients:

	Estimate	Std. Error	t value	Pr(> t)
(Intercept)	54.8318	6.5517	8.369	0.000158 ***
Palaeolatitude	0.1325	0.2001	0.662	0.532360

Residual standard error: 12.37 on 6 degrees of freedom

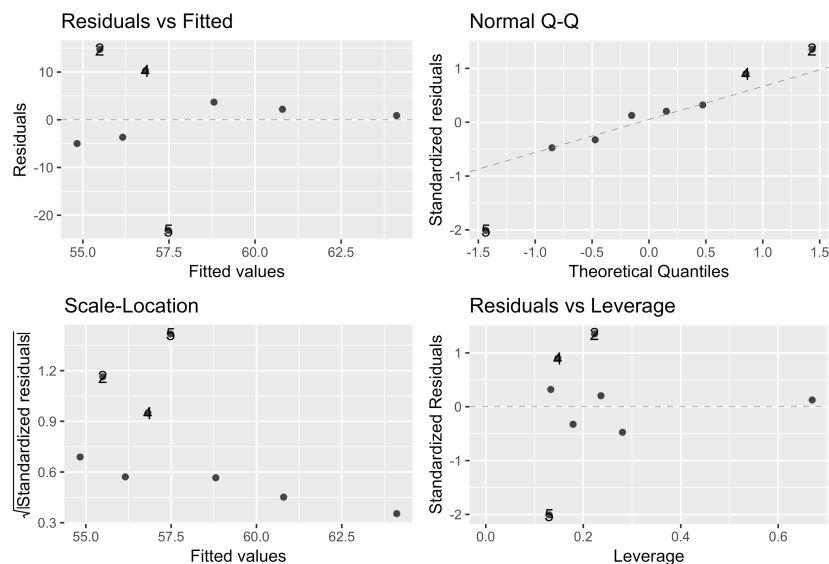
Multiple R-squared: 0.06813, Adjusted R-squared: -0.08718

F-statistic: 0.4387 on 1 and 6 DF, p-value: 0.5324

INTERPRETATION

- R squared = 0.07: approximately 7% of variation in size can be explained by the model.
- The residual standard error indicates that using the model to predict size from palaeolatitude, results 68.3% of the times in an error smaller than ± 12 mm.
- The slope (*estimate*) of the palaeolatitude equals 0.13, indicating that an increase of 1° palaeolatitude is associated with an increase of 0.13 mm in size.
- The p-value of the palaeolatitude, equals 0.53: it implies that the null hypothesis (i.e. that slope of palaeolatitude = 0) cannot be rejected.

DIAGNOSTIC PLOTS



SMITHIAN (SOUTHERN HEMISPHERE): SIZE VS PALAEO LATITUDE

Call:

```
lm(formula = medians ~ Palaeolatitude, data = dd_SM_lat_Sh)
```

Coefficients:

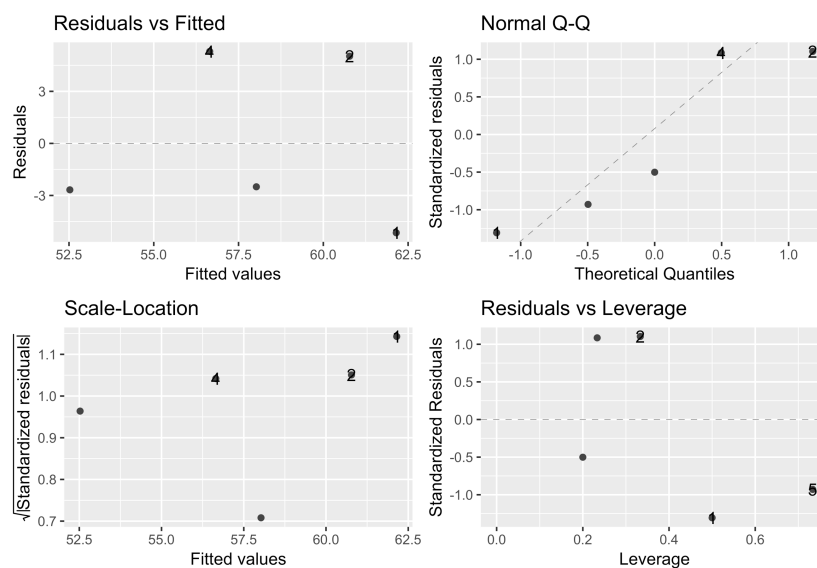
	Estimate	Std. Error	t value	Pr(> t)
(Intercept)	52.5250	4.7748	11.000	0.00161 **
Palaeolatitude	-0.2750	0.2036	-1.351	0.26964

Residual standard error: 5.576 on 3 degrees of freedom
Multiple R-squared: 0.3782, Adjusted R-squared: 0.1709
F-statistic: 1.824 on 1 and 3 DF, p-value: 0.2696

INTERPRETATION

- R squared = 0.4: approximately 40% of variation in size can be explained by the model (i.e. by the variation in palaeolatitude).
- The residual standard error indicates that using the model to predict size from palaeolatitude results 68.3% of the times in an error smaller than ± 5.6 mm.
- The slope (*estimate*) of the palaeolatitude equals -0.27: hence an increase of 1° palaeolatitude is associated with a decrease of 0.27 mm in size.
- The p-value of the palaeolatitude, equals 0.27. It implies that the Null Hypothesis (i.e. that slope of palaeolatitude = 0) cannot be rejected.

DIAGNOSTIC PLOTS



SPATHIAN (NORTHERN HEMISPHERE): SIZE VS PALAEO LATITUDE

```
lm(formula = medians ~ Palaeolatitude, data = dd_SP_lat_Nh)
```

Coefficients:

	Estimate	Std. Error	t value	Pr(> t)
(Intercept)	46.94182	3.40738	13.78	7.44e-07 ***
Palaeolatitude	-0.05097	0.11337	-0.45	0.665

Residual standard error: 7.144 on 8 degrees of freedom

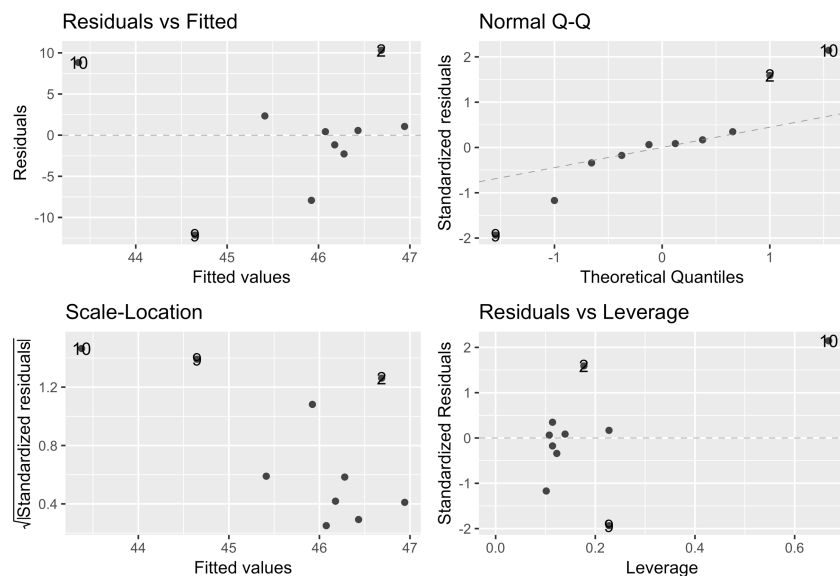
Multiple R-squared: 0.02464, Adjusted R-squared: -0.09728

F-statistic: 0.2021 on 1 and 8 DF, p-value: 0.6649

INTERPRETATION

- R squared: indicates that approximately 2% of variation in size can be explained by the model (i.e. by the variation in palaeolatitude).
- The residual standard error indicates that using the model to predict size from, results 68.3% of the times in an error smaller than ± 7 mm.
- The slope (*estimate*) of the palaeolatitude equals -0.05: an increase of 1° palaeolatitude is thus associated with a decrease of 0.05 mm in size.
- The p-value of the palaeolatitude, equals 0.66 and implies that the null hypothesis (i.e. that slope of palaeolatitude = 0) cannot be rejected.

DIAGNOSTIC PLOTS



SPATHIAN (SOUTHERN HEMISPHERE): SIZE VS PALAEOLATITUDE

Call:

```
lm(formula = medians ~ Palaeolatitude, data = dd_SP_lat_Sh)
```

Coefficients:

	Estimate	Std. Error	t value	Pr(> t)
(Intercept)	33.7850	22.0709	1.531	0.223
Palaeolatitude	-0.8535	0.9411	-0.907	0.431

Residual standard error: 25.77 on 3 degrees of freedom

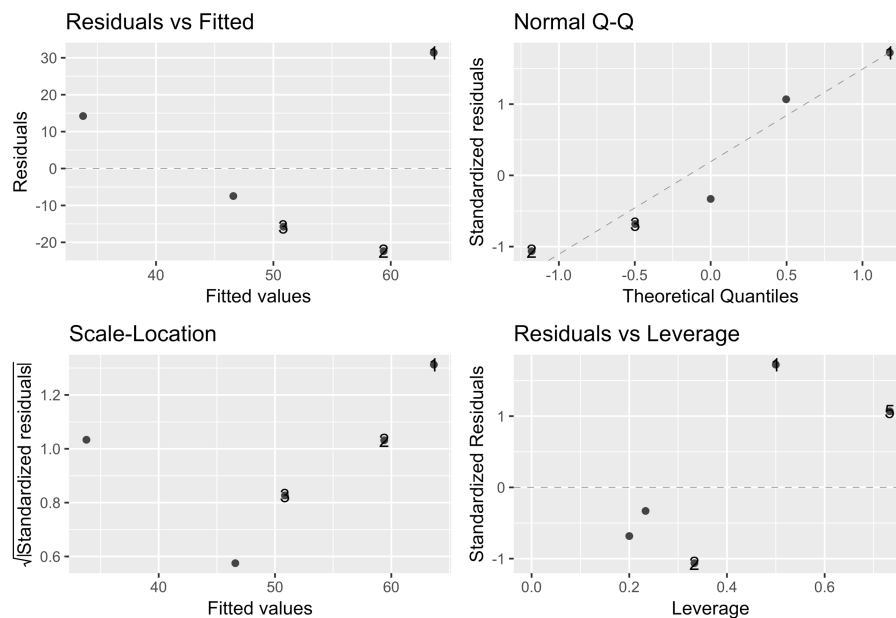
Multiple R-squared: 0.2152, Adjusted R-squared: -0.04644

F-statistic: 0.8225 on 1 and 3 DF, p-value: 0.4313

INTERPRETATION

- R squared = 0.21: approximately 21% of variation in size can be explained by the model.
- The residual standard error indicates that using the model to predict size from palaeolatitude results 68.3% of the times in an error smaller than ± 25 mm.
- The slope (*estimate*) of the palaeolatitude equals -0.8 and indicates that an increase of 1° palaeolatitude is associated with a decrease of 0.8 mm in size.
- The p-value of the palaeolatitude, equals 0.43: hence the null hypothesis (i.e. that slope of palaeolatitude = 0) cannot be rejected.

DIAGNOSTIC PLOTS



SMITHIAN + SPATHIAN: SIZE VS PALAEOLONGITUDE

Call:

```
lm(formula = medians ~ Palaeolongitude, data = dd_m_lon)
```

Coefficients:

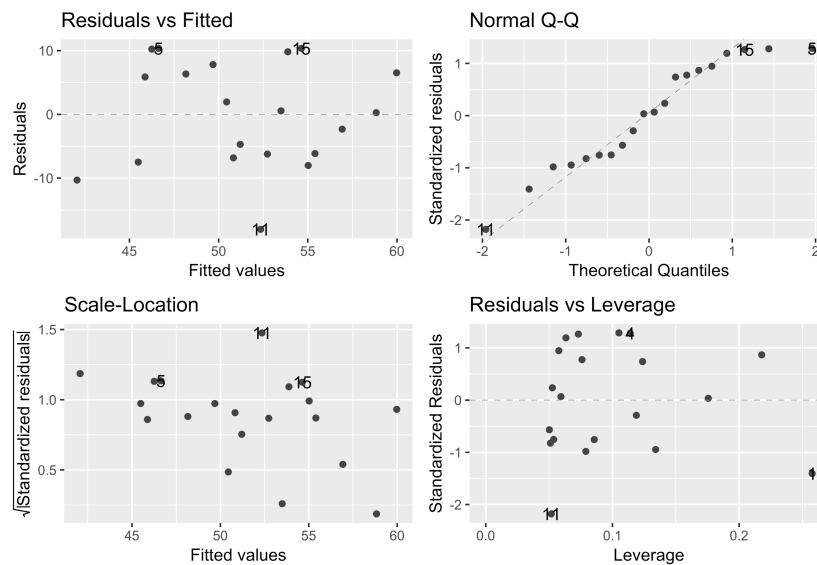
	Estimate	Std. Error	t value	Pr(> t)
(Intercept)	49.30372	2.10447	23.428	6.18e-15 ***
Palaeolongitude	0.07622	0.03132	2.433	0.0256 *

Residual standard error: 8.506 on 18 degrees of freedom
Multiple R-squared: 0.2475, Adjusted R-squared: 0.2057
F-statistic: 5.921 on 1 and 18 DF, p-value: 0.02561

INTERPRETATION

- R squared = 0.25: approximately 25% of variation in size can be explained by the model (i.e. by the variation in palaeolongitude).
- The residual standard error indicates that using the model to predict size from palaeolongitude results 68.3% of the times in an error smaller than ± 8 mm.
- The slope (*estimate*) of the palaeolongitude equals 0.08; this indicates that an increase of 1° palaeolongitude is associated with an increase of 0.08 mm in size.
- The p-value of the palaeolongitude, equals 0.02. Being it smaller than 0.05, it implies that the null hypothesis (i.e. that slope of palaeolongitude = 0) can be rejected.

DIAGNOSTIC PLOTS



SMITHIAN + SPATHIAN: SIZE VS PALAEOLONGITUDE WITHOUT -95° LONGITUDE

Call:

```
lm(formula = medians ~ Palaeolongitude, data = dd_m_lon)
```

Coefficients:

	Estimate	Std. Error	t value	Pr(> t)
(Intercept)	50.6686	2.2494	22.525	4.25e-14 ***
Palaeolongitude	0.0529	0.0344	1.538	0.142

Residual standard error: 8.257 on 17 degrees of freedom

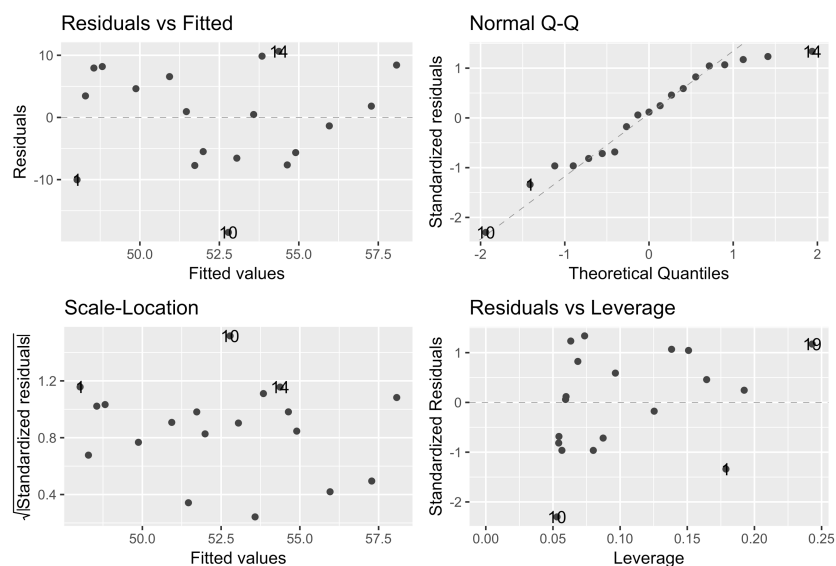
Multiple R-squared: 0.1221, Adjusted R-squared: 0.07051

F-statistic: 2.365 on 1 and 17 DF, p-value: 0.1425

INTERPRETATION

- R squared = 0.12: approximately 12% of variation in size can be explained by the model (i.e. by the variation in palaeolongitude).
- The residual standard error indicates that using the model to predict the size from palaeolongitude results 68.3% of the times in an error smaller than ± 8 mm.
- The slope (*estimate*) of the palaeolongitude equals 0.05 and indicates that an increase of 1° palaeolongitude is associated with an increase of 0.05 mm in size.
- The p-value of the palaeolongitude, equals 0.14 and implies that the null hypothesis (i.e. that slope of palaeolongitude = 0) cannot be rejected.

DIAGNOSTIC PLOTS



SMITHIAN: SIZE VS PALAEOLONGITUDE

Call:

```
lm(formula = medians ~ Palaeolongitude, data = dd_SM_m_lon)
```

Coefficients:

	Estimate	Std. Error	t value	Pr(> t)
(Intercept)	5.864e+01	4.835e+00	12.128	8.16e-09 ***
Palaeolongitude	8.293e-04	6.644e-02	0.012	0.99

Residual standard error: 17.18 on 14 degrees of freedom

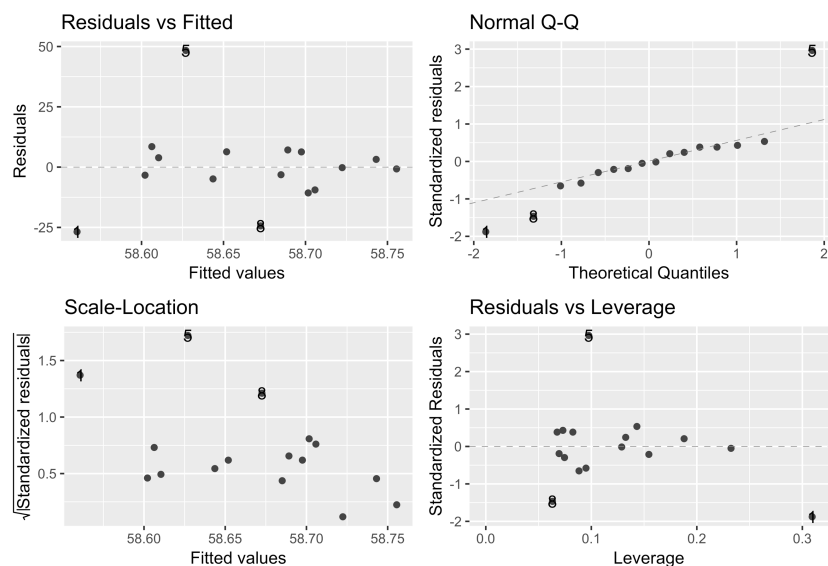
Multiple R-squared: 1.113e-05, Adjusted R-squared: -0.07142

F-statistic: 0.0001558 on 1 and 14 DF, p-value: 0.9902

INTERPRETATION

- R squared = $1.1 \cdot 10^{-5}$: indicates that approximately 0.001% of variation in size can be explained by the model.
- The residual standard error shows that using the model to predict the size from palaeolongitude results 68.3% of the times in an error smaller than ± 17 mm.
- The slope (*estimate*) of the palaeolongitude equals 0.0008; hence an increase of 1° palaeolongitude is associated with an increase of 0.0008 mm in size.
- The p-value of the palaeolongitude, equals 0.99. Hence the null Hypothesis (i.e. the slope of palaeolongitude = 0) can be rejected.

DIAGNOSTIC PLOTS



SPATHIAN: SIZE VS PALAEOLONGITUDE

Call:

```
lm(formula = medians ~ Palaeolongitude, data = dd_SP_m_lon)
```

Coefficients:

	Estimate	Std. Error	t value	Pr(> t)
(Intercept)	47.34709	6.35045	7.456	1.37e-06 ***
Palaeolongitude	0.18449	0.09547	1.933	0.0712 .

Residual standard error: 22.91 on 16 degrees of freedom

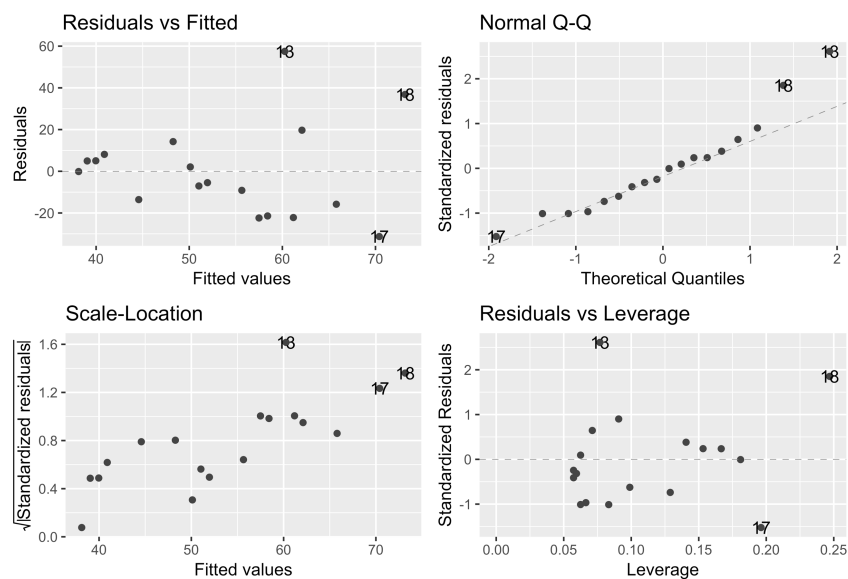
Multiple R-squared: 0.1892, Adjusted R-squared: 0.1386

F-statistic: 3.735 on 1 and 16 DF, p-value: 0.0712

INTERPRETATION

- R squared = 0.18: approximately 18% of variation in size can be explained by the model.
- The residual standard error shows that using the model to predict the size from palaeolongitude results 68.3% of the times in an error smaller than ± 22 mm.
- The slope (*estimate*) of the palaeolongitude equals 0.18: an increase of 1° palaeolongitude is thus associated with an increase of 0.18 mm in size.
- The p-value of the palaeolongitude, equals 0.07. Hence the null hypothesis (i.e. the slope of palaeolongitude = 0) can be rejected.

DIAGNOSTIC PLOTS



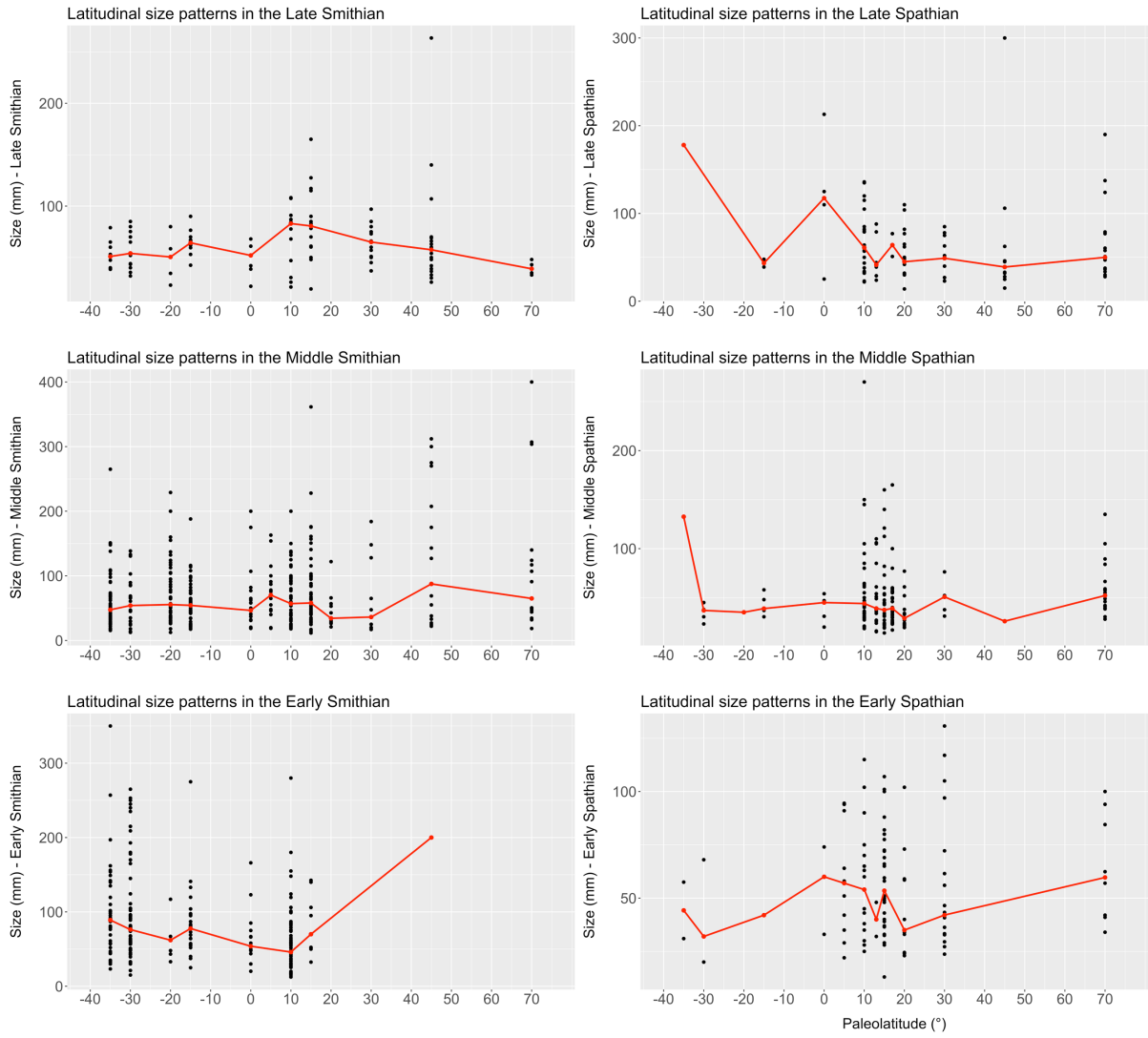


Figure B1

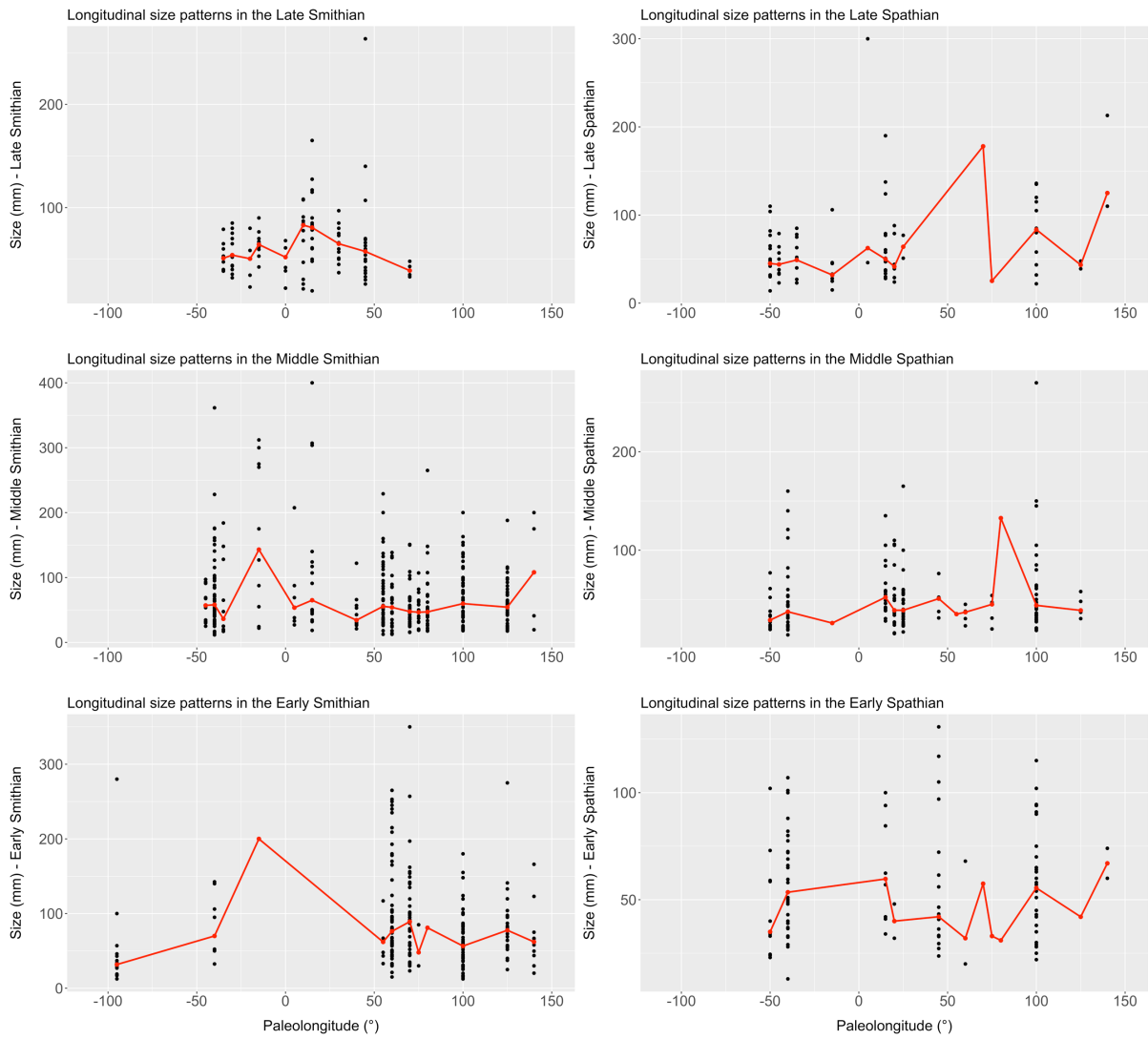


Figure B2

Personal declaration

I hereby declare that the submitted thesis is the result of my own, independent work. All external sources are explicitly acknowledged in the thesis.

A handwritten signature in black ink, reading "Lara Locatelli". The signature is written in a cursive style with a large initial "L" and "L" for the last name.

Lara Locatelli

Matriculation number: 10-947-794

Zurich, January 2019